EFFECT OF LIQUID FILM VELOCITY DISTRIBUTION ON THE DIRECT CONTACT CONDENSATION

A THESIS
SUBMITTED TO
THE COLLEGE OF ENGINEERING
UNIVERSITY OF BASRAH
IN PARTIAL FULFILLMENT OF
THE REQUIREMENTS FOR THE DEGREEOF
MASTER OF SCINCE
IN
MECHANICAL ENGINEERING

By
Ammar Ali Ojimi
(B. Sc. Mech. Eng.)

February 2003

بِسْمِ اللَّهِ الرَّحْمَنِ الرَّحِيم

إِنَّ فِي خَلْقِ السَّمَاوَاتِ وَالْأَرْضِ وَاخْتِلافِ
اللَّيْلِ وَالنَّهَارِ لَآيَاتٍ لِأُولِي الْأَلْبَابِ
{١٩٠} الَّذِينَ يَذْكُرُونَ اللّه قِيَاماً وَقُعُوداً
وَعَلَى جُنُوبِهِمْ وَيَتَفَكَّرُونَ فِي خَلْقِ
السَّمَاوَاتِ وَالْأَرْضِ رَبَّنَا مَا خَلَقْتَ هَذَا
بَاطِلاً سُبْحَانَكَ فَقِنَا عَذَابَ النَّارِ{١٩١}
رَبَّنَا إِنَّكَ مَنْ تُدْخِلِ النَّارَ فَقَدْ أَخْزَيْتَهُ
وَمَا لِلظَّالِمِينَ مِنْ أَنْصَارٍ {١٩٢} رَبَّنَا
إِنَّنَا سَمِعْنَا مُنَادِياً يُنَادِي لِلْإِيمَانِ أَنْ
آمِنُوا بِرَبِّكُمْ فَآمَنَّا رَبَّنَا فَاغْفِرْ لَنَا
ذُنُوبَنَا وَكَفِّرْ عَنَّا سَيِّئَاتِنَا وَتَوَفَّنَا مَعَ
الْأَبْرَارِ {١٩٣} رَبَّنَا وَآتِنَا مَا
وَعَدْتَنَا عَلَى رُسُلِكَ وَلا تُخْزِنَا يَوْمَ
الْقِيَامَةِ إِنَّكَ لا تُخْلِفُ الْمِيعَادَ {١٩٤}

صَدَقَ الله العَلِيُ العَظِيْم

آيات من سورة آل عمران المباركه

الإهداء

إلى شفعائي في أخرتي ودنياي محمد وال محمد صلوات الله عليه وعليهم أجمعين.

إلى الشمعة التي أنارت لي طريقي بدعائها...والدتي الحبيبة

إلى والدي... حباً واعتزازاً

إلى اخوتي الأعزاء

حسين ,كاظم, اسعد ومرتضى

إلى أخواتي العزيزات

إلى أحبائي وأصدقائي

اهدي هذا الجهد المتواضع

عمار

Certification

I certify that this thesis is prepared under my supervision at the University of Basrah, as a partial requirement for the degree of Master of scince in Mechanical Engineering.

Signature:

Name: Prof. Dr. Abdul-Muhsin A. Rageb

(Supervisor)

Data: 25 /2 /2003

In view of the available recommendations, I forward this thesis for debate by the examining committee.

Signature:

Name: Dr. Ameen A. Nassar

(Head of Mech. Eng. Dept.)

Data: 25 /2 /2003

Examining Committee's Report

We certify that we have read this thesis titled " **EFFECT OF LIQUID FILM VELOCITY DISTRIBUTION ON THE DIRECT CONTACT CONDENSATION**" which is being submitted by **Ammar Ali Ojimi** and as examining committee, examined the student in its contents. In our opinion it is adequate for the partial fulfilment of the degree of Master of scince in Mechanical Engineering.

Signature:
Name: Dr. A. M. Al-Chalaby
(Member and Chairman)
Data: 29 /6 /2003

Signature:
Name: Prof. Dr. S. E. Najim
(Member)
Data: 29 /6/2003

Signature:
Name: Dr. K. Y. Al-Salman
(Member)
Data: 29/6 /2003

Signature:
Name: Prof. Dr. A. M. Rageb
(Supervisor)
Data: / /2011

Approval of College of Engineering

Signature:
Name: Dr. Asaad Saleem
(Dean of Engineering collage)
Data: / /2003

ACKNOWLEDGMENTS

Thanks to God before everything who lightened may away during hard times.

The author would like to thank his supervisor professor Dr. Abdul-Muhsin A. Rageb for his much valued advice, assistance, and tuition during the various stages of this work, which was beyond any expectations.

Sincere thanks are also due professor Dr. A. H. Ghailan, the dean of the College of Engineering, and professor Dr. R. S. Fayadh, the dean's assistance for scientific affairs, and Dr. Ameen A. Nassar, the head of Mechanical Engineering Department for extending the facilities, which enable me to complete this work.

The author wishes to thank Dr. S. I. Najim for his help offered whenever required, and Dr. K. Y. Al-Salman for his expert advice, and providing important references.

The author would also like to thank Mr. Hussein. S. Saltan and all the teaching staff the college of engineering for their help offered whenever required. Thanks are also extended to the staff of Mechanical department computer center and the college library for the being very helpful.

Finally, I wish to express my sincere thanks to my family and friends for their support, patience, and understanding throughout the stages of this work.

Abstract

The present work is a theoretical investigation of the influence of variation of the velocity profiles on the direct contact condensation process of saturated vapor on a fully developed subcooled laminar liquid film flowing over an adiabatic solid surface. A theoretical model based on the heat balance and thermal energy equation is developed to describe the condensation performance of vapor on a thin liquid film having different types of velocity profiles. The theoretical model considers the fact that both velocity distribution and temperature gradients are taken as a variable along the flow line which can give more exact solution than previous works. Three type of velocity profiles for the liquid film, were chosen in this analysis, these are: uniform, linear, and semi-parabolic velocity distribution.

Analytical method was employed to two types of these profiles mainly uniform and linear profile. Also, the study includes development of a numerical procedure to the third type of the used profiles that is the semi-parabolic velocity profile.

The obtained results demonstrated the main parameters that control the condensation process and these are Prandtl number (Pr), Reynolds number (Re), and Subcooling number (S). The results gave informations about the process in term of Nusselt number, bulk temperature, and condensation rate.

The results of the present model are compared with the other theoretical predictions; the agreement between the results was satisfactory. Also, the results are compared with the experimental result obtained by other author, the agreement between the result was accepted.

Contents

List of Symbols

Symbols	Description	Units
a	Dimensionless wave amplitude	
A_1,A_2,A_3	Constant Coefficients	
A_n	Constant defined in eq.(3.60)	
c_p	Specific heat of liquid	J/kg.K
C_1,C_2,C_3	Constant Coefficients	
C_n	Constant defined in eq.(3.30)	
C_j	j th expansion coefficient defined in Eq.(3.107)	
D	Coefficient matrix eq.(3.105)	
D^t	Transpose of D	
f	Function of x^+	
g	Gravitational acceleration	m/s^2
	Function of y^+	
g	The eigenvectors associated with D	
g_{ij}	i th element of j th eigenvector of D	
h	Heat transfer coefficient	$W/m^2.K$
h_{ij}	i th element of j th eigenvector of D^t	
h_{fg}	Latent heat of evaporation	J/kg
J_P	Bessel function of the first kind , p th order	
k	Thermal conductivity of liquid	W/m.K
L	Wave length	m
$\dot{m}$	Mass flow rate of liquid	kg/s
Nu_x	Local Nusselt number , $(h_x \delta_o/k)$	
Pe	Peclet number,($(4\bar{u}_o \delta_o$)/α	
Pr	Prandtl number , (υ/α)	
q''	Heat flux	W/m^2
Re	Film Reynolds number , $(4\bar{u}_o \delta_o$)/υ	
S	Subcooling number , $(C_P(T_s-T_o))/h_{fg}$	
T	Temperature	K
u	Film velocity	m/s
x	Coordinate parallel to flow	m
y	Coordinate normal to flow	m

Greek Symbol

α	Thermal diffusivity	m^2/s
γ_n	Eigenvalues of the second case , eq.(3.56)	
β_j	Eigenvalues of the third case (of D matrix) , eq.(3.71)	
Δ	Difference	
δ	Film thickness	M
λ_n	Eigenvalues of the first case , eq.(3.26)	
μ	Dynamic viscosity	kg/m.s
υ	Kinematics viscosity	m^2/s
ρ	Density	kg/m^3
τ	Shear stress	N/m^2

Subscript

Symbol	Description
b	Bulk
i	General grid point
l	Liquid
O	Value at x=0
S	Saturation
St	Steam
V	Vapor
w	Wall(solid surface)
x	Local

Superscript

Symbol	Description
+	Dimensionless
-	Average

Chapter One

INTRODUCTION

Chapter One

INTRODUCTION

1.1 General

Condensation is the heat transfer process by which a vapor is changed in to a liquid by removing the latent heat of condensation. Four basic types of condensation are generally recognized: dropwise, filmwise, direct contact, and homogeneous type of condensation. In dropwise condensation, the drops of liquid form from the vapor at particular nucleation sites on a solid surface, and the drops remain separate during growth until carried away by gravity or vapor shear. In filmwise condensation, the drops initially formed and quickly coalesce to produce a continuous liquid film on the surface through which heat must be transferred to condense more vapor. In direct contact condensation, the vapor condenses directly on the subcooled liquid surface. In homogeneous condensation, the liquid phase forms directly from supersaturated vapor, away from any macroscopic surface, it is however, general assumed that, in practice, there are sufficient number of dirt or mist particles present in the vapor to serve as nucleation sites [1]. Efforts are continuing on means to predict the heat transfer coefficient for condensation more accurately, and to increase the heat transfer coefficient. This will result in reduced condenser size and would increase significantly the attractiveness of condensers in applications such as steam cars [2]. The direct contact condensation shows higher heat transfer rate than other type of condensation.

1.2 Direct Contact Condensation

Direct contact condensation is a phenomenon of interest in a variety of industrial applications, such as reflux condenser, tubular contractor, in cooling of rocket engines, during the work of last stage of steam turbines. In chemical engineering industry (e.g., mixing-type-heat exchanger, degasers, sea-water desalting by multiple distillation) and by energy conversion applications, such as geothermal and solar system. Condenser of this type are employed because of their higher heat transfer rates, trouble free operation and smaller initial capital outlay in comparison with the conventional indirect heat exchanger equipment [3,4,5,6]. In recent year the direct contact condensation has been of major important in connection with the nuclear industry (e.g., pressurizer under normal operating conditions, steam-water interaction in safety analysis). In the case of loss of coolant in a pressurized water reactor (PWR), the emergency cooling water (in a subcooled conditions) is injected into pressure vessel (which is filling with a steam in saturation or superheated condition) to prevent over heating [7]. Also, this process is employed for part of safety system in the European Simplified Boiling Water Reactor (ESBWR) where, in the case of an accident, condensable vapor is injected into subcooled liquid to help depressurize the system [8].

The direct contact condensation occurs when steam bought to contact with a moving liquid layer (in subcooled condition). The liquid layer flows along a solid surface, with free surface. The liquid motion may be induced by the body force (e.g., gravity force) or surface forces due to second phase moving (e.g., shear stress) or pressure drop force. The second phase in contact with the free surface of the film may be either a gas or a second (immicible) liquid, which may be at rest or in

motion relative to the solid surface on which the film flows. Thin liquid film flow is a special case of two-phase flow. The rate of transport heat between the two phases may be depend on the nature of these phases [9]. The direct contact condensation is always concerned with condensation of single vapor on a falling liquid film of identical chemical composition. Water was the most widely used substance because of its practical importance.

Several experimental and theoretical studies have been carried out on local condensation rates on the direct contact condensation process for several years (Murty 1974, Tamir 1976, Bankoff 1979, … etc). From the experiential results a large number of empirical correlations have been developed. Most of the theoretical studies of the direct contact condensation process were based on the assumptions of the constant velocity and temperature gradient used in the energy equation [Celata et al. 1989, Ragab 1993, Mikielwicz et al. 1995, … etc.]. These assumption is very rough approximation indeed (for example in semi-parabolic velocity profile case the velocity of the surface of liquid layer equals 1.5 of the average velocity), and may be lead to error for some cases (thick liquid layer or not well mixed flow). It allows a simpler solution of the problem. Non of these works took into account the effect of variable velocity and temperature gradient of the liquid layer on the condensation process. For the liquid layers treated here, three possible liquid velocity profile with variable temperature gradient, are assessed in a first attempt to model the process of direct contact condensation without imposing sever assumption on the velocity or temperature profile.

1.3 Objectives of the study

The main points that will be considered in this investigation are:

1. To developed theoretical model for the direct contact condensation process of saturated vapor condensed on a fully developed laminar, subcooled liquid films flow over an adiabatic solid surface with different velocity profiles (uniform, linear, and semi-parabolic velocity profile) where the liquid films may be driven by pressure drop, interfacial shear stress and gravity forces.
2. To study the effect of various parameters that control the direct contact condensation process for different case of the velocity profile employed here.
3. To compare the most important condensation parameters obtained by using the three present models, find which type of velocity give best performance.
4. To compare the result with that obtained from the approximated theoretical works carried out by other authors, and with published experimental works.

Chapter Two

LITERATURE REVIEW

Chapter Two

LITERATURE REVIEW

2.1 Introduction

Condensation is the process by which a vapor is changed to a liquid by removing the latent heat of condensation from the vapor. There are four basic modes or mechanisms of condensation generally recognized: dropwise, filmwise, homogeneous, and direct contact condensation.

The earliest work in this field was done by Nusselt [10] 1916. Who investigated the laminar filmwise condensation under certain specified assumptions, where the liquid film was flowing with semi-parabolic Nusselt velocity profile.

2.2 Direct Contact Condensation

The condensation of vapor on the liquid is called direct contact condensation. In this type the latent heat is transferred directly to the liquid .The direct contact condensation of vapor on liquid show higher intensity of heat transfer than the other type of condensation, for this reason this process has been an attractive subject of study for many investigators.

Studies in this field can be classified into three branches:

1- Direct Contact Condensation on Liquid Layer.
2- Direct Contact Condensation on Liquid Jets.
3- Direct Contact Condensation on Liquid Droplets.

Which has been the subject of intensive studies for several decades.

2.2.1 Direct Contact Condensation on Liquid Layer:

Several experimental and theoretical studies have been carried out for local condensation in direct contact with stratified two-phase flow. As a result, a number of empirical correlations on the condensation heat transfer coefficient have been developed. At the same time theoretical investigation were also performed to description this process.

In 1974, Murty and Sastri [11] studied analytically the direct contact condensation of the saturated vapor on a cold falling liquid film along an inclined wall. The region can conveniently be termed as thermally developing and the one beyond is the thermally developed region. The velocity and temperature distribution in their analysis were assumed as

$$u = 4u_o f_1\left[\frac{f_2+2}{3}y^+ - y^{+2}\right] \quad \ldots (2.1)$$

$$T = 1-2\eta+\eta^2 \quad \ldots (2.2)$$

$$\eta = \frac{\delta}{\delta_t}(1-y^+) \quad \ldots (2.3)$$

where δ_t, Thermal boundary layer thickness and f_1, f_2 are arbitrary function of x.

The average temperature in the liquid film, the dimensional film thickness, the local Nusselt number and the effectiveness, where found to depend on parameters such as α', Pr, S and γ'.

Where

$$\alpha' = \frac{\rho g \delta_o^2 \sin\theta}{u_{\max}\mu} \quad \ldots (2.4)$$

$$\gamma' = \frac{\rho_l \mu_l}{\rho_v \mu_v} \quad \ldots (2.5)$$

This result showed that the dimensionless film thickness decrease for increase of α' and experiences a local minimum in the down stream. The local Nusselt number is decreasing with increasing distance from leading edge of the channel up to a constant value for fully developed flow. Increase in α' and Pr increase the Nusselt number. Effectivness increase with increasing α' and decrease with Pr.

Finkelstein and Tamir [12] 1976 performed experimental measurements of the interfacial heat transfer coefficient, at various saturation pressures, for the direct contact condensation at several vapors on a liquid film of a similar chemical composition. They investigated the flowing vapors: water, carbon tetrachloride, methanol, n-pentane, methylenechloride, feron-113, dichloro-ethane and carbon disulfide. The flow of the liquid was maintained laminar over a wide range of operating condition .In all cases, the interfacial resistance was found to be appreciable compared with the overall average resistance. Hence, value of condensation coefficients (ratio of actual to the maximum condensation rate) was found to be much lower than unity.

Bankoff et al. [13] 1979 measured local steam condensation rate in a co-current horizontal stratified flow of steam and subcooled water in a 305 mm × 64 mm rectangular channel 1.56 m long. Electrically heated pitot tubes were used to measure steam mass flow rate at four locations along the centerline. In addition to axial steam flow profile, the inlet water and steam flow rate, the inlet and outlet water temperature, and the depth

of the water layer a long the channel were also measurement. The experimental data indicate that the local condensation rates increases with increasing steam flow rates, water flow rate and the degree of subcooling.

Segev and Collier [14] 1980 developed one-dimensional model to describe the flow behavior of liquid film draining down a heated wall, in the presence of countercurrent vapor flow. In developing the conservation equations they considered a well-mixed turbulent liquid film for which the velocity and temperature profiles assumed to be uniform. The effects of nonequilibrium void generation at the walls and condensation of countercurrent vapor on the penetrating liquid film interface, as well as on the bypassed liquid, had been considered. The condensation on the liquid film was described by using a heat transfer coefficient developed for co-current flow in a horizontal channel, as no data on countercurrent condensation were readily available in that time. The good agreement obtained for a counter current flow in an annulus suggests that the condensation mass flow rate did not depend strongly on geometry and vapor flow.

Kim and Bankoff [15] 1983 studied the condensation in the counter-current stratified flow of vapor and subcooled water in rectangular channel (380 mm × 38 mm and 1.27 m long) inclined 33 degree to the horizontal. The variables in the experiment were the inlet water and vapor flow rates and the inlet water temperature. Condensation heat transfer coefficients were determined as a function of local vapor and water flow rates and degree of subcooling. In all cases the local heat transfer coefficient increases with distance from the water inlet. The

result were correlated in term of turbulent Nusselt number to give the following relation

$$Nu_t = 0.061 \mathrm{Re}_t^{1.12} \mathrm{Pr}^{0.5} \quad \ldots (2.6)$$

and

$$\left.\begin{aligned} Nu_t &= \frac{h\lambda_t}{k} \\ \mathrm{Re}_t &= \frac{u_t \lambda_t}{\nu} \end{aligned}\right\} \quad \ldots (2.7)$$

where u_t, λ_t turbulent velocity and length scale. For horizontal co-current steam-water flow, the scale was $u_t = 0.3\bar{u}, \lambda_t = \delta$.

Kim and Bankoff [16] 1983 used a similar test section as [8] (380 mm×75 mm rectangular channel) measured local condensation heat transfer coefficient for counter current stratified flow of steam and cold water at atmospheric pressure at inclination of 4^o from the horizontal. In the rang $800 < \mathrm{Re_l} < 15000, 2500 < \mathrm{Re_v} < 30000$, they sought for correlation for Nusselt number finding

$$Nu = 0.63 \times 10^{-5} \mathrm{Re}_v^{0.9} \mathrm{Re}_l^{0.75} \mathrm{Pr}^{0.81} \quad \ldots (2.8)$$

which correlated the data. They also proposed a correlation for turbulent Nusselt number.

$$Nu_t = 0.134 \mathrm{Re}_v^{0.96} \mathrm{Pr}^{0.5} \quad \ldots (2.9)$$

The dependence upon the turbulent Reynolds number had been increased compared to the smooth interface models. This was reasonable, however,

since the influence of vapor Reynolds number that is crucial for the rough interface, appears only in the length and velocity scales.

In 1984, Lim et al. [17] measured the condensation rates of atmospheric steam on subcooled water in a co-current horizontal channel (63.5 mm × 304.8 mm and 1.601 m long). The experiments were performed at atmospheric pressure with slightly superheated steam, and examined the effects of steam flow rates(0.4-0.16 kg/s), water flow rate (0.2-1.45 kg/s), inlet water temperatures (25 ^{o}C and 50 ^{o}C), inlet water layer thickness (0.9 cm, 1.59 cm, 2.22 cm) on condensation rates. The heat transfer coefficients were found to vary from (1.3-20 kW/m^2. ^{o}C), depending on weather the interfaces were smooth or wavy and increases with steam and water flow rates.

In 1985, Kim et al. [3] measured local condensation heat transfer coefficients and interfacial shear stresses for counter current stratified flow of steam and subcooled water in rectangular channels (2.1 m long and 0.38 wide). Two channel depths (=0.075 and 0.038 m) and three inclination (4, 30 and 90 degree) were employed. They developed correlation of the interfacial friction factor f_i. Which was a function of the liquid Reynolds number only. The correlation for adiabatic interfacial factor $f_{i,a}$ obtained by a lest-squares methods was,

$$f_{i,a} = a\,\mathrm{Re}_L + b \qquad \ldots (2.10)$$

where a= 0.14 * 10^{-5} and b=0.021 for the nearly horizontal flow and a= 0.16 * 10^{-5} and b=0.025 for nearly vertical flow.

The measured interfacial friction factors f_i were compared with $f_{i,a.}$. The results showed that $f_{i,a}$ is much smaller than f_i, except for relatively low liquid subcooling. The relation between them is:

$$f_i - f_{i,a} = Cf_i \quad \ldots (2.11)$$

where the constant C was estimated to be 0.754 by a least-squares fit to the present data.

The following relation correlated the turbulent Nusselt number

$$Nu_t = n_1 \, \mathrm{Re}_t^{n_2} \, \mathrm{Pr}^{n_3} \quad \ldots (2.12)$$

where the coefficient n_1-n_3 are determined empirically. By least-squares linear regression, n_3 was found to be 0.465±0.045 with a 95% confidence limit.

The exponent n_2 was found to increase with the inclination angles, as follows,

$$\left.\begin{aligned} n_1 &= 0.0141 - 0.111(\sin\theta)^{0.93} \quad , \\ n_2 &= 0.96 - 0.425(\sin\theta)^{2.2} \end{aligned}\right\} \quad \ldots (2.13)$$

In 1986, Celata et al. [18] studied experimentally the direct contact condensation of stagnant saturated steam on slowly moving subcooled water with reference to a horizontal flat geometry. The experimental variables were the inlet water flow rate and temperature together with inlet steam temperature. Heat transfer coefficient did not show, practically, dependence on either inlet water temperature or inlet steam temperature but only on inlet water flow rate. They proposed correlations for the Nusselt number, as a function of Reynolds number and Prandtl numbers, which are

$$Nu = 0.021 \mathrm{Re}^{1.31} \mathrm{Pr}^{1.8} \qquad for\ Pe < 400 \qquad \ldots (2.14)$$

$$Nu = 0.043 \mathrm{Re}^{1.31} \mathrm{Pr}^{1.06} \qquad for\ 400 < Pe < 1500 \qquad \ldots (2.15)$$

$$Nu = 0.033 \mathrm{Re}^{4/3} \mathrm{Pr}^{1.1} \qquad for\ Pe > 1500 \qquad \ldots (2.16)$$

The agreement was reasonably good, within the experimental accuracy.

Celata et al. [19] 1987 studied experimentally the direct contact condensation of superheated steam (practically stagnant) on subcooling water with very low interfacial velocity (2-5 cm/sec). The steam at superheated temperature up to 200 ^{o}C and the inlet water temperature was up to 80 ^{o}C. The steam and water flow rates are measured up to 20 and 120 kg/h respectively. They presented a theoretical dissertation before the experimental results and show that the total thermal power (thermal power due to steam de-superheating, thermal power due to condensation and thermal power due to condensed subcooling (to the outlet liquid temperature)) and consequently the total heat transfer coefficient did not show appreciable dependence on superheated steam temperature. So it could practically evaluated by mean of available correlation for saturated steam condition. The direct contact heat transfer coefficient is linked to the overall one and is slightly dependent on the degree of steam superheating, as experimentally confirmed.

In 1989, Celata et al. [4] investigated experimentally the interaction between saturated or superheated steam in quasi-stagnant conditions and subcooled water in horizontal flow within a rectangular duct test section (42.5 mm × 19.7 mm). Four water level were tested (4, 6, 8 and 10 mm) and the heat transfer surface was 18.2 cm^2. Water average velocity ranged (0.5-20 cm/sec), while saturated steam temperature was varied (105-150

^{o}C), superheated steam temperature was varied from 20 to 70 ^{o}C where carried out at pressure (0.2 Mpas.).

A theoretical analysis based on assuming uniform velocity profile on liquid layer was achieved, and proposed a correlation for total thermal conductivity as

$$k_{tot} = k + k_{turb.} \quad \ldots (2.17)$$

$$k_{turb.} = k[a\,\mathrm{Re}^{b}\,\mathrm{Pr}^{c} - 1] \quad \ldots (2.18)$$

where k is the molecular thermal conductivity, $k_{turb.}$, turbulent thermal conductivity. And a, b and c constants have the values as: a= 0.21, b=0.34 , c=-0.24 .

A comparison of the model with experimental data shows that the water turbulent conductivity was introduce in the model only for data point with Reynolds number greater than 1250. For data characterized by a lower Reynolds number, the model works with the molecular value of the water thermal conductivity. Practically, the model is a laminar-turbulent description of the direct contact condensation process.

In 1993, Rageb [20] developed a theoretical approach to study the condensation of the steam on subcooled liquid film on a heated surface. The analysis based on assuming the velocity distribution in laminar liquid film as given by

$$u^{+} = -\frac{G}{2}y^{+} + (T + G\delta^{+})y^{+} \quad \ldots (2.19)$$

and the energy equation was solved using the average of this distribution. Who was given special consideration to evaporation of the formed film. The results demonstrated that the main parameters effecting the condensation were also effecting the evaporation. Furthermore, the local

film thickness, the average temperature difference and the average Nusselt number were found to depend on many factor such as the subcooled number S, Peclet number Pe, heating ratio R, gravity and shear parameters (G and T).

Where

$$\left.\begin{aligned} R &= \frac{q''_w}{\frac{k}{\delta_o}(T_s - T_o)} \\ G &= \frac{g\delta_o^2}{\nu u_o} \\ T &= \frac{\tau_o \delta_o}{\rho \nu u_o} \end{aligned}\right\} \quad \ldots (2.20)$$

In 1995, Mikielewicz and Rageb [7] presented an approximate theoretical solution of the direct-contact condensation of steam with saturation temperature on subcooled liquid layer, which flow on an adiabatic solid surface. The steam was flow co-currently with the liquid layer and condenses on the liquid interface. The analysis was based on simplified energy equation, in which the temperature gradient in the direction of the liquid flow was taken from the average energy balance and used the same average velocity distribution as in Ragab [20] 1993. An adequate solution for the direct contact condition was obtained. The solution considers a few parameter controlling the condensation processes as the Pe, S, G, and T. They also found that the main effect on the liquid layer thickness was attributed to the subcooling number, while the effect of the other parameters is less significant. The theoretical results obtained were compared with experimental results for other authors. Satisfactory

agreement was obtained when only about 10 % of variation in the average Nusselt number was observed for two extreme cases, the gravity and shear stress driven film.

Karapantsios et al. [5] 1995 measured the local condensation heat transfer rate for steam-air mixtures in direct contact with subcooled water layer inside a vertical tube over the range of liquid flow rates (1.7-17.5 g/s.cm). The gas mixture is maintained effectively stagnant during the tests and the major resistance to heat transfer is due to the large amount of noncondensables. They presented a theoretical model to account for some additional thermal resistance on liquid side, by decomposing the liquid film in to a wavy 'nonresistant' region and laminar substrate region where temperature gradients may prevail. In the second region they employed the parabolic velocity distribution, that is

$$u_{sub}(y') = \frac{g\delta_o^2}{2\nu}\left(1-\left(\frac{y'}{\delta_o}\right)^2\right) \qquad \ldots (2.21)$$

where, $u_{sub}(y')$, velocity distribution in the substrate, y' , normal direction measured from interface surface. Heat transfer coefficient was found to depend not only on the steam concentration but also on the liquid flow rates. Furthermore, the dependence of heat transfer coefficients on the liquid flow rates is attributed to the dynamic interaction between the interfacial waves and gas layer.

Karapantsios and karabelas [21] 1995 examined an intermittent (periodic) liquid flow rate as a means to enhance local condensation rates in a vertical column where quasi-stagnant vapor gas mixtures come in direct contact with falling wavy liquid layer. The gas mixture being effectively stagnant was responsible for the major resistance to heat

transfer due to its relatively large concentration of noncondensables. Flow intermittence was found to improve heat transfer rates by as much as an order of magnitude. The local condensation heat transfer coefficients depend greatly on both liquid flow mode and liquid flow rate. Statistical analysis of the measured local fluctuations of film thickness revealed that condensation was responsible only for slight modifications of isothermal liquid surface morphology. There was also evidence that increase liquid wave velocities aid the interfacial transport process.

In 1996, Karapantsios et al. [22] carried out an experimental and theoretical studies of condensation from air –steam mixture on a falling water layer. This layer was wavy turbulent while the gas phase is kept saturated with steam. Experiments were conducted with the gas mixture effectively stagnant compared with the fast moving liquid film. Measurements are also made under a mild vacuum applied on the gas phase. Heat transfer coefficients averaged over the entire length of the condensing surface tend to increase by decreasing the liquid flow rate, by increasing the steam fraction and by applying a mild vacuum on the gas phase. However for the cases examined, there was a liquid flow rate above which the heat transfer coefficient becomes almost constant. Numerical predictions were made for fully developed turbulent film using an eddy diffusivity model. The result indicated that for a system with a large a mount of noncondensable gases the temperature profile in the liquid film is nearly uniform and that the major resistance to condensation resided in the gas phase. The analysis also showed that the relative contribution of sensible heat transferred through the gas phase was small relative to the latent heat released upon condensation. Comparison of the

predictions with experimental data suggested that a significant parameter in this analysis was the gas diffusion boundary layer thickness, which seems to be comparable in size with the liquid film thickness. Finally, the possibility was discussed of correlating condensation heat transfer coefficients with already available statistical characteristics of the falling wavy layer. Theoretical predictions based on this idea were in good agreement with obtained data.

In 1999, Rageb [23] developed an analytical study of direct contact condensation of saturated vapor on a cold laminar falling film at the entrance length. The velocity and temperature profile within the boundary layer were taken in the form

$$\frac{u}{u_\delta} = 2(\frac{y}{\delta}) - (\frac{y}{\delta})^2 \quad \ldots (2.22)$$

$$\frac{T - T_o}{T_s - T_o} = 1 - 2(\frac{\delta_f - y)}{\delta_f} + (\frac{\delta_f - y}{\delta_t})^2 \quad \ldots (2.23)$$

where

u_δ: Velocity at $y = \delta$

δ_f: Film thickness

δ_t: Thermal boundary layer thickness

The investigation was carried out for both accelerating and decelerating subcooled liquid film. The local Nusselt number, liquid film thickness and the entrance length where found to depend on parameters such as Pr, S and G (as defined in equation 2.20). The Nusselt number for fully developed flow was compared with the theory developed by Mikielewicz and Rageb [7] the present analysis gives about 10 % higher values which may be considered as good agreement.

In 2001, Lieth [6] studied analytically the process of the direct contact condensation of vapor on subcooled laminar wavy liquid film flowing over an adiabatic solid surface. The heat balance and a simplified energy equation were used. The heat balance was done for smooth film subjected to the same conditions as that for the wavy flow. The energy equation is simplified by considering the local temperature gradient in flow direction is equal to the bulk temperature gradient. Semi-parabolic velocity profile was used to describe the velocity distribution through out the liquid film, that is

$$u^{+} = 3(y^{+}\delta^{+} - \frac{1}{2}y^{+2}) \quad \ldots (2.24)$$

The result of the theoretical model are compared with some other theoretical predications to justify the validity of the theoretical model, and the result found to be in agreement.

Davis and Yadigaroglu [8] 2002,presented a method for solving condensation problems involving in a more general flow known as a "falker-skan" flow, where vapor is injected into a liquid pool at a constant velocity, resulting in a movement of the vapor-liquid interface at another velocity. They used this method to solve the problem of saturated vapor flowing in direct contact over subcooled liquid. They found a correlation for the vapor blowing parameter (or mass transfer rate) versus the Jacob number ($c_p(T_\infty-T_o)/h_{fg}$)and the ratio of the vapor to liquid free-stream velocities, the liquid Prandtl number and the density ratio. Finally, they investigated trends for the non-dimensional liquid heat transfer coefficient and non-dimensional interfacial pressure difference.

Recently, Al-Salman [9] 2002, did an investigation of direct contact condensation process of saturated vapor on fully developed subcooled laminar wavy falling film flowing over an adiabatic wall, he developed a new theoretical model based on the mass, momentum and energy conservation equations in addition to the overall heat balance equation, to describe the condensation performance of vapor on thin liquid film for different waves shapes. The theoretical model was give information about the dynamics of the direct contact condensation process in term of condensation rates and heat transfer characteristics. Also, he performed an experimental, investigation by carrying several experimental measurements for condensing saturated steam directly on subcooled laminar wavy falling water film. The results show that the waviness of the liquid film increases the heat transfer rates up to several tenths of a percent. He obtained a good agreement between the theoretical and the experimental results.

2.2.2 Direct Contact Condensation on Liquid Jets:

The process of condensation on liquid jet in which the coolant is injected as a series of jets or solid sheets and falls down trough a relatively quiescent vapor have been studies by many investigators.

In 1976, Benedek [24] investigated experimentally the problem of heat transfer at the condensation of steam on turbulent water jet. According to the measurement the heat transfer coefficient was found to depend on the water velocity and the mount of air being present at the condensation, on other hand it did not depend on the pressure and steam velocity.

In 1989, Kim and Mills, [25], [26] studied experimentally and theoretically the condensation on coherent turbulent liquid jet. The purpose of the experimental part [25] was obtain a data based for liquid side heat transfer coefficient. The Stanton number was found to be essentially independent of jet diameter, but it depends on the length, velocity, surface tension and viscosity. In the theoretical part [26] they evaluated the suitability of simple algebraic model for eddy diffusivity.
Various eddy diffusivity models, of varying degree of complexity, were evaluated through comparison with experimental data. Numerical solutions were also obtained for laminar jets.

Lui et al. [27] 1989 studied experimentally the direct contact condensation on a fragment circular jet. In this study the water was injected through a nozzle to glass chamber. The experimental was done for different inlet velocities and inlet temperature. The measured heat transfer rates for these conditions are presented in the terms of percent coolant utilized, which is defined as

$$\text{Percent of coolant utilized} = 1 - \frac{(T_s - T)}{(T_s - T_o)} \qquad \ldots(2.26)$$

where

T: average jets temperature.

The experimental data indicated that at low air concentrations, the percent coolant utilized decreases with increasing Subcooled number.

Celata et al. [28] 1989 carried out an experiment on the direct condensation of steam on subcooled liquid jets. Results regarding the effect of nozzle diameter and length as well as the jet velocity are reported. It is particular interest the influence of the nozzle length on the

jet heating, a longer nozzle giving rise to a less heat transfer between steam and the liquid jet.This is probably due to the different velocity profile that issuing jet present in the two nozzles. Once the liquid jet is in the steam environment, after leaving the nozzle it tend to assume a flat radial velocity profile. The velocity profile adjustment causes an increase of the local turbulence, increasing the heat transfer. In case of turbulent jets if the length of the nozzle is sufficient to allow an appreciable or fully velocity profile development, the extent of this effect is limited to reduce superficial layer with a consequent reduction of the heat transfer.

2.2.3 Direct Contact Condensation on Liquid Droplets:

Direct contact condensation of vapor on dispersed droplets of subcooled liquid has many industrial applications, particularly in the chemical and nuclear industries. Consequently, numerous studies have been conducted on this subject.

In 1973, Ford and Lekic [29] studied the growth of drops during condensation in direct contact between liquid drops and vapor. An approximate correlation for this process was obtained from theoretical considerations. They performed an experimental investigation of condensations of steam on water drops of three different diameters and with different initial subcooling of drops below the saturation temperature of steam. They used high-speed photography to analyze the growth of drops during condensation.

Ford and Lekic [30] 1980 carried out a theoretical study of the direct contact condensation of a pure vapor on a spray of subcooled water drops. Theoretical consideration includes the analysis of drop size

distribution, motion of drops, and heat transfer rate. Droplet diameter was found to be the most important parameter, affecting thermal utilization (or the average spray temperature). They performed experimental investigation of steam condensing on a spray of subcooled water drop, using three full cone nozzles at different pressure drops.
Comparison of the values of thermal utilization obtained experimentally and those predicated by the model showed good agreement. The values of thermal utilization obtained indicate that this a highly efficient way of condensing pure steam.

In 1984, Hijikata et al. [31] investigated experimentally and theoretically the direct contact condensation of vapor to falling cooled droplets identical in material with the vapor. Heat transfer of direct contact condensation to a droplet was rate-controlled by the heat transfer in the droplet. Experimental results show that the heat transfer coefficient about ten times higher than that of the solid sphere and about four times higher than the theoretical value. A theoretical analysis had been carried out with adequate consideration to the deforming oscillation of the droplet due to surface tension and it is clarified that the analytical solution well explains the experimental results.

In 1991, Celata et al. [32] performed an experiment of direct contact condensation of saturated steam on subcooled water sprays characterized by droplets of uniform size, to test the influence of droplet diameter and velocity on the heat transfer rate. The performed continuous measurements of the average droplet temperature along the axis of the spray jet. The condensation efficiency and local heat transfer coefficient

were calculated as functions of the main parameters involved (droplet diameter and velocity, thermodynamic condition of the fluids).

Chapter Three

THEORETICAL ANALYSIS

Chapter Three

THEORETICAL ANALYSIS

3.1 Introduction

Condensation in two-phase system causes variations in the amount and distribution of each phase [5]. These changes, inturn, induce variation in the local heat transfer processes. Because of continuos change of all the thermal and hydraulic properties of the flow, the situation at any point a long the transfer surface may never be truly full developed either thermally or hydrodynomicaly. However, in order to describe the momentum and energy field inside the two phases a pseudo-equilibrium is customarily adopted in the literature.

In this chapter the heat balance and energy equation are solved for subcooled liquid film flowing on an adiabatic solid surface, with three types of velocity distribution on which saturated steam is condensed, to study the heat transfer characteristics of process with various velocity profiles.

The governing equations of the problem are presented based on the following assumptions;

1. The liquid film is laminar, steady, and fully developed.
2. The subcooled liquid film on which condensation occurs is flowing on adiabatic surface.
3. The steam in saturated temperature condensed on the liquid-vapor interface.
4. The increment of condensed mass on the analyzed control volumes is small enough to be neglected the normal component of velocity.

5. Any wave, which may be present due to steam up-flow, is neglected.
6. The thermo-physical properties of fluid are constant.
7. The viscous dissipation within the liquid is negligible.

The physical model that is considered in the present work is showing in fig. (3.1).

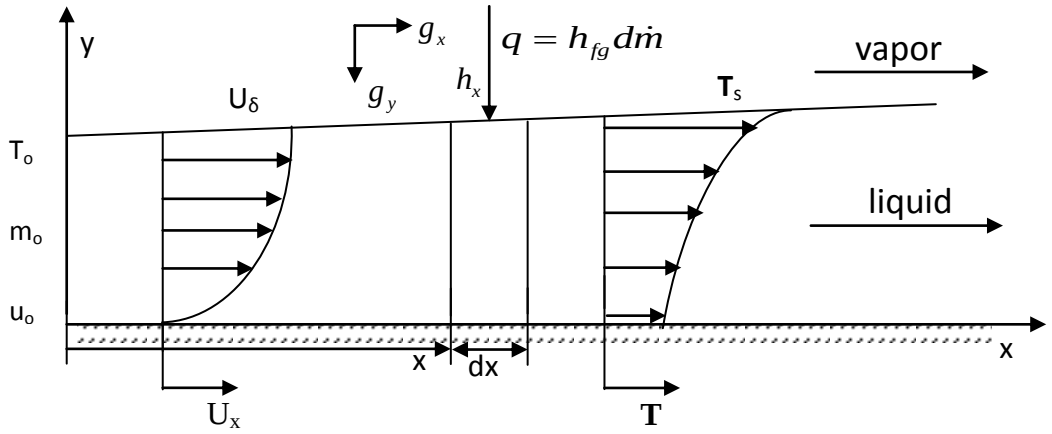

Fig. (3.1) general direct-condensation model

3.2 Heat Transfer Models

The models will be developed for direct contact condensation of saturated vapor on subcooled liquid layer corresponding to different velocity profiles. The liquid layer flows on an adiabatic solid surface with inlet mass flow rates $\dot{m}_o$ and subcoled inlet temperature T_o. Steam with saturation temperature T_s flows co-currently with the liquid layer. Using the above assumptions, the heat balance for these models may be described by term representing the latent heat of vapor condensation and terms represently the sensible heat of interface.

$$d\dot{m}h_{fg} + d\dot{m}c_p T_s + \dot{m}c_p T_b = (\dot{m} + d\dot{m})c_p (T_b + dT_b) \qquad \ldots (3.1)$$

Simplification of the heat balance equation, neglecting minor value ($d\dot{m}c_p dT$), and the value ($c_p(T_s-T_b)$) because it is small enough in comparison with the value (h_{fg}) [7], the heat balance equation becomes

$$\dot{m}c_p dT_b = h_{fg} d\dot{m} \quad \ldots (3.2)$$

Subjected to the boundary condition

$$T = T_o \qquad \dot{m} = \dot{m}_o \qquad at \qquad x = 0 \quad \ldots (3.3)$$

Equation (3.2) can be rearranged using the dimensionless form and becomes

$$\frac{d\dot{m}^+}{\dot{m}^+} = -SdT_b^+ \quad \ldots (3.4)$$

and equation (3.3) as

$$T_b^+ = 1 \qquad \dot{m}^+ = 1 \qquad at \qquad x^+ = 0 \quad \ldots (3.5a)$$

where

$$T_b^+ = \frac{T_s - T_b}{T_s - T_o} \quad \ldots (3.5b)$$

$$\dot{m}^+ = \frac{\dot{m}}{\dot{m}_o} \quad \ldots (3.5c)$$

$$S = \frac{c_p(T_s - T_o)}{h_{fg}} \quad \ldots (3.5d)$$

$$x^+ = \frac{x}{\delta_o} \quad \ldots (3.5e)$$

After integration and satisfying the boundary condition gives

$$\dot{m}^+ = \exp\{S(1-T_b^+)\} \quad \ldots (3.6)$$

Thus its appears that $\dot{m}^+$ can not be determined from the above equation, since there is no other relation to determine T_b^+. So that using the energy equation instead of the heat balance a new solution for T_b^+ can be estimated. The appropriates energy equation for this problem can be written as Özisk [33]

$$u(y)\frac{\partial T}{\partial x} = \alpha \frac{\partial^2 T}{\partial y^2} \quad \ldots (3.7)$$

The boundary conditions used in this problem are:

1) $T = T_o \qquad x = 0 \qquad 0 \le y \le \delta_o \quad \ldots (3.8a)$

2) $\frac{\partial T}{\partial y} = 0 \qquad x > 0 \qquad y = 0 \quad \ldots (3.8b)$

3) $T = T_s \qquad x > 0 \qquad y = \delta \quad \ldots (3.8c)$

Introducing the dimensionless variable into equation (3.7) and equation (3.8a,b, c), it yields

$$\frac{\mathrm{Re}}{4}\mathrm{Pr}\,u^+(y^+)\frac{\partial T^+}{\partial x^+} = \frac{\partial^2 T^+}{\partial y^{+2}} \quad \ldots (3.9)$$

And

1) $T^+ = 1 \qquad x^+ = 0 \qquad 0 \le y^+ \le 1$ … (3.10a)

2) $\dfrac{\partial T^+}{\partial y^+} = 0 \quad x^+ > 0 \qquad y^+ = 0$ … (3.10b)

3) $T^+ = 0 \qquad x^+ > 0 \qquad y^+ = \delta^+$ … (3.10c)

Where

$$T^+ = \frac{T_s - T}{T_s - T_o} \quad \text{… (3.11a)}$$

$$u^+ = \frac{u}{\bar{u}_o} \quad \text{… (3.11b)}$$

$$\delta^+ = \frac{\delta}{\delta_o} \quad \text{… (3.11c)}$$

$$y^+ = \frac{y}{\delta_o} \quad \text{… (3.11d)}$$

$$\mathrm{Re} = \frac{4\bar{u}_o \delta_o}{\upsilon} \quad \text{… (3.11e)}$$

$$\mathrm{Pr} = \frac{\upsilon}{\alpha} \quad \text{… (3.11f)}$$

And $\bar{u}_o$ can be defined as

$$\bar{u}_o = \frac{1}{\delta_o}\int_0^{\delta_o} u(y)dy \qquad \ldots (3.12)$$

To obtain the solution of equation (3.9) and estimates the value of $T^+(x^+, y^+)$, an expression for velocity profile is needed. In this work three types of velocity profiles have been assumed; these are (fig. (3.2)).

1. Uniform velocity profile.
2. Linear velocity profile.
3. Semi-parabolic velocity profile.

And by substitution each type of these profiles in equation (3.9) a new solution can be obtained.

3.2.1 Analysis with Uniform Velocity Profile

In this case the velocity profile to be considered is uniform in y and x directions, and it can be written as following;

$$u(y) = u_o \qquad 0 \le y \le \delta(x) \qquad \ldots (3.13)$$

or in nondimensional form the above equation becomes

$$u^+ = 1 \qquad 0 \le y^+ \le \delta^+ \qquad \ldots (3.14)$$

where

$$u^+ = \frac{u(y)}{\bar{u}_o} \qquad \ldots (3.15)$$

Substitution of equation (3.14) into equation (3.9) gives

$$\frac{\mathrm{Re}}{4}\mathrm{Pr}\frac{\partial T^{+}}{\partial x^{+}}=\frac{\partial^{2}T^{+}}{\partial y^{+2}} \quad \ldots (3.16)$$

This equation can be solved using the separation of variables method [34]. The method of separation of variables consists of seeking particular " product solution" of equation (3.16) in the form

$$T^{+}(x^{+},y^{+})=f(x^{+}).g(y^{+}) \quad \ldots (3.17)$$

Where f is a function of x^{+} alone and g is a function of y^{+} alone.

If equation (3.17) is introduced into equation (3.16), and after separating the variables gives

$$\frac{\mathrm{Re}}{4}\mathrm{Pr}\frac{1}{f}\frac{df}{dx^{+}}=\frac{1}{g}\frac{d^{2}g}{dy^{2}}=-\lambda^{2} \quad \ldots (3.18)$$

Where $(-\lambda^{2})$ is the separation constant.

Thus the two ordinary differential equations are

$$\frac{df}{dx^{+}}+\frac{4\lambda^{2}f}{\mathrm{Re}\,\mathrm{Pr}}=0 \quad \ldots (3.19)$$

$$\frac{d^{2}g}{dy^{+2}}+\lambda^{2}g=0 \quad \ldots (3.20)$$

And the solution of these equations may be written as

$$f=C_{1}\exp(-\frac{4\lambda^{2}}{\mathrm{Re}\,\mathrm{Pr}}x^{+}) \quad \ldots (3.21)$$

$$g=C_{2}\sin(\lambda y^{+})+C_{3}\cos(\lambda y^{+}) \quad \ldots (3.22)$$

The general solution is

$$T^+(x^+, y^+) = f.g = C_1 \exp(-\frac{4\lambda^2}{\mathrm{Re\,Pr}} x^+)(C_2 \sin(\lambda y^+) + C_3 \cos(\lambda y^+)) \quad \ldots (3.23)$$

The constant (C_1, C_2 and C_3) in this equation are found using the boundary conditions. Applying equation (3.10b), the solution is reduces to

$$\mathrm{T}^+(x^+, y^+) = C_3 \cos(\lambda y^+) \exp(-\frac{4\lambda^2}{\mathrm{Re\,Pr}} x^+) \quad \ldots (3.24)$$

Using the boundary condition at the interface equation (3.10c) yields

$$C_3 \cos(\lambda \delta^+) \exp(-\frac{4\lambda^2}{\mathrm{Re\,Pr}} x^+) = 0, \quad \ldots (3.25)$$

This requires the eigenvalues λ_n to be positive roots of $\cos(\lambda_n \delta^+) = 0$, that is

$$\lambda_n = \frac{1}{\delta^+}(\frac{\pi}{2}(2n+1) \qquad n = 0,1,2,.... \quad \ldots (3.26)$$

Thus it follows that any particular solution has the form

$$T_n^+ = C_n \cos(\lambda_n y^+) \exp(-\frac{4\lambda_n{}^2}{\mathrm{Re\,Pr}} x^+) \quad \ldots (3.27)$$

The solution satisfied the boundary condition equation (3.10a) is obtain by summing all possible solutions:

$$T^+ = \sum_{n=0}^{\infty} C_n \cos(\lambda_n y^+) \exp(-\frac{4\lambda_n^2}{\mathrm{Re\,Pr}} x^+) \quad \ldots (3.28)$$

The constant C_n are found from boundary condition at the beginning of flow

$$1 = \sum_{n=0}^{\infty} C_n \cos(\lambda_n y^+) \quad \ldots (3.29)$$

Multiplying equation (3.29) by ($\cos \lambda_m y^+$), integrating from 0 to 1.0 and making use of the orthogonal property [35] of the eigenfunctions (see appendix A) gives for C_n:

$$C_n = \frac{\int_0^1 \cos(\lambda_n y^+) dy^+}{\int_0^1 \cos^2(\lambda_n y^+) dy^+} = \frac{2\sin \lambda_n}{\lambda_n + \frac{1}{2}\sin(2\lambda_n)} \quad \ldots (3.30)$$

The temperature distribution is then finally found to be

$$T^+ = \sum_{n=0}^{\infty} \frac{2\sin(\lambda_n)}{\lambda_n + \frac{1}{2}\sin(2\lambda_n)} \cos(\lambda_n y^+) \exp(-\frac{4\lambda_n^2}{\mathrm{Re\,Pr}} x^+) \quad \ldots (3.31)$$

with λ_n as given by equation (3.26).

This equation represents the temperature distribution in the liquid layer.

Using the definition of the bulk temperature along the flow in the following form;

$$T_b^+ = \frac{\int_0^{\delta^+} u^+ T^+ dy^+}{\int_0^{\delta^+} u^+ dy^+} \quad \ldots (3.32)$$

and substitution of the expressions obtained for both velocity, equation (3.14) and temperature distribution, equation (3.31), gives

$$T_b^+ = \frac{\int_0^{\delta^+} \left\{ \sum_{n=0}^{\infty} \frac{2\sin(\lambda_n)}{\lambda_n + \frac{1}{2}\sin(2\lambda_n)} \cos(\lambda_n y^+) \exp(-\frac{4\lambda_n{}^2}{\mathrm{Re\,Pr}} x^+) \right\} dy^+}{\int_0^{\delta^+} dy^+} \quad \ldots (3.33)$$

After integration of this equation, yields

$$T_b^+ = \frac{1}{\delta^+} \sum_{n=0}^{\infty} \frac{2\sin(\lambda_n)}{\lambda_n(\lambda_n + \frac{1}{2}\sin(2\lambda_n))} \sin(\lambda_n y^+) \exp(-\frac{4\lambda_n^2}{\mathrm{Re\,Pr}} x^+) \quad \ldots (3.34)$$

The dimensionless mass flow rate can be defined as;

$$\dot{m}^+ = \int_0^{\delta^+} u^+(y^+) dy^+ \quad \ldots (3.35)$$

and using the expression for velocity, equation (3.14) gives

$$\dot{m}^+ = \delta^+ \quad \ldots (3.36)$$

To obtain the film thickness, equation (3.34) and equation (3.36) are substitute into equation (3.6) and the result will be

$$\delta^+ = \exp\left\{ S[1 - \frac{1}{\delta^+} \sum_{n=0}^{\infty} \frac{2\sin(\lambda_n)}{\lambda_n(\lambda_n + \frac{1}{2}\sin(2\lambda_n))} \sin(\lambda_n \delta^+) \exp(-\frac{4\lambda_n^2}{\mathrm{Re\,Pr}} x^+)] \right\}$$

… (3.37)

Using this equation the film thickness at any position along the flow can be obtains and so the total mass flow rate of condensation can be determined.

Heat Transfer Coefficient:

The local heat transfer coefficient may b obtained from heat balance at the interface of liquid – vapor as;

$$h_x = \frac{q''}{(T_s - T_b)} \quad \text{… (3.38)}$$

Where

$$q'' = -k \left. \frac{\partial T}{\partial y} \right|_{y=\delta} \quad \text{… (3.39)}$$

Substitution of equation (3.39) into equation (3.38) gives

$$h_x = -\frac{k}{(T_s - T_b)} \left. \frac{\partial T}{\partial y} \right|_{y=\delta} \quad \text{… (3.40)}$$

Further arrangement the above equation becomes

$$\frac{h_x \delta_o}{k} = -\frac{\delta_o}{(T_s - T_b)} \frac{\partial T}{\partial y}\bigg|_{y=\delta} \quad \ldots (3.41)$$

Or in dimensionless form the above equation yields

$$Nu_x = -\frac{1}{T_b^+} \frac{\partial T^+}{\partial y^+}\bigg|_{y^+=\delta^+} \quad \ldots (3.42)$$

Where

$$Nu_x = \frac{h_x . \delta_o}{k} \quad \ldots (3.43)$$

Using equation (3.34) and the derivative of equation (3.31) at the liquid-vapor interface, equation (3.42) it becomes

$$Nu_x = \frac{\delta^+ \sum_{n=0}^{n} \frac{\sin(\lambda_n)}{1 + \frac{1}{2\lambda_n}\sin(2\lambda_n)} \sin(\lambda_n \delta^+) \exp(-\frac{4\lambda_n^2}{\mathrm{Re\,Pr}} x^+)}{\sum_{n=0}^{\infty} \frac{\sin(\lambda_n)}{\lambda_n^2 + \frac{\lambda_n}{2}\sin(2\lambda_n)} \sin(\lambda_n \delta^+) \exp(-\frac{4\lambda_n^2}{\mathrm{Re\,Pr}} x^+)} \quad \ldots (3.44)$$

This equation represents the local Nusselt number in the longitude direction of the flow.

3.2.2 Analysis with Linear Velocity Profile

In this case the shear stresses forces may be the force which driven the liquid layer on the solid surface, and velocity distribution can be written as

$$u(y) = \frac{\tau_w}{\mu} y \qquad 0 \le y \le \delta(x) \qquad \ldots (3.45)$$

or in the dimensionless form

$$u^+ = 2y^+ \qquad 0 \le y^+ \le \delta^+ \qquad \ldots (3.46)$$

By substitution equation (3.46) into equation (3.9) it becomes

$$\frac{\mathrm{Re}}{2} \mathrm{Pr}\, y^+ \frac{\partial T^+}{\partial x^+} = \frac{\partial^2 T^+}{\partial {y^+}^2} \qquad \ldots (3.47)$$

This equation can be solved using the separation of variables methods and can be written in the form

$$T^+(x^+, y^+) = f(x^+) g(y^+) \qquad \ldots (3.17)$$

Using the above equation, equation (3.47) can be written as;

$$\frac{\mathrm{Re}}{4} \mathrm{Pr} \frac{1}{f} \frac{df}{dx^+} = \frac{1}{y^+ g} \frac{d^2 g}{dy^{+2}} = -\frac{9}{4}\gamma^2 \qquad \ldots (3.48)$$

where $(-\frac{9}{4}\gamma^2)$ is the separation constant.

From equation (3.48) the following equations can be obtains

$$\frac{df}{dx^+} + \frac{9\gamma^2}{2\,\mathrm{Re}\,\mathrm{Pr}} f = 0 \qquad \ldots (3.49)$$

And

$$\frac{d^2 g}{dy^{+2}} + \frac{9}{4}\gamma^2 y^+ g = 0 \qquad \ldots (3.50)$$

Equation (3.49) may be integrated to give

$$f = A_1 . \exp(-\frac{9\gamma^2}{2\,\mathrm{Re}\,\mathrm{Pr}} x^+) \qquad \ldots (3.51)$$

and equation (3.50) may be solved using the Bessel function [33] to gives The solution (see appendix B) as

$$g = \sqrt{y^+}[A_2 J_{1/3}(\gamma y^{+3/2}) + A_3 J_{-1/3}(\gamma y^{+3/2})] \qquad \ldots (3.52)$$

Thus the general solution is

$$T^+(x^+, y^+) = f.g = A_1 \exp(-\frac{9\gamma^2}{2\,\mathrm{Re}\,\mathrm{Pr}} x^+)[\sqrt{y^+}(A_2 J_{1/3}(\gamma y^{+3/2}) + A_3 J_{-1/3}(\gamma y^{+3/2})] \qquad \ldots (3.53)$$

where A_1, A_2 and A_3 are constants that can be found from boundary conditions.

Applying the boundary condition expressed by equation (3.10b) gives $A_2 = 0$ Since $J_{-2/3}(0) = \infty$, therefore equation (3.53) becomes

$$T^+(x^+, y^+) = A_3\sqrt{y^+}\,J_{-1/3}(\gamma\, y^{+3/2})\exp(-\frac{9\gamma^2}{2\,\mathrm{Re}\,\mathrm{Pr}}x^+) \qquad \ldots (3.54)$$

Satisfying the boundary condition at the vapor-liquid interface expressed by equation (3.10c) yields

$$A_3\sqrt{\delta^+}\,J_{-1/3}(\gamma\delta^{+3/2})\exp(-\frac{9\gamma^2}{2\,\mathrm{Re}\,\mathrm{Pr}}x^+) = 0 \qquad \ldots (3.55)$$

This requires the eigenvalues γ_n to be positive roots of $J_{-1/3}(\gamma\delta^{+3/2}) = 0$, from which it is found that

$$\gamma = \frac{1}{\delta^{+3/2}}(1.8664, 4.9879, 8.1243, 11.2635, 14.4038, 17.5445, \ldots) \qquad \ldots (3.56)$$

Thus it follows that any particular solution is of the form

$$T_n^+ = A_n\sqrt{y^+}\,J_{-1/3}(\gamma_n y^{+3/2})\exp(\frac{9\gamma_n^2}{2\,\mathrm{Re}\,\mathrm{Pr}}x^+) \qquad \ldots (3.57)$$

and the general solution is obtained by summing all possible solutions:

$$T_n^+ = \sqrt{y^+}\sum_{n=1}^{\infty}A_n J_{-1/3}(\gamma_n y^{+3/2})\exp(-\frac{9\gamma_n^2}{2\,\mathrm{Re}\,\mathrm{Pr}}x^+) \qquad \ldots (3.58)$$

The constant A_n are found from boundary condition at the flow inlet, equation (3.10a), thus

$$1 = \sqrt{y^+}\sum_{n=1}^{\infty}A_n J_{-1/3}(\gamma_n y^{+3/2}) \qquad \ldots (3.59)$$

Multiplying equation (3.54) by ($y^{+3/2} J_{-1/3}(\gamma_m y^{+3/2})$). Integrating from 0 to 1.0 and making use of the orthogonal properly [35] of the eigenfunctions (see appendix A) gives the value for A_n:

$$A_n = \frac{\int_0^1 y^{+3/2} J_{-1/3}(\gamma_n y^{+3/2}) dy^+}{\int_0^1 y^{+2} J^2_{-1/3}(\gamma_n y^{+3/2}) dy^+} = \frac{2}{\gamma_n J_{2/3}(\gamma_n)} \quad \ldots (3.60)$$

The temperature distribution is then finally found to be

$$T^+ = \sqrt{y^+} \sum_{n=1}^{\infty} \frac{2}{\gamma_n J_{2/3}(\gamma_n)} J_{-1/3}(\gamma_n y^{+3/2}) \exp(-\frac{9\gamma_n^2}{2\,\mathrm{Re}\,\mathrm{Pr}} x^+) \quad \ldots (3.61)$$

with $J_{-1/3}(\gamma_n \delta^{+3/2}) = 0$ as given by equation (3.56)

Using the above equation and equation (3.46) for velocity distribution into equation (3.32) the bulk temperature can be written as;

$$T_b^+ = \frac{\int_0^{\delta^+} 2y^+ \{\sqrt{y^+} \sum_{n=1}^{\infty} \frac{2}{\gamma_n J_{2/3}(\gamma_n)} J_{-1/3}(\gamma_n y^{+3/2}) \exp(-\frac{9\gamma_n^2}{2\,\mathrm{Re}\,\mathrm{Pr}} x^+)\} dy^+}{\int_0^{\delta^+} 2y^+ dy^+} \quad \ldots (3.62)$$

and by integrating this equation and after rearrangement the result becomes

$$T_b^+ = \frac{8}{3\delta^+} \sum_{n=1}^{\infty} \frac{J_{2/3}(\gamma_n \delta^{+3/2})}{\gamma_n^2 J_{2/3}(\gamma_n)} \exp(-\frac{9\gamma_n^2}{2\,\mathrm{Re}\,\mathrm{Pr}} x^+) \quad \ldots (3.63)$$

This equation represents the bulk temperature distribution in the liquid layer for this case.

The mass flow rate can be obtained, using equation (3.35) and after applying equation (3.46), yields

$$\dot{m}^{+} = \delta^{+2} \qquad \ldots (3.64)$$

By substitution equation (3.63) and equation (3.64) in to equation (3.6) and after rearrangement the resulting equation, becomes

$$\delta^{+} = \left\{ \exp[S\{1 - \frac{8}{3\delta^{+}} \sum_{n=1}^{\infty} \frac{J_{2/3}(\gamma_n \delta^{+3/2})}{\gamma_n^2 J_{2/3}(\gamma_n)} \exp(-\frac{9\gamma_n^2}{2\,\mathrm{Re}\,\mathrm{Pr}} x^{+}\}] \right\}^{\frac{1}{2}} \ldots (3.65)$$

The film thickness of the liquid layer for this case can be evaluates by this equation, and therefore the total mass flow rate and the condensation rate can be also evaluated.

Heat Transfer Coefficient:

The temperature gradient in the interface for this case can be determines using the derivative of equation (3.61) and written as;

$$\left.\frac{\partial T^{+}}{\partial y^{+}}\right|_{y^{+}=\delta^{+}} = -3\delta^{+} \sum_{n=1}^{\infty} \frac{J_{2/3}(\gamma_n \delta^{+2/3})}{J_{2/3}(\gamma_n)} \exp(-\frac{9\gamma_n^2}{2\,\mathrm{Re}\,\mathrm{Pr}} x^{+}) \qquad \ldots (3.66)$$

By substitution the above equation and equation (3.63) into equation (3.42) and simplified the result the local Nusselt number for this case becomes

$$Nu_x = \frac{9\delta^{+2}\sum_{n=1}^{\infty}\frac{J_{2/3}(\gamma_n\delta^{+3/2})}{J_{2/3}(\gamma_n)}\exp(\frac{-9\gamma_n^2}{2\,\mathrm{Re}\,\mathrm{Pr}}x^+)}{8\sum_{n=1}^{\infty}\frac{J_{2/3}(\gamma_n\delta^{+3/2})}{\gamma_n^2 J_{2/3}(\gamma_n)}\exp(\frac{-9\gamma_n^2}{2\,\mathrm{Re}\,\mathrm{Pr}}x^+)} \quad \ldots (3.67)$$

Using this equation the local Nusselt number in the liquid layer along the flow direction can be obtained.

3.2.3 Analysis with Semi-Parabolic Velocity Profile

Semi-parabolic velocity profile (Nusselt velocity profile) is assumed to describe the velocity distribution when the flow is driven by gravity force, it can be written as

$$u(y) = \frac{g}{\nu}(y\delta - \frac{y^2}{2}) \qquad 0 \le y \le \delta(x) \quad \ldots (3.68)$$

using the dimension less form it can be written as

$$u^+ = 3(y^+\delta^+ - \frac{1}{2}y^{+2}) \qquad 0 \le y^+ \le \delta^+ \quad \ldots (3.69)$$

By using equation (3.9) the flowing equation can be obtains

$$\frac{\mathrm{Re}}{4}\mathrm{Pr}\left\{3(y^+\delta^+ - \frac{1}{2}y^{+2})\right\}\frac{\partial T^+}{\partial x^+} = \frac{\partial^2 T^+}{\partial y^{+2}} \quad \ldots (3.70)$$

The analytical solution for this type of differential equation is very complicated therefore; a numerical procedure is developed to solve this equation. That was development of the numerical procedure adopted by El-Ariny and Aziz [37], for the case of heat transfer in plane Couette flow.

Utilizing the method of separation of variables by writing $T^+ = f(x^+).g(y^+)$, equation (3.70) can be separated into

$$\frac{\mathrm{Re}}{4}\mathrm{Pr}\frac{1}{f}\frac{df}{dx^+} = \frac{1}{u^+ g}\frac{d^2 g}{dy^{+2}} = -\beta \qquad \ldots (3.71)$$

Where $(-\beta)$ is the arbitrary constant of separating of variables.

From equation (3.71) one can obtains

$$\frac{df}{dx^+} + \frac{4\beta}{\mathrm{Re}\,\mathrm{Pr}} f = 0, \qquad \ldots (3.72)$$

$$\frac{dg^2}{dy^+} + \beta u^+ g = 0 \qquad \ldots (3.73)$$

the solution of equation (3.72) can be found as

$$f = C_1 \exp(-\frac{4\beta}{\mathrm{Re}\,\mathrm{Pr}} x^+) \qquad \ldots (3.74)$$

while equation (3.73) can be solve numerically.

The central finite different formula [34] for the second derivative of the eigefunction ($g(y^+)$) can be formulated as following (figure (3.3))

$$\left.\frac{d^2 g}{dy^{+2}}\right|_i = \frac{g_{i+1} - 2g_i + g_{i-1}}{(\Delta y^+)^2} \qquad \ldots (3.75)$$

writing the differential equation (3.73) using the above equation, with grid size (Δy^+), one obtains for point i (figure (3.4)).

$$\frac{1}{(\Delta y^{+2})}(g_{i-1} - 2g_i + g_{i+1}) = -\beta\, g_i u_i^+ \quad \ldots (3.76)$$

where

$$\Delta y^+ = \frac{\delta^+}{n} \quad \ldots (3.77)$$

n =Number of grid

Rearrangement of equation (3.76) gives

$$-D_i g_{i-1} + 2D_i g_i - D_i g_{i+1} = \beta\, g_i \quad \ldots (3.78)$$

i=1,2,3,……,n

with

$$D_i = \frac{1}{(\Delta y^+)^2 u_i^+} \quad \ldots (3.79)$$

Applying equation (3.78) for *n* points, a set of algebraic equations is obtains as

Node number	*finite different equation*	
1	$D_1(-g_o + 2g_1 - g_2) = \beta\, g_1$	… (3.80)
2	$D_2(-g_1 + 2g_2 - g_3) = \beta\, g_2$	
3	$D_3(-g_2 + 2g_3 - g_4) = \beta\, g_3$	
⋮	⋮	
n	$D_n(-g_{n-1} + 2g_n - g_{n+1}) = \beta\, g_n$	

From the boundary condition at the solid surface equation (3.10b) one can obtain that

$$\frac{dg}{dy^+} = \frac{g_2 - g_o}{2\Delta y^+} = 0 \qquad \ldots (3.81)$$

this equation leads to $g_2 = g_o$.

The finite difference equations can be written in the matrix form as shown in equation (3.82).

$$\begin{bmatrix} 2D_1 & -2D_1 & 0 & 0 & 0 & . & . & 0 & 0 & 0 \\ -D_2 & 2D_2 & -D_2 & 0 & 0 & . & . & 0 & 0 & 0 \\ 0 & -D_3 & 2D_3 & -D_3 & 0 & . & . & . & . & 0 \\ 0 & 0 & -D_4 & 2D_4 & -D_4 & . & . & . & . & 0 \\ . & . & . & . & . & . & . & . & . & \\ . & . & . & . & . & . & . & . & . & \\ 0 & . & . & . & . & . & -D_{n-1} & 2D_{n-1} & -D_{n-1} & \\ 0 & 0 & . & . & . & . & 0 & -D_n & 2D_n & \end{bmatrix} \begin{bmatrix} g_1 \\ g_2 \\ g_3 \\ g_4 \\ . \\ . \\ g_{n-1} \\ g_n \end{bmatrix} = \beta \begin{bmatrix} g_1 \\ g_2 \\ g_3 \\ g_4 \\ . \\ . \\ g_{n-1} \\ g_n + \frac{D_n}{\beta} g_{n+1} \end{bmatrix}$$

$\ldots$ (3.82)

where g_{n+1} is to be determined from boundary condition at the interface surface equation (3.10c).

Equation (3.82) can be also written as

$$\mathbf{Dg} = \beta \mathbf{g} \qquad \ldots (3.83)$$

where **D**, represent the coefficient matrix and ***g***, represent the eigenvectors.

The solution of equation (3.70) can be written using the above equation and equation (3.74), as

$$T_i^+ = \sum_j C_j g_{ij} \exp(-\frac{4\beta_j}{\mathrm{Re\,Pr}} x^+) \quad \ldots (3.84)$$

In this equation, g_{ij} is the ith element of jth eigenvector. The eigenvalues (β_j) are obtained from ***D*** matrix.

Subsequently, the corresponding eigenvectors are determined by solving the system of equations (equation (3.82)) for each eigenvalue.

To determine C_j, the forgoing is applied to the transpose of D i.e., D^t. The eigenvectors of D and D^t possess the orthogonal property [37] and thus, applying the boundary condition at the inlet of flow, equation (3.10a) at point i, that is $x^+ = 0, T^+ = 1$, the coefficient C_j can be obtained and written as

$$C_j = \frac{\sum_{i=1}^{n} h_{ij}}{\sum_{i=1}^{n} h_{ij} g_{ij}} \quad \ldots (3.85)$$

where h_{ij} represents the ith element of the jth eigenvectors of $\boldsymbol{D}^t$. By applying equation (3.85) and the eigenvalues (β_j) in the equation (3.84) it becomes

$$T_i^+ = \sum_{j=1}^{n} \left[\frac{\sum_{i=1}^{n} h_{ij}}{\sum_{i=1}^{n} h_{ij} g_{ij}} \right] g_{ij} \exp(-\frac{4\beta_j}{\mathrm{Re\,Pr}} x^+) \quad \ldots (3.86)$$

The bulk temperature T_b^+ is next calculated according to its definition

$$T_b^+ = \frac{\int_0^{\delta^+} u^+ T^+ dy^+}{\int_0^{\delta^+} u^+ dy^+} \quad \ldots (3.32)$$

To determine T_b^+ the numerator in this equation was integrated using Simpson's rule.

The dimensionless mass rate is determined using the velocity profile equation (3.69) and equation (3.35), thus

$$\dot{m}^+ = \delta^{+3} \quad \ldots (3.87)$$

The film thickness is found by substitution of the bulk temperature T_b^+ that was calculated from previously step, into equation (3.6) and by using equation (3.87) it can be written as

$$\delta^+ = \left[\exp\{S(1-T_b^+)\}\right]^{\frac{1}{3}} \quad \ldots (3.88)$$

To this point both the bulk temperature and condensate film thickness can be calculate ,also the total mass flow rate and the condensation rate can be calculated numerically.

Heat Transfer Coefficient

The local Nusselt number for this case are obtain using equation (3.42), that is

$$Nu_x = -\frac{1}{T_b{}^+}\frac{\partial T^+}{\partial y^+}\bigg|_{y^+=\delta^+} \quad \ldots (3.42)$$

The derivative of the temperature distribution used in this equation is obtain by using polynomial fitted to previously computed T_i^+ values from equation (3.86), and by substitution of the value of δ^+ that evaluated from equation (3.88) in the derivative and using the above equation, the local Nusselt number can be evaluates.

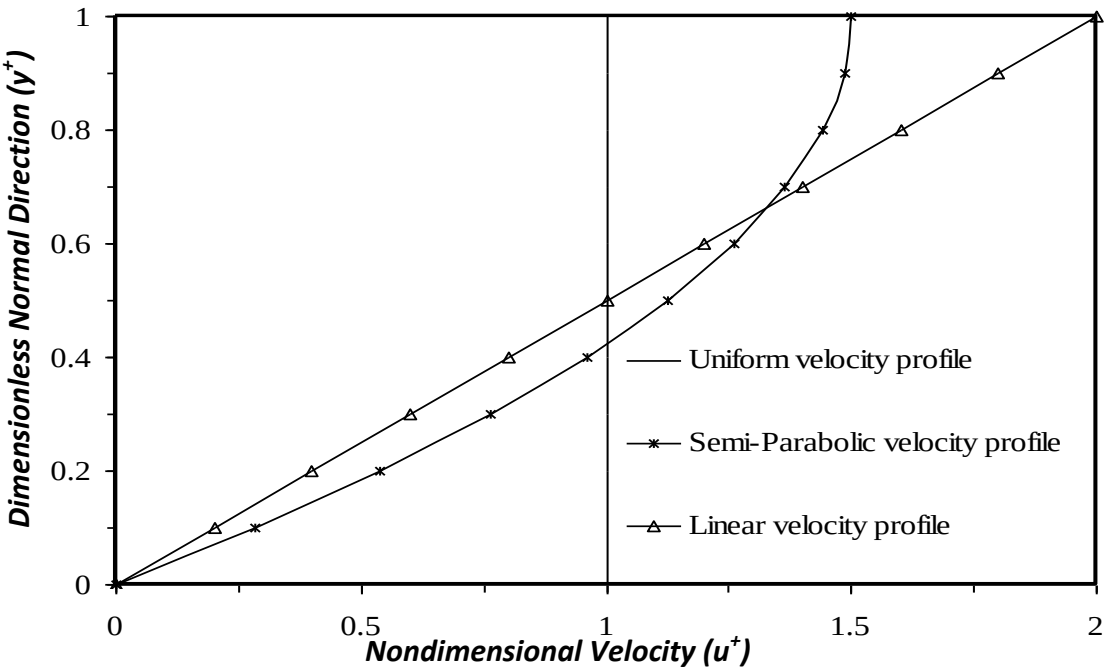

Figure(3.2) Dimensionless Velocity Profiles(X^+=0.0)

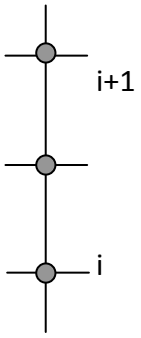

Figure (3.3) Arrangement of Grid point

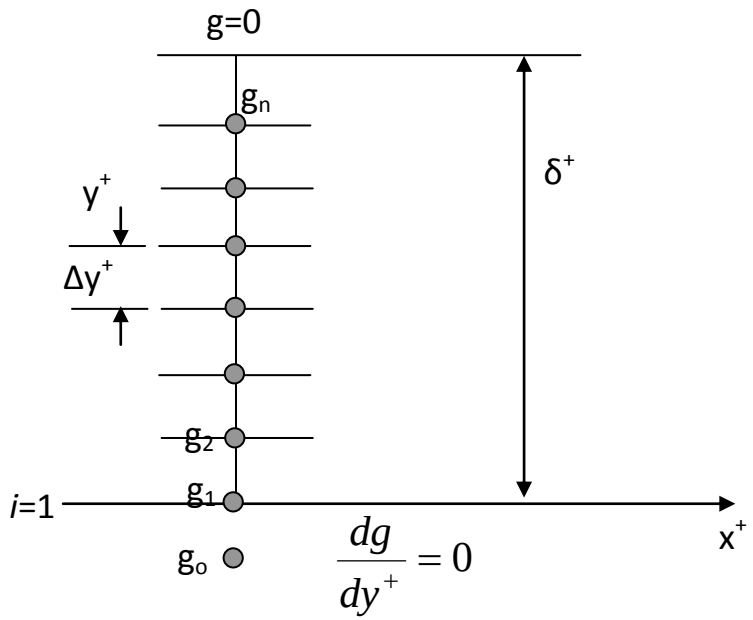

Figure (3.4) The mesh of the Numerical solution

Chapter Four

RESULTS AND DISCUSSION

Chapter Four

RESULTS AND DISCUSSION

In order to investigate the direct contact condensation process, the obtained equations are solved for the important parameters of this process, these are the local Nusselt number, bulk temperature of liquid layer and the local film thickness in the flow direction. The evaluation of these parameters is essential for designing and applications of the direct contact condensation systems. The previous investigations of the direct contact condensation on laminar smooth film were based on two simplified assumptions.

The first was the velocity profile of liquid layer is assumed to be constant in the two direction of flow when it is employed in the energy equation. The second assumption was the temperature gradient used in the energy equation in the direction of the flow is independent on the normal coordinate to the flow, so that it was easy to solve the problem using these assumptions. In this study, the velocity profile in the liquid layer and the temperature gradient are taken as a variable (i.e. actual velocity and temperature profile), therefore in some cases a completely different methods are used to obtain the solution. Three types of velocity profiles of the liquid layer are used in this analysis to show the difference between the value of the various condensation parameters obtained using the three present models, and to find which type of velocity profile gives the best performance.

The procedure followed in this chapter includes separate presentation of the results and discussion of each model which corresponds to one type of velocity profile and the comparison between

the most important condensation parameters. In addition a comparison between the present theoretical work (for linear case) and the theoretical work deduced by Mikielewicz and Rageb [7], and (for semi-parabolic case) with the theoretical and experimental results obtained by Al-Salman [9] are also performed.

4.1 Direct Contact Condensation on a Liquid Layer Flowing with Uniform Velocity Profile

The solution of the mathematical model for this case was carried out analytically and the calculation was done using computer program (see flow chart in the appendix C). Different important parameters, which control the efficiency of the condensation process, were taken as variables in this study. These parameters are Prandtl number (Pr), Reynolds number (Re) and the subcooling number (S). The values of these parameters were chosen according to the more common cases of condensation on laminar fully developed flow, which exist in the literature. Also these value agree with the experimental evidence and observations. The range of these parameters are:

1- Prandtl number (Pr) vary from 1.0 to 6.0.
2- Reynolds numbers (Re) vary from 400 to 1500.
3- Subcooling number (S) vary from 0.025 to 0.15.

4.1.1 Local Nusselt Number

The theoretical predication of the local Nusselt number for this case obtains by using equation (3.44). The variation of the local Nusselt number with axial distance in direction of flow is shown on Figures 4.1 to

4.3. The general trend, which is clear in these figures, is the decrement of Nusselt number along the axial distance. This may be occurs due to the increment of condensate layer thickness that accompanied by increment the resistance to heat transfer. The effect of condensation controlling parameter (Pr, Re, S) can be explained as:

i. Effect of Prandtl Number on the Local Nusselt Number:

Figure 4.1 shows the relation between the local Nusselt number and the axial distance for various values of Prandtl number (for constant condensation parameter Re and S). From this figure it is observed that the value of local Nusselt number decreases with the axial distance a long the flow for all the selected Prandtl number. For fixed axial distance a long the flow, the increment of Prandtl number leads to increases the heat transfer coefficient and so that the local Nusselt number increases. That may be attributed to the variation of the thermal properties of the liquid caused by the variation of Prandtl number ($\Pr = \frac{\nu}{\alpha}$, where ν, characterizes the fluids transport properties with respect to the transport of momentum and α, doing the same for the transport of heat [38]). Also, from this figure it noted that all the curves are converge after a distance from the inlet in the flow direction because of the elevation of the liquid temperature that leads to reduce condensation process.

ii. Effect of Reynolds Number on the Local Nusselt Number:

The effect of the Reynolds number on the variation of the local Nusselt number with the axial distance (while the other parameter are kept constant) are shown in figure 4.2. As it is obvious from this figure,

Nusselt number decreases with the increment of axial distance and at fixed axial position along the flow, for various value of Reynolds number it can noted that the increase of Reynolds number gives increment in the Nusselt number. This increment may be due to the increment of the mass flow rates, which increase the heat capacity and the initial film thickness.

iii. Effect of Subcooling on the Local Nusselt Number:

Figure 4.3 shows the effect of subcooling number on the local Nusselt number, while the other parameters are kept constant. The local Nusselt number decreases with the axial distance for various value of subcooling number. The Nusselt number is defined by ($h\delta_o / k$), therefore, its value depends on the value of ($h\delta_o$). However, the variation of heat transfer coefficient (h) is vary small with various subcooling number (equation 3.40) and δ_o is independent on the subcooling temperature (T_o), therefore effect of subcooling number has negligible effect on the local Nusselt number.

4.1.2 Local Dimensionless Bulk Liquid Temperature

The evaluation of the local dimensionless bulk temperature (T_b^+) of the liquid layer flowing with uniform velocity profile is obtained from equation (3.33). The change of T_b^+ with the axial distance along the flow direction due to condensation at the vapor-liquid interface is shown in figure (4.4) to (4.6) for different selected condensation parameters.

The general tend in these figure is the reduction of T_b^+ (from initial unity value at the beginning of flow) with x^+. This reduction in the bulk liquid temperature is due to the heat gained by the liquid phase as a result

of condensation process. The effect of the condensation parameters on the local bulk temperature are given as:

i. Effect of Prandtl Number on the Local Bulk Temperature:

Figure 4.4 gives the effect of Prandtl number on the dimensionless bulk temperature (keeping the other parameters Re and S constant). The increment in the Prandtl number is accompanied by substantial increase in the dimensionless bulk temperature. This increment may be due to increase the momentum transport properties as Prandtl number increase, that leads to increase the heat transfer from vapor.

ii. Effect of Reynolds Number on the Local Bulk Temperature:

Figure 4.5 clearly shows the influence of Reynolds number of the liquid layer, when all other condensation parameters (Pr and S) are constant, on the dimensionless bulk temperature. As Reynolds number increases, the dimensionless bulk temperature increases. This is related to the higher initial film thickness δ_o and liquid mass flow rate.

iii. Effect of Subcooling Number on the Dimensionless Bulk Temperature:

No substantial influence of the subcooling number on the dimensionless bulk temperature along the axial distance is observed as it is shown in figure 4.6. This occurs because the subcooling number is behaving as a potential of condensation which dependent on the subcooling inlet temperature. And since both the subcooling number and dimensionless bulk temperature are two parameters defined relative to the

inlet temperature (equation (3.5b,d)). The influence of the subcooling number on the bulk temperature will not appear when it is defined in dimensionless form.

4.1.3 Dimensionless Film Thickness

The dimensionless film thickness (δ^+) along the condensation line for the case uniform velocity profile is calculated by equation (3.37). The variation of dimensionless film thickness with the axial distance are indicates in figures 4.7 to 4.9 for different selected parameters (Pr, Re and S). The general behavior that observed in these figures is the increment of the dimensionless film thickness along the flow direction. This increment is due to the continuous condensation process at the vapor-liquid interface.

i. Effect of Prandtl Number on the Dimensionless Film Thickness:

Figure 4.7 shows the variation of the dimensionless film thickness with the axial distance for various values of Prandtl number where the other controlling parameters (Re and S) are kept constant. It is noted that the dimensionless film thickness decreases for increases of the Prandtl number. This may be due to the decreases in the thermal diffusivity for the liquid layer that leads to reduce the ability of liquid to condesate vapor.

ii. Effect of Reynolds Number on the Dimensionless Film Thickness:

Figure 4.8 shows the effect of the liquid layer Reynolds number on the dimensionless film thickness, as one would expect the dimensionless film thickness is decreasing with increasing Reynolds number of the

liquid layer when the major system parameters Pr, S are kept constant. This is attributed to the more rapid growth of initial film thickness δ_o than the local film thickness of the liquid layer due to the condensation as Reynolds number increases.

iii. Effect of Subcooling Number on the Dimensionless Film Thickness:

The influence of the subcooling number on the dimensionless film thickness is demonstrated in figure (4.9), while the other parameters (Pr and Re) are kept constant. This figure indicates that the increase in the subcooling number is accompanied by increasing in the dimensionless film thickness. This may be due to the fact the subcooling number acts during condensation as a potential of condensation and therefore, the increment of the subcooling number increase the ability of liquid to condensate vapor which leads to increase the dimensionless film thickness.

The dimensionless liquid mass flow rate for this case have the same behavior and trend as the dimensionless film thickness which can be observed from equation (3.36).

4.2 Direct Contact Condensation on Liquid layer Flowing with Linear Velocity Profile

Analytical method was used to solve the mathematical model for this case; the calculation was carried out using computer program (see flow chart in appendix D). The evaluation of the condensation result are obtained for the local Nusselt number, equation (3.67), dimensionless bulk temperature, equation (3.63), and the dimensionless film thickness,

equation (3.65). The main governing condensation parameters in this case are also Prandtl number, Reynolds number and Subcooling number. These parameters are selected and used in the calculation are the same as those used in the first case. The influence of each one of these parameters on condensation characteristics were the other parameter are kept constant, are demonstrated in figure 4.10 – 4.18.

From these figure it is very obvious that the local Nusselt number, dimensionless bulk temperature and the dimensionless film thickness have the same trends as that for the case of uniform velocity profile. At the same times, the dimensionless velocity at the vapor – liquid interface becomes higher for the linear velocity profile case in comparison with the other velocity cases (Fig. 3.2). Therefore the local Nusselt number shown in figures (4.10 – 4.12) become high due to increase the interfacial velocity between the two phase, which lead to increase the heat transfer rate. The dimensionless bulk temperature is reduce as shown in figures (4.12 – 4.14) due to enhancement of the heat transfer through the vapor-liquid interface. The dimensionless liquid mass flow rate is calculated using equation (3.64) is increasing due to increase the ability of liquid to absorb heat from vapor and condensate the vapor. The dimensionless film thickness decrease with increase the velocity for this case as shown figures (4.15 –4.18) since it is proportional to square root of the dimensionless mass flow rate (equation (3.64)).

4.3 Direct Contact Condensation on Liquid Layer Flowing with Semi-Parabolic Velocity Profile

Numerical calculations of the theoretical model for this case are done according to the numerical solution given in section (3.2.3), using

the computer program (see flow chart appendix E). The grid size used is $\Delta y^+ = (\delta^+ / 12)$. The number of eigenvalues equals to the number of unknown temperatures at grid points. To assess the accuracy of the developed procedure, the numerical solution for the dimensionless temperature distribution obtained with grid size of $\Delta y^+ = (\delta^+ / 12)$ was compared with the analytical solution of the uniform case, equation (3.31). The comparison is shown in figure (4.28). Excellent agreement was obtained which indicated high accuracy of the present developed procedure. The local Nusselt number, dimensionless bulk temperature and the dimensionless film thickness are evaluated based on the numerical method. The controlling condensation parameters are also Prandtl number, Reynolds number and Subcooling number and selected as the same that use in the previous cases. The effect of each one of these parameters on the condensation results were all other parameters are constant, are shown in figures 4.19-4.27.

From these figures the same trends as in the previous case can be observed for the local Nusselt number, dimensionless bulk temperature and the dimensionless film thickness. Also, from utilized figure (3.2) we can see that the interfacial velocity between the liquid vapor phases for this case is large than the velocity in the uniform flowing case but smaller than the linear one. Which may be the reason for that the value of local Nusselt number (figs.4.19-4.21) become higher than for uniform velocity but less than that for linear velocity profile. The dimensionless bulk temperature (figs.4.22-4.24) and the dimensionless mass flow rate values are in between the uniform and semi-parabolic velocity profiles. That may be due to the same reasons discussed in previous cases. The dimensionless

film thickness (figs.4.25-4.27) decease in comparison with the uniform case since it is proportional to the cubic root of the dimensionless mass flow rate (equation (3.87)).

4.4 The Comparison Between the Present Models Using the Three Types of Velocity Profiles

The important aspect of the analysis is the study of the effect of flow velocity profile of the liquid layer on the condensation characteristics during the condensation process, so the comparison of the results of each model with the other can clarified the fact of the velocity profiles.

In this study, it is evident from the previous sections and by utilized figure (3.2), that there is difference in the condensation rate of the vapor for different velocity cases. That may be attributed to the different of the velocity gradient at the vapor-liquid interface. Also, the velocity gradient may have an effect on the shear stress at the vapor-liquid interface. The interfacial shear stress, which increases with increasing the velocity gradient, enhances the condensation process.

The comparison between the local Nusselt number, dimensionless bulk temperature and the dimensionless mass flow rate of the three cases of flowing velocity profile which employed in this study are illustrate in figure 4.29-4.31 (while the controlling parameter are kept constant as (Pr=1.0, Re=1000, S=0.1).

The effect of velocity profile of the liquid layer on the local Nusselt number is shown in figure 4.29. From this figure, one can be noticed that the local Nusselt number increases, as velocity at the surface of liquid layer ($u^{+}_{y^{+}=\delta^{+}}$) become higher. This effect may be due to the increasing in

the heat exchanging between the vapor and liquid phase, that leads to increase the heat transfer coefficient of the condensation process and so the local Nusselt number.

Figure 4.30 is drawn to show the effect of ($u^+_{y^+=\delta^+}$) on the dimensionless bulk temperature, which declare that higher value of ($u^+_{y^+=\delta^+}$) lead to a lower value of the dimensionless bulk temperature. This may be due to increasing in the heat transfer coefficient when interfacial velocity increases and that lead to reduce the dimensionless bulk temperature.

The dimensionless liquid mass flow rate increase with increasing ($u^+_{y^+=\delta^+}$) as shown in figure (4.31). The dimensionless film thickness may be decrease since it dependent on the different root of the dimensionless mass flow rate for each case of velocity. The increasing in the dimensionless mass flow rate may be due to increasing the heat transfer through the vapor-liquid interface, leading to increasing the ability of liquid to absorb heat from vapor and condensations it.

4.5 Comparison the Results of the Present Model with the Previous Approximate Theoretical Works.

The results of the present model (for linear case) were compared with that obtained by Mikielewicz and Rageb [7] as in figures 4.32 and 4.33. Taking the same condensation parameters (Pr=10. Re=1600,S=0.125).

Figure 4.32 shows the comparison between the local Nusselt number for both studies and figure 4.33 shows the comparison for local film thickness.

From these figure similar trend is observed for both local Nusselt number and local film thickness obtained from both the present model and from [7].

It is clear that the local Nusselt number for the present work is slightly smaller, which may be due to the fact that model [7] did not consider the effect of the velocity distribution and temperature gradient through the liquid film on the condensation process and depends on the average values.

Also the local film thickness is slightly higher in comparison with the local film thickness obtained by [7]. That may be related to the same previous reason. In general the comparison between the results of these two models shows good agreement.

Also the present model results (for semi-parabolic case) is compared with the theoretical work of Al-Salman [9] as shows in figures 4.34 and 4.35. The input data was (a=0.2, L^{+}=80,S=0.125) and taken for two cases of Peclet number (Pe=500 and Pe=4000). The figure (4.34) shows a difference about 20٪ since that model was developed for wavy flow. The agreement between the results of the two models is a satisfactory.

In figure 4.35 the local mass flow rates evaluated using the present model was compared with that obtained from Al-Salman results. From this figure, similar trend and good agreement between the results are obtained.

4.6 Comparison the Results of the Present Model with the Experimental Results of the others.

In order to prove the validity of the present model, the results obtained were compared with experimental data corresponding to the cocurrent flow on a vertical channel {2m long, 0.3m wide, and 0.08m high}, obtained by Al-Salman[9].

The local heat transfer coefficients for semi-parabolic case predicated from the present model were compared with the experimental data of Al-Salman[9] in figures 4.36-4.37 .The theoretical results obtained from the present model is based on condensation parameters obtained from the experimental data, These calculated parameters are used as input data to the theoretical model.

Figure 3.36 corresponds to the experimental data: m_o=0.0694 kg/s, T_o=32^{o}C and a=0.2,while figure 3.37 is drawn for the same data except m_o=0.0833 kg/s and a=0.26.

It is obvious from these figures, that a similar trend is achieved for both the experimental data and the result of the present model. The shift of the experimental data above the result of the present model may be attributed to the fact that the experimental data is concerned the case of a wavy flow, which enhances the heat transfer coefficients.

The shift between the experimental data and the result of the present model can be noticed to be constant, so the result of the present model can be multiplied by a factor to agree with the experimental data, this mean that this present model can be used to take into account the effect of the wavy flow.

Concerning the dimensionless mass flow rate, figure 3.38 shows the comparison between the experimental and theoretical mass flow rate

calculated using the present analysis. This figure shows a good agreement between the predicted mass flow rate compared with the experimental one. That proves the validity of using the present model.

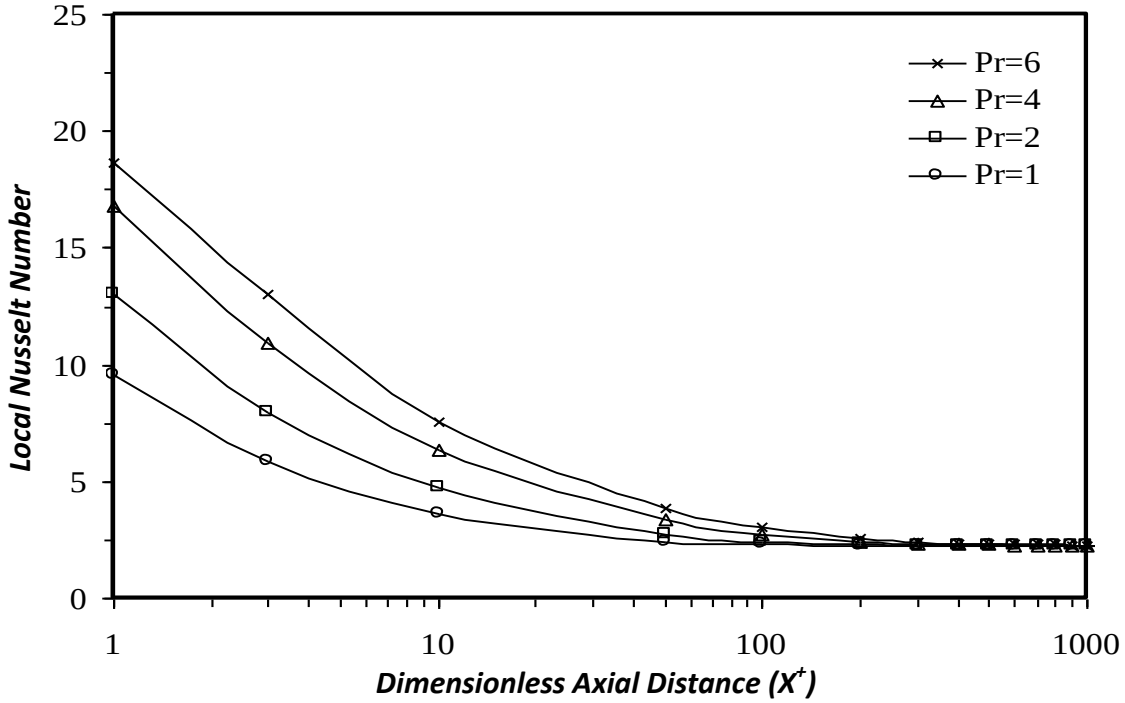

Fig. 4.1 Effect of Prandtl Number on the Local Nusselt Number (uniform velocity profile) Re=1000 S=0.1 .

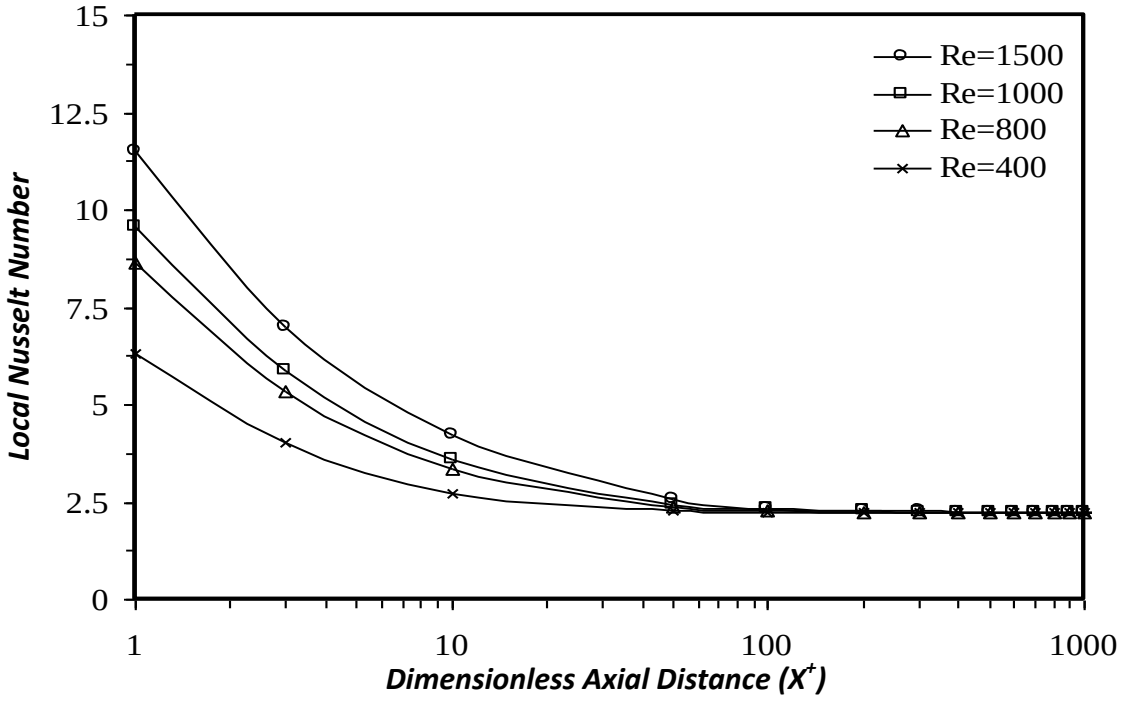

Fig. 4.2 Effect of Reynold Number on the Local Nusselt Number (uniform velocity profile) Pr=1. S=0.1 .

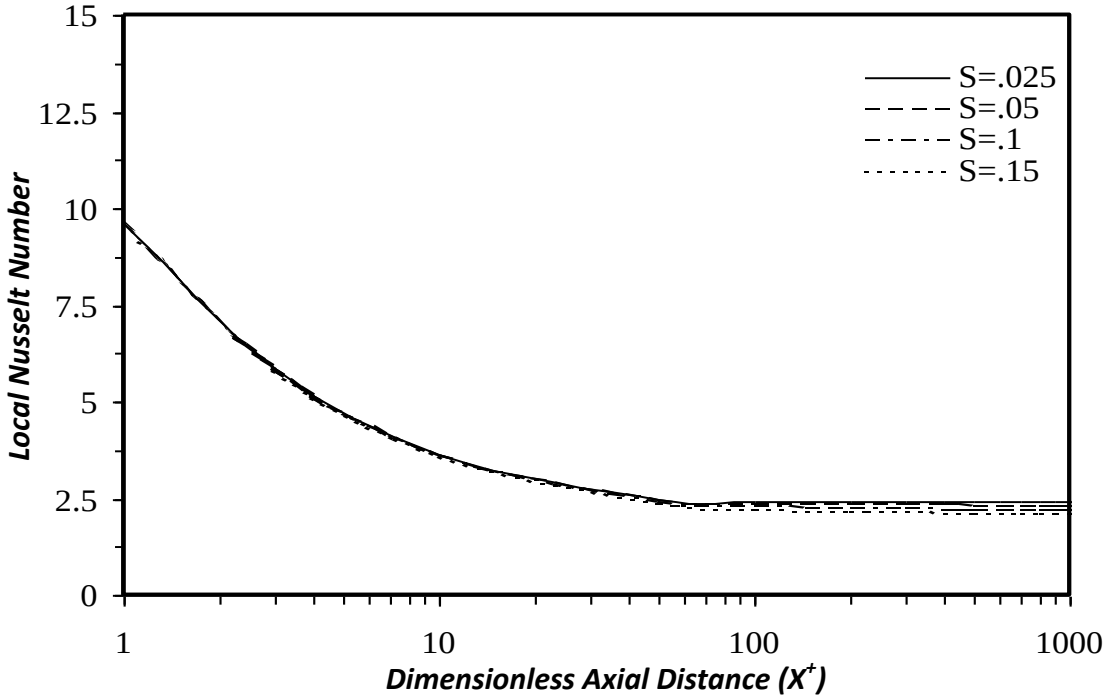

Fig. 4.3 Effect of Subcooled Number on the Local Nusselt Number (uniform velocity profile) Re=1000 Pr=1 .

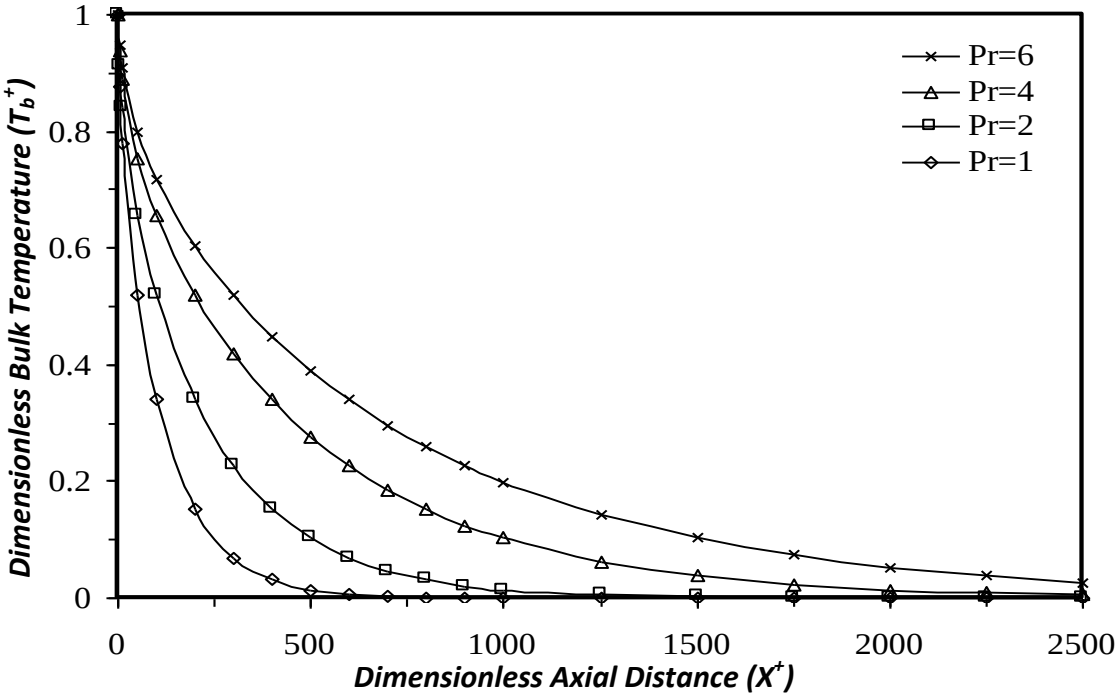

Fig. 4.4 Effect of Prandtl Number on the Local Dimensionless Bulk Liquid temperature (uniform velocity profile) Re=1000 S=0.1 .

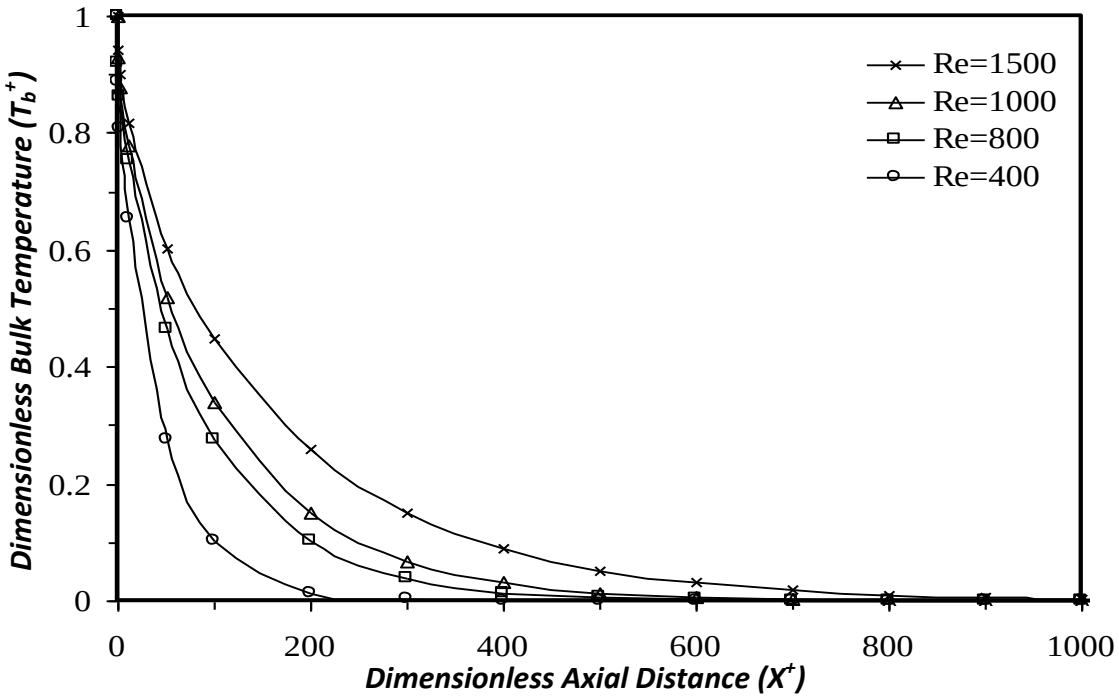

Fig. 4.5 Effect of Reynold Number on the Local Dimensionless Bulk Liquid temperature (uniform velocity profile) Pr=1. S=0.1 .

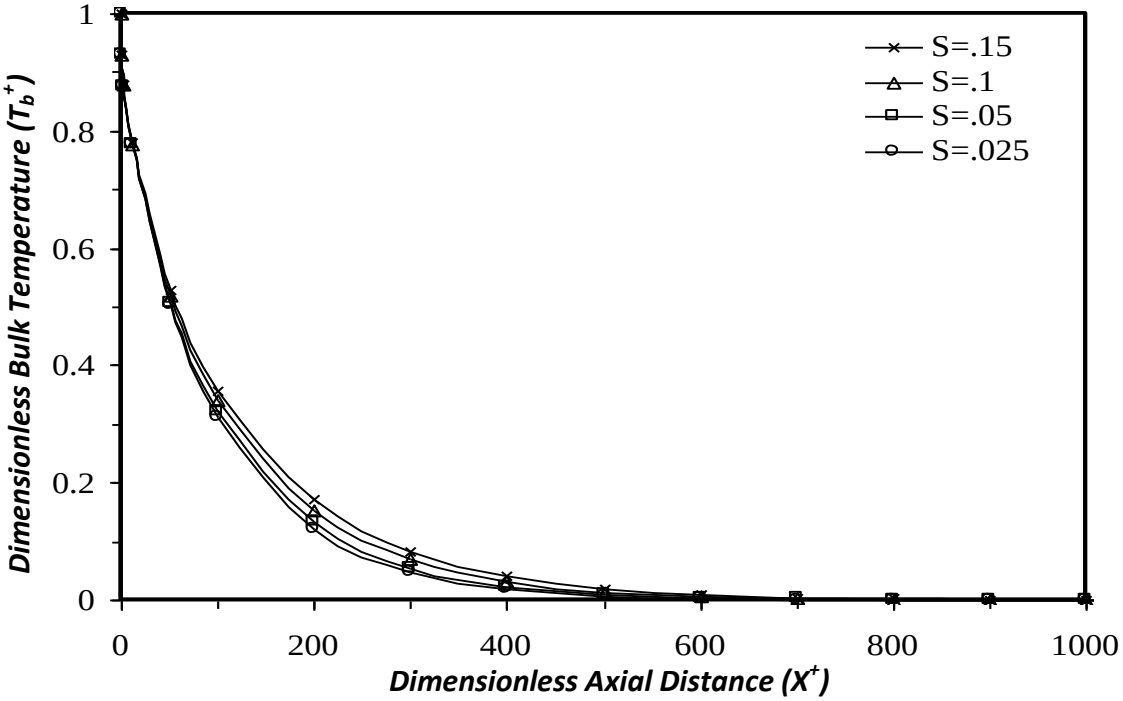

Fig. 4.6 Effect of Subcooling Number on the Local Dimensionless Bulk Liquid temperature (uniform velocity profile) Re=1000 Pr=1.0 .

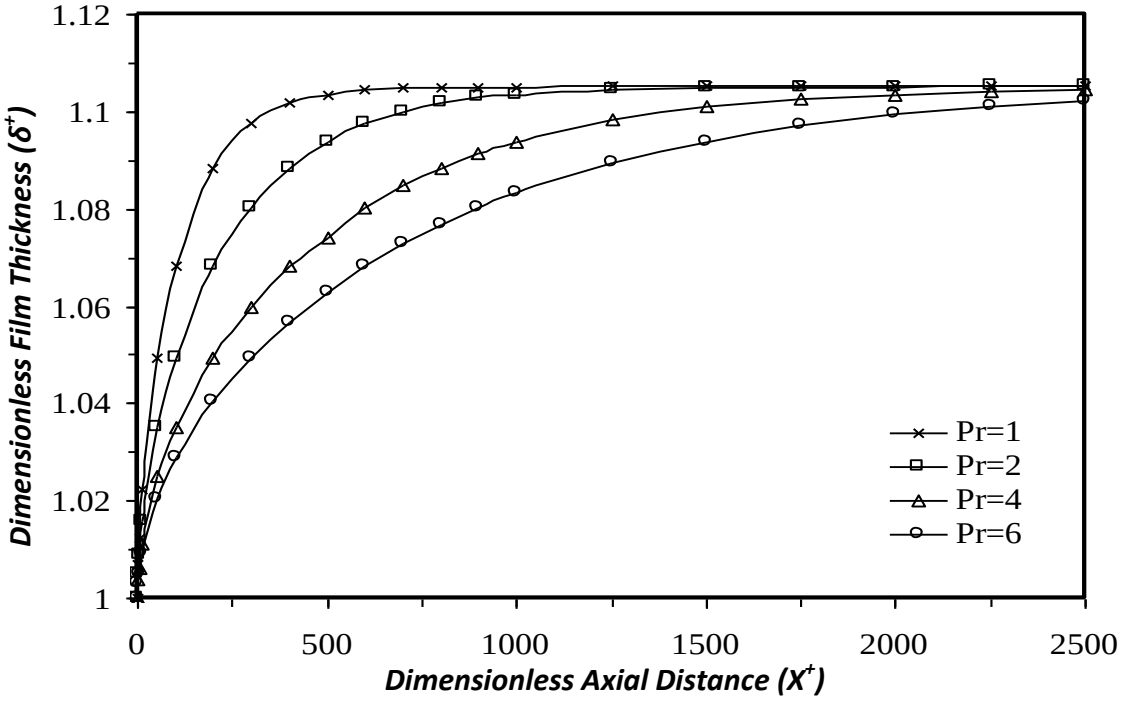

Fig. 4.7 Effect of Prandtl Number on the Local Dimensionless Film Thickness (uniform velocity profile) Re=1000 S=0.1 .

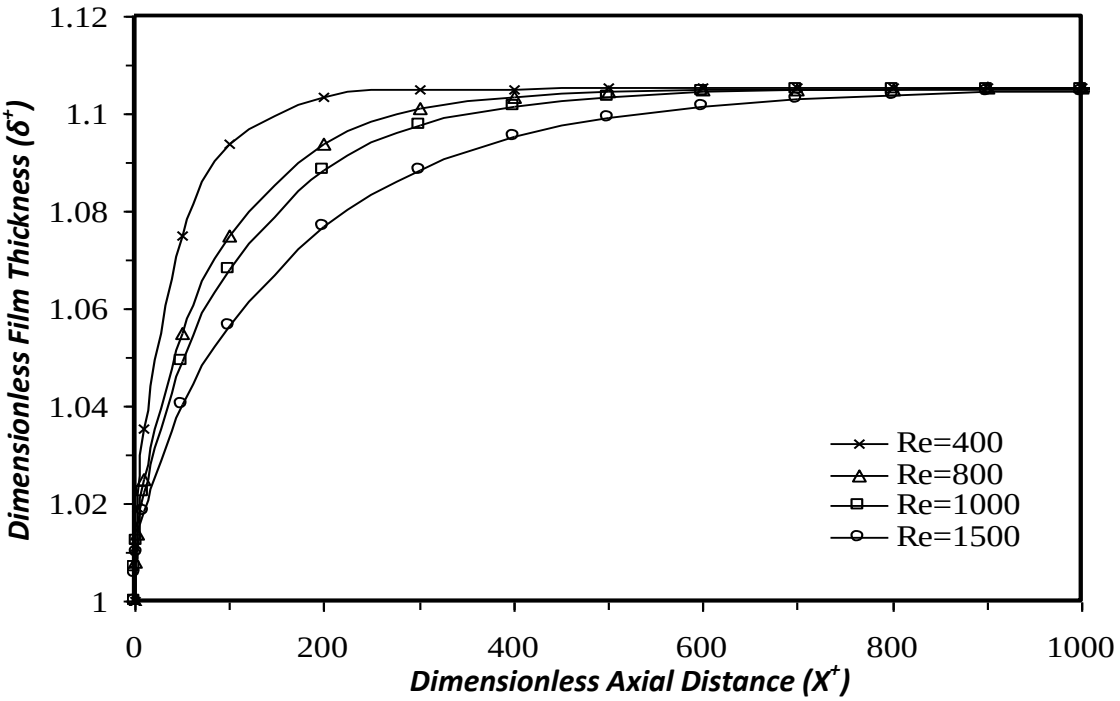

Fig. 4.8 Effect of Reynold Number on the Local Dimensionless Film Thickness (uniform velocity profile) Pr=1. S=0.1 .

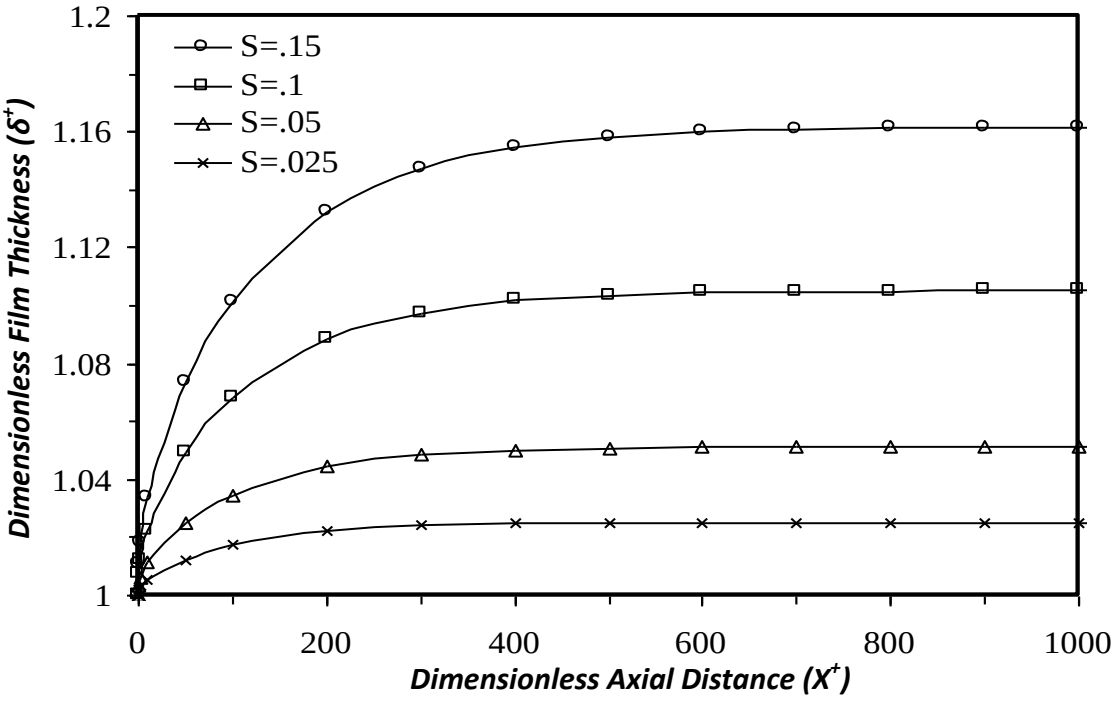

Fig. 4.9 Effect of Subcooling Number on the Local Dimensionless Film Thickness (uniform velocity profile) Re=1000 Pr=0.1 .

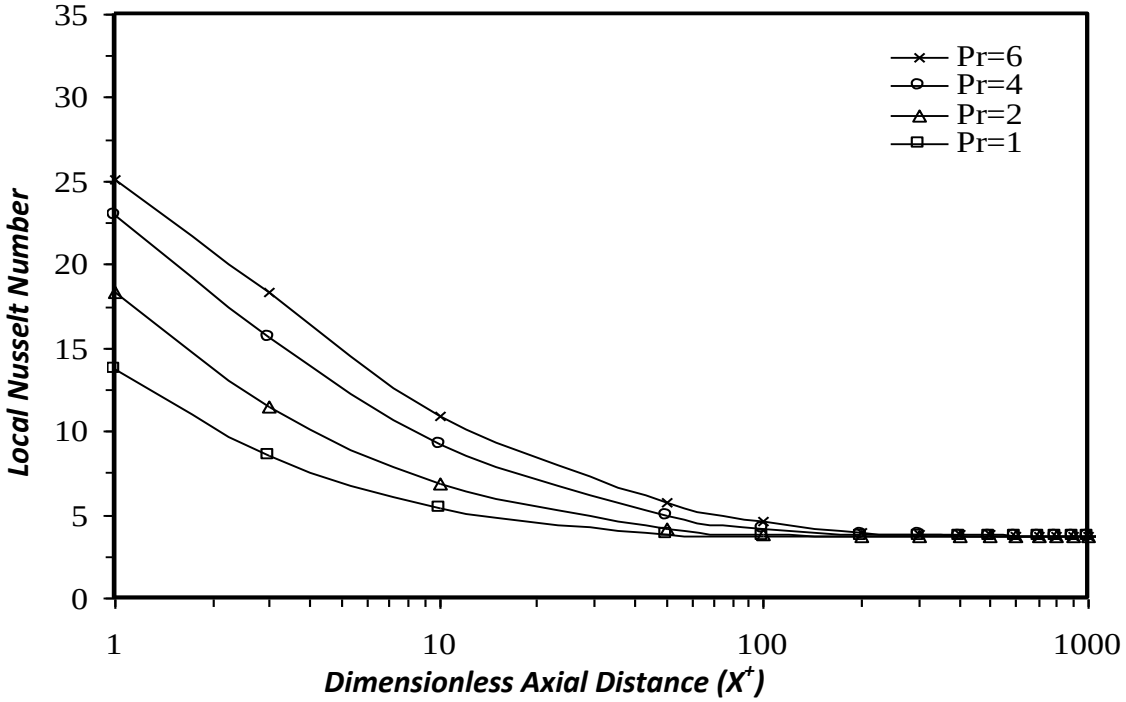

Fig. 4.10 Effect of Prandtl Number on the Local Nusselt Number (linear velocity profile) Re=1000 S=0.1 .

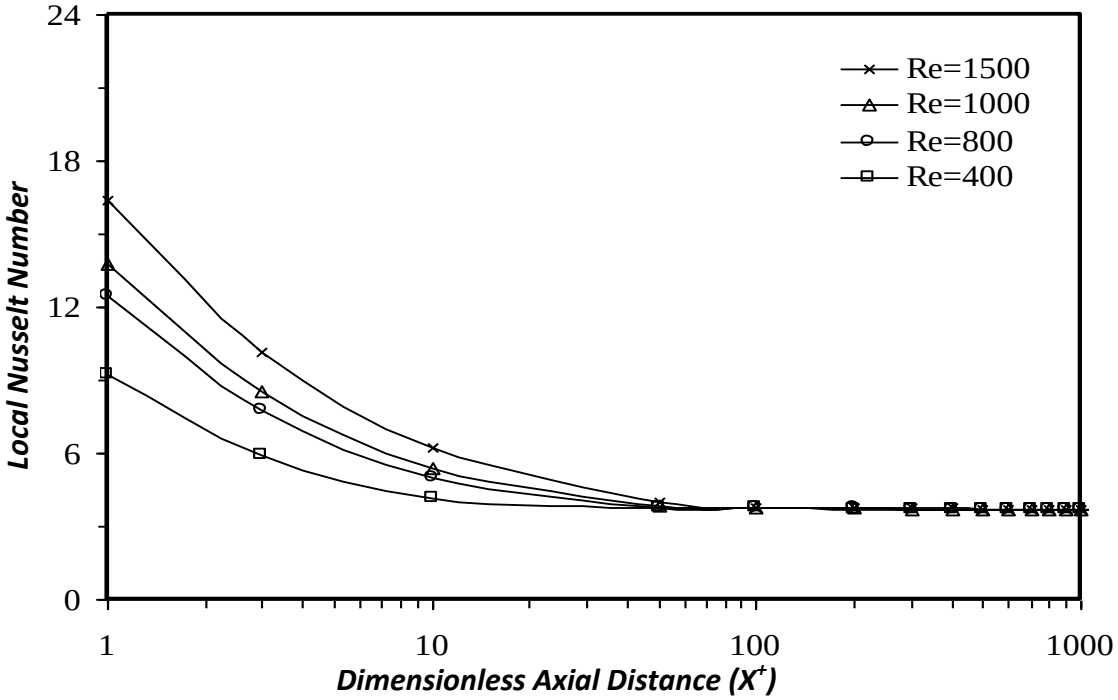

Fig. 4.11 Effect of Reynold Number on the Local Nusselt Number (linear velocity profile) Pr=1. S=0.1 .

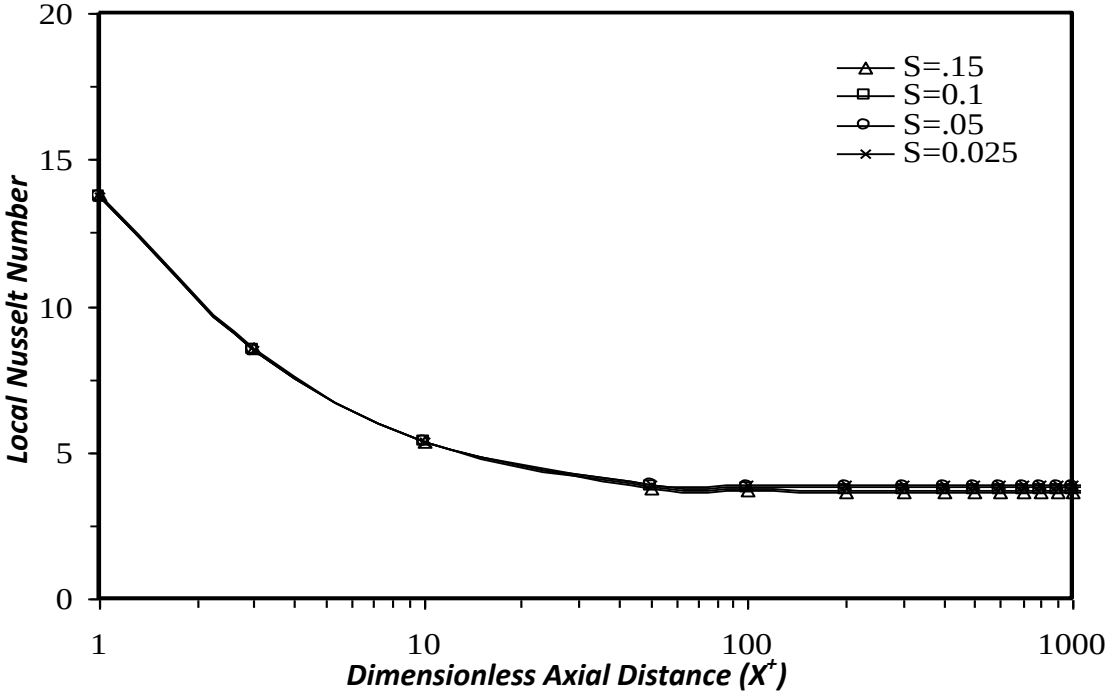

Fig. 4.12 Effect of Subcooled Number on the Local Nusselt Number (linear velocity profile) Re=1000 Pr=1 .

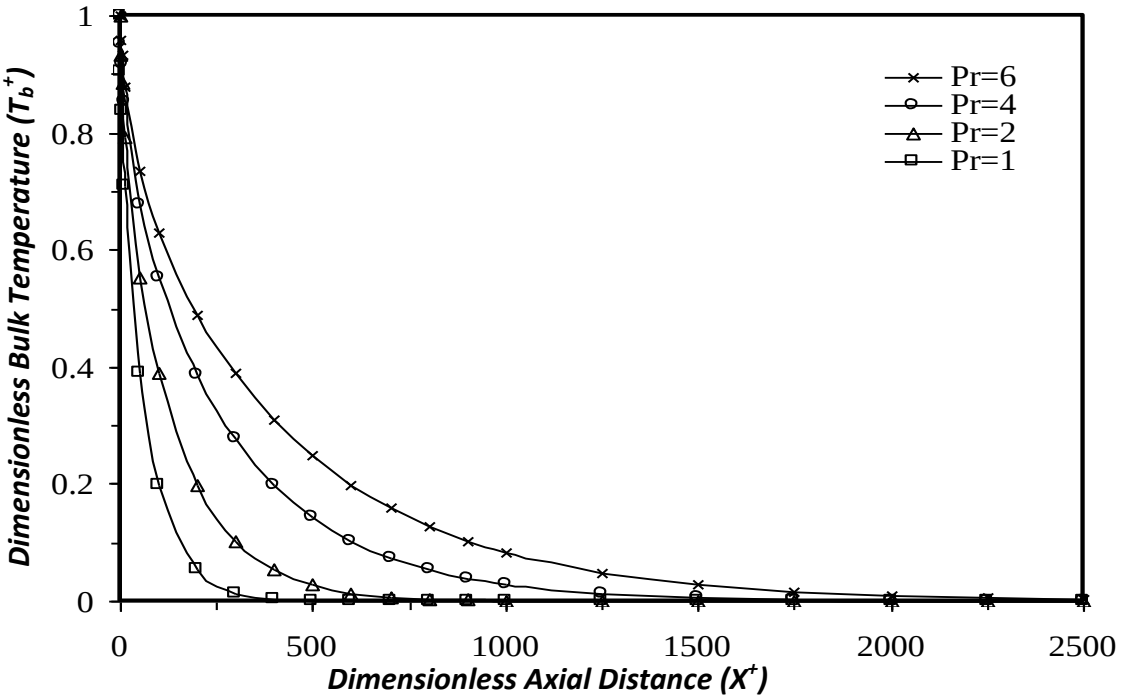

Fig. 4.13 Effect of Prandtl Number on the Local Dimensionless Bulk Temperature (linear velocity profile) Re=1000 S=0.1 .

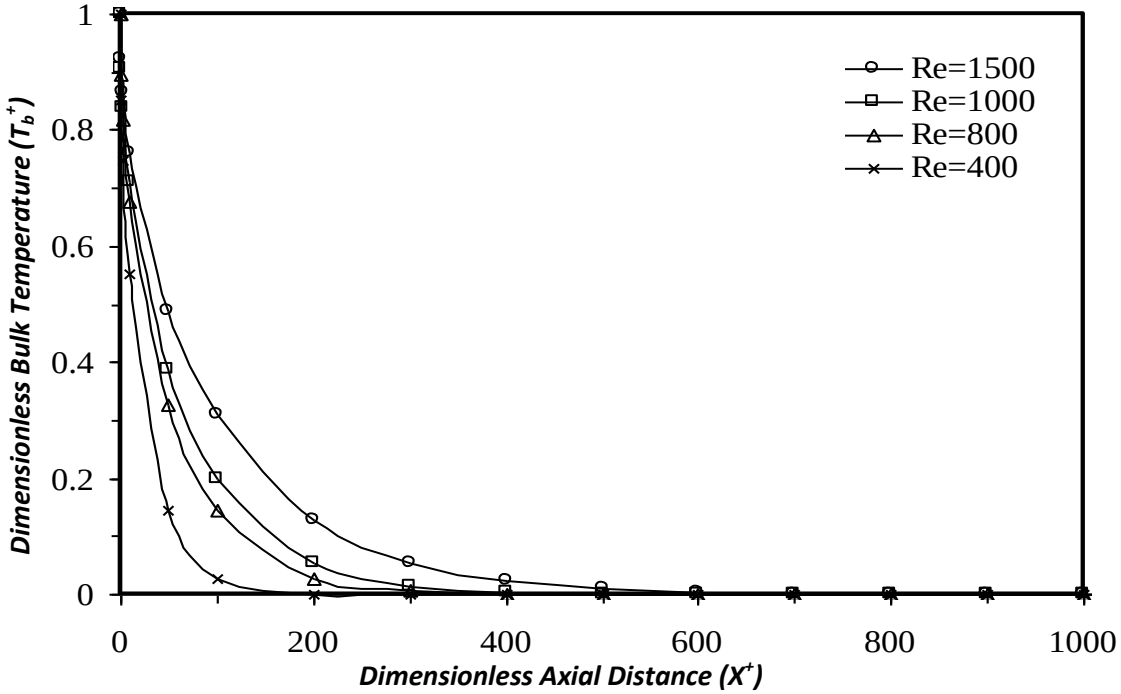

Fig. 4.14 Effect of Reynold Number on the Local Dimensionless Bulk Temperature (linear velocity profile) Pr=1. S=0.1 .

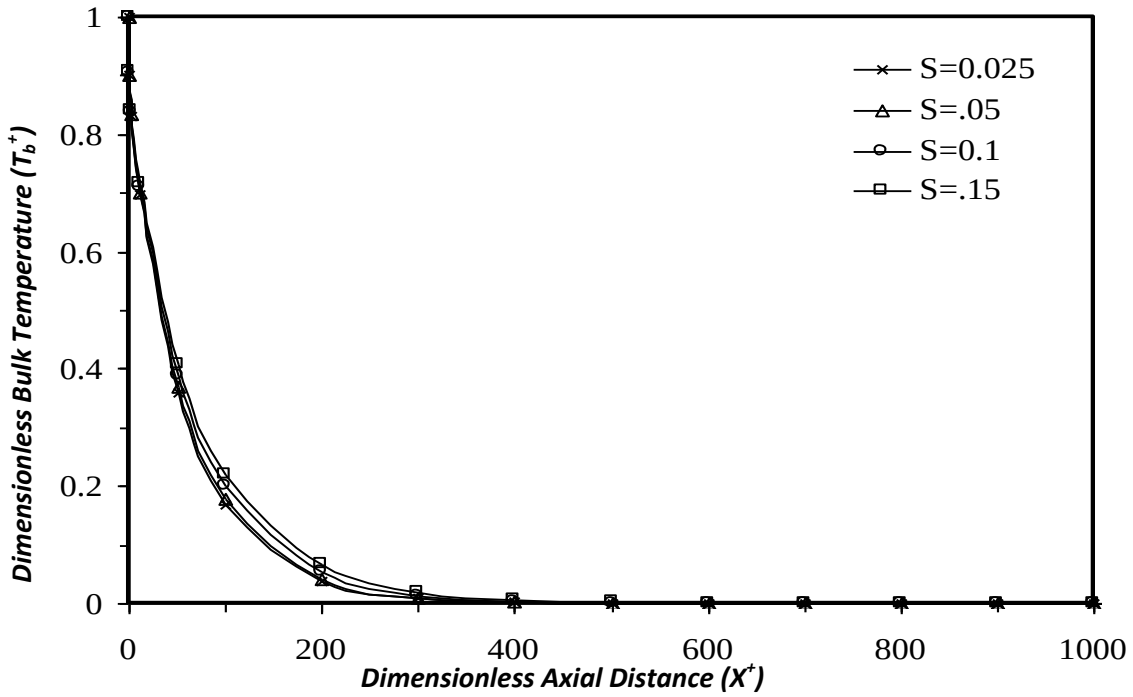

Fig. 4.15 Effect of Subcooling Number on the Local Dimensionless Bulk Temperature (linear velocity profile) Re=1000 Pr=1.0 .

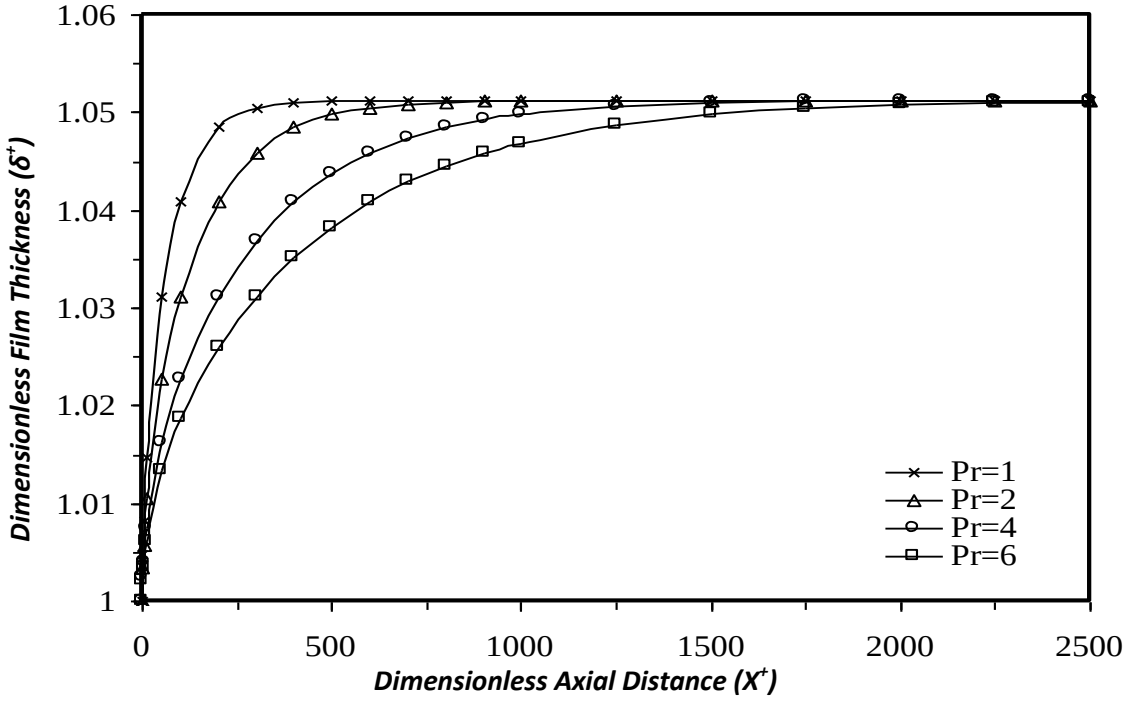

Fig. 4.16 Effect of Prandtl Number on the Local Dimensionless Film Thickness (linear velocity profile) Re=1000 S=0.1 .

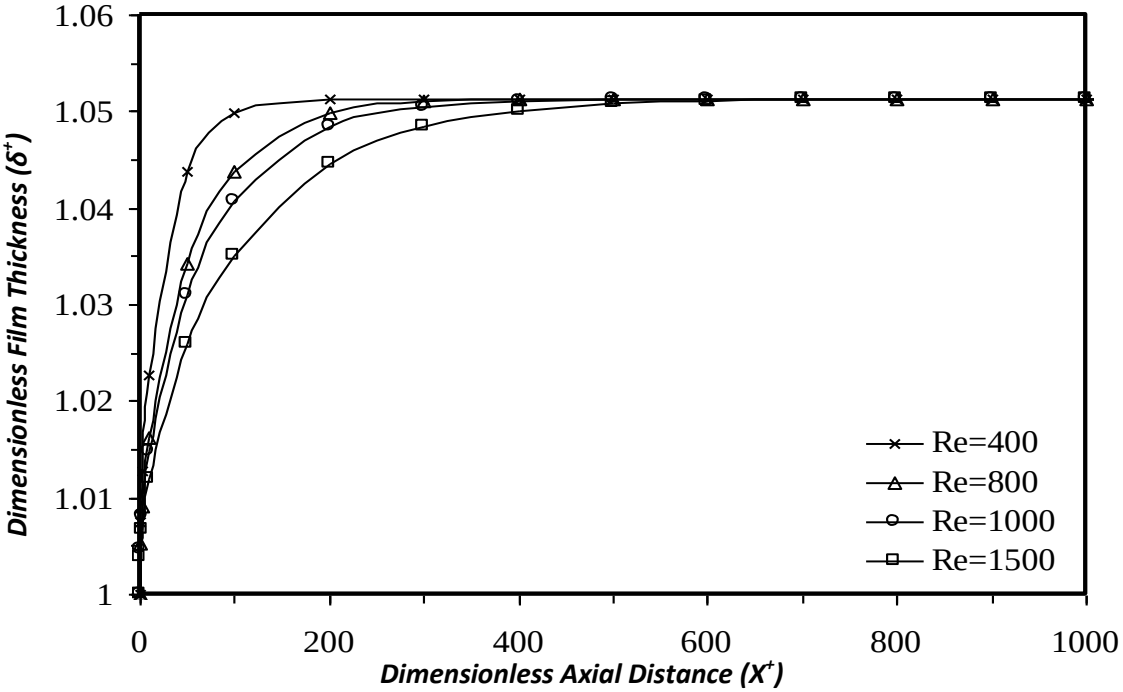

Fig. 4.17 Effect of Reynold Number on the Local Dimensionless Film Thickness (linear velocity profile) Pr=1. S=0.1 .

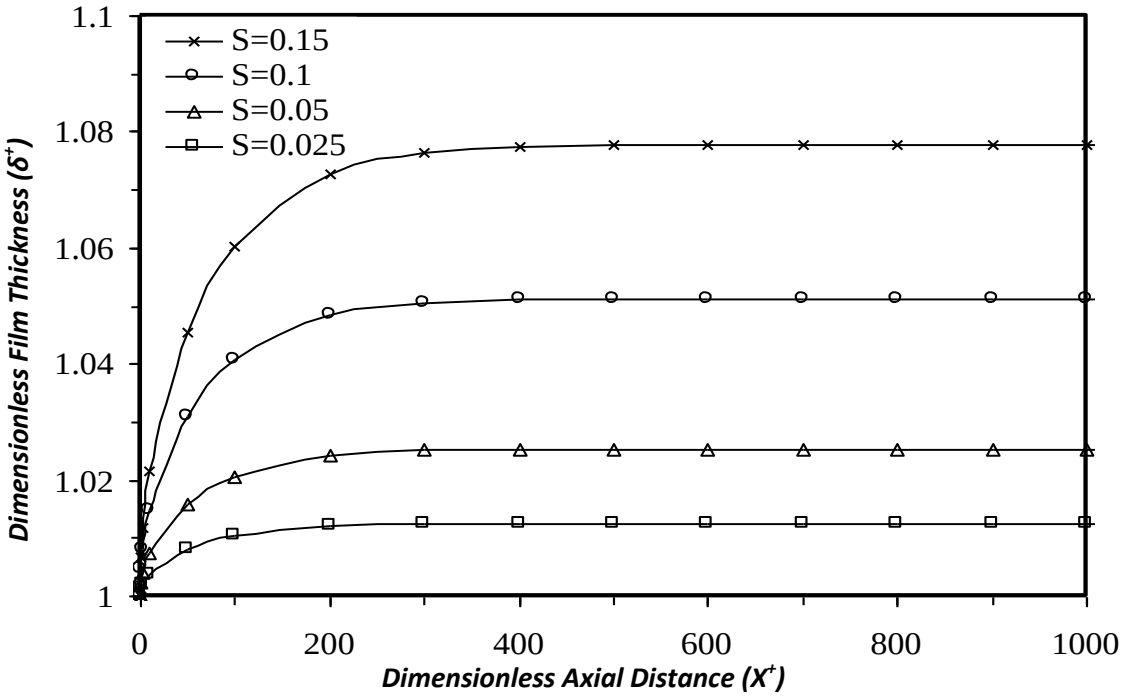

Fig. 4.18 Effect of Subcooling Number on the Local Dimensional Film Thickness (linear velocity profile) Re=1000 Pr=0.1 .

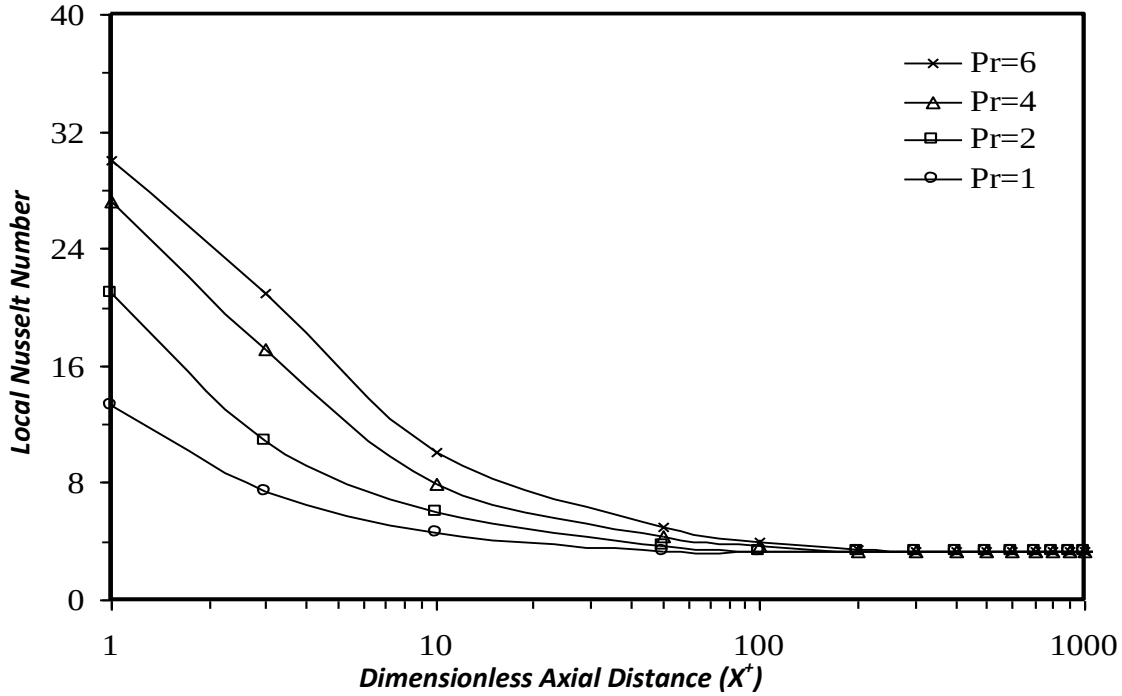

Fig. 4.19 Effect of Prandtl Number on the Local Nusselt Number (semi-parabolic velocity profile) Re=1000 S=0.1 .

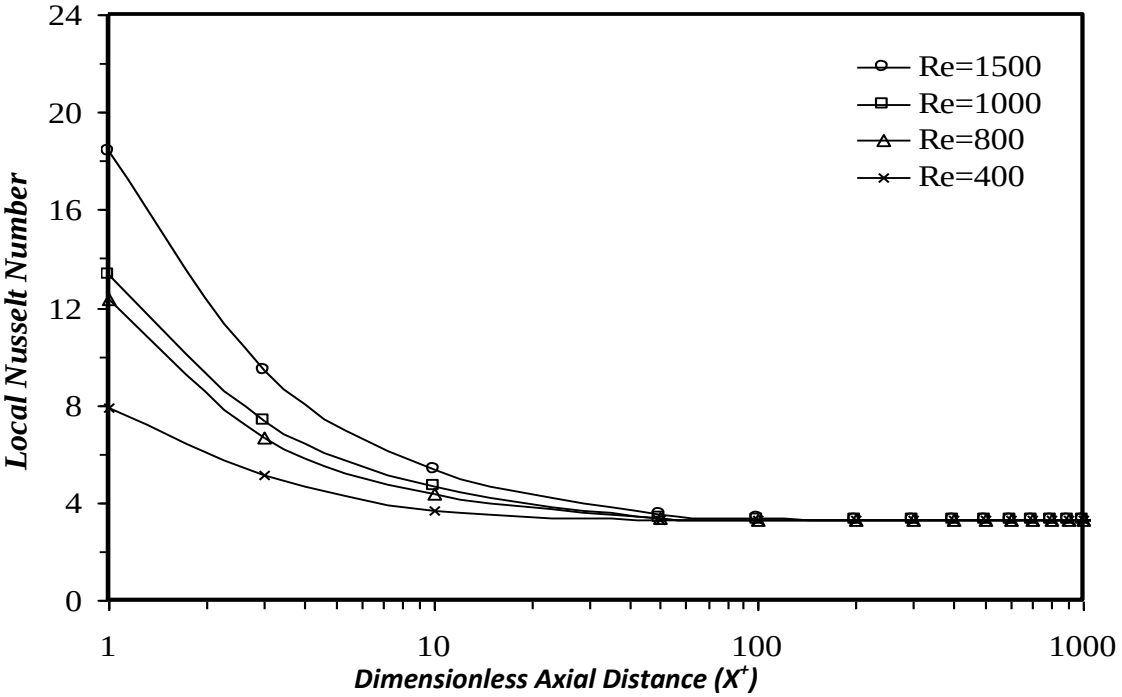

Fig. 4.20 Effect of Reynold Number on the Local Nusselt Number (semi-parabolic velocity profile) Pr=1. S=0.1 .

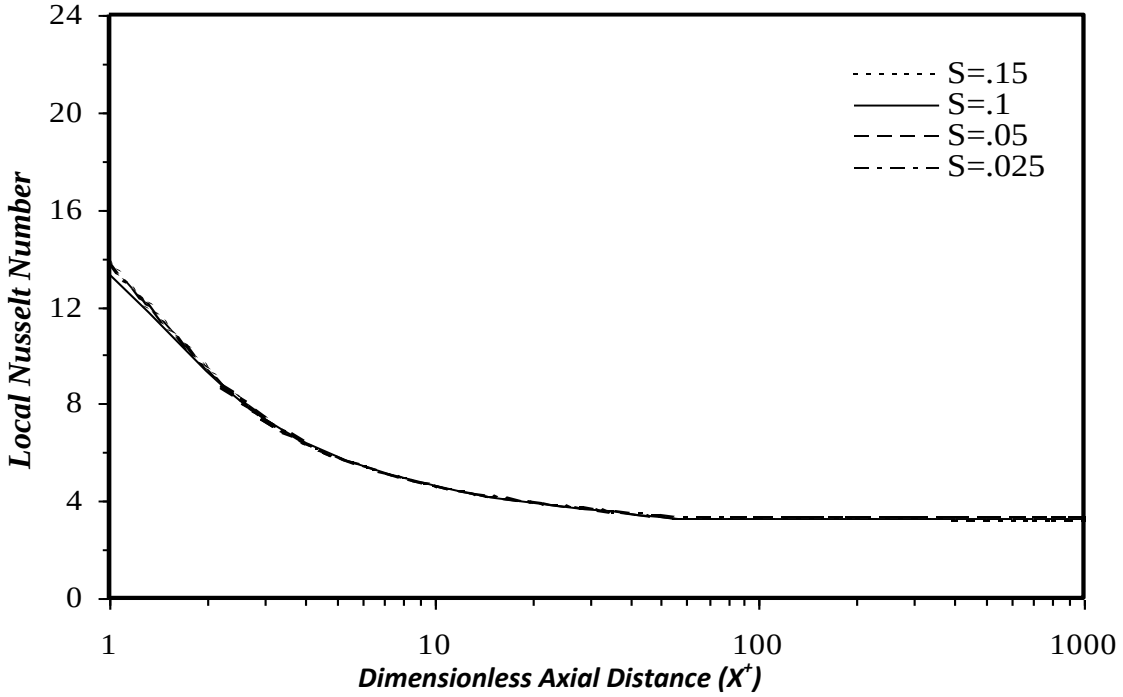

Fig. 4.21 Effect of Subcooling Number on the Local Nusselt Number (semi-parabolic velocity profile) Re=1000 Pr=1 .

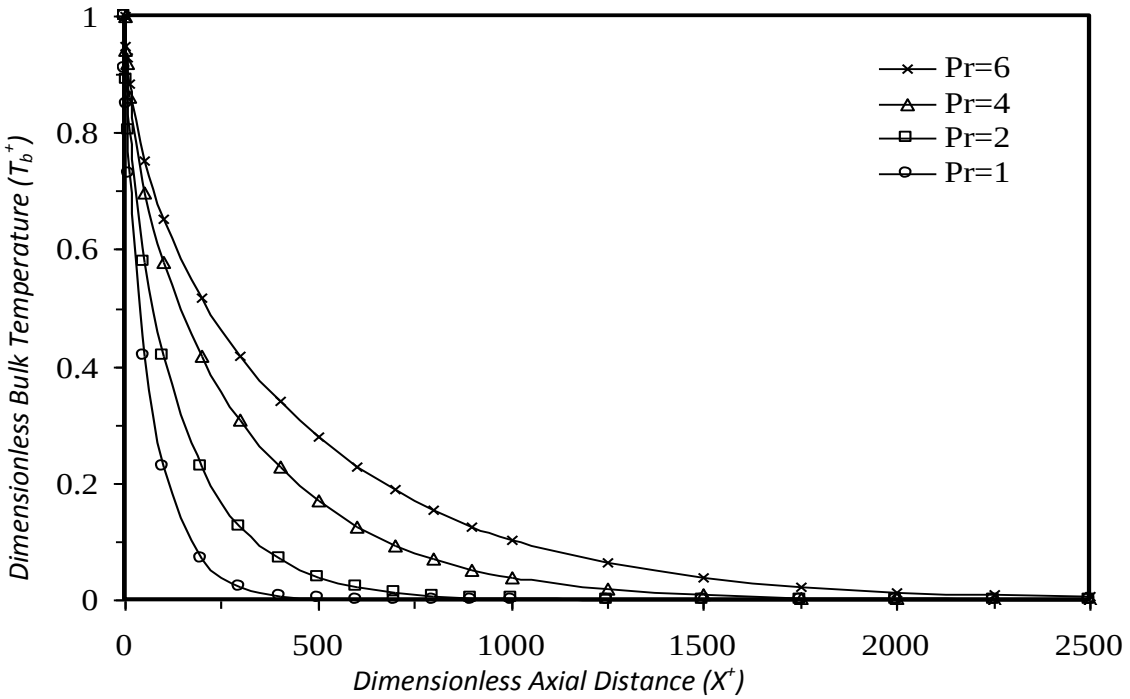

Fig. 4.22 Effect of Prandtl Number on the Local Dimensionless Bulk Liquid Temperature (semi-parabolic velocity profile) Re=1000 S=0.1 .

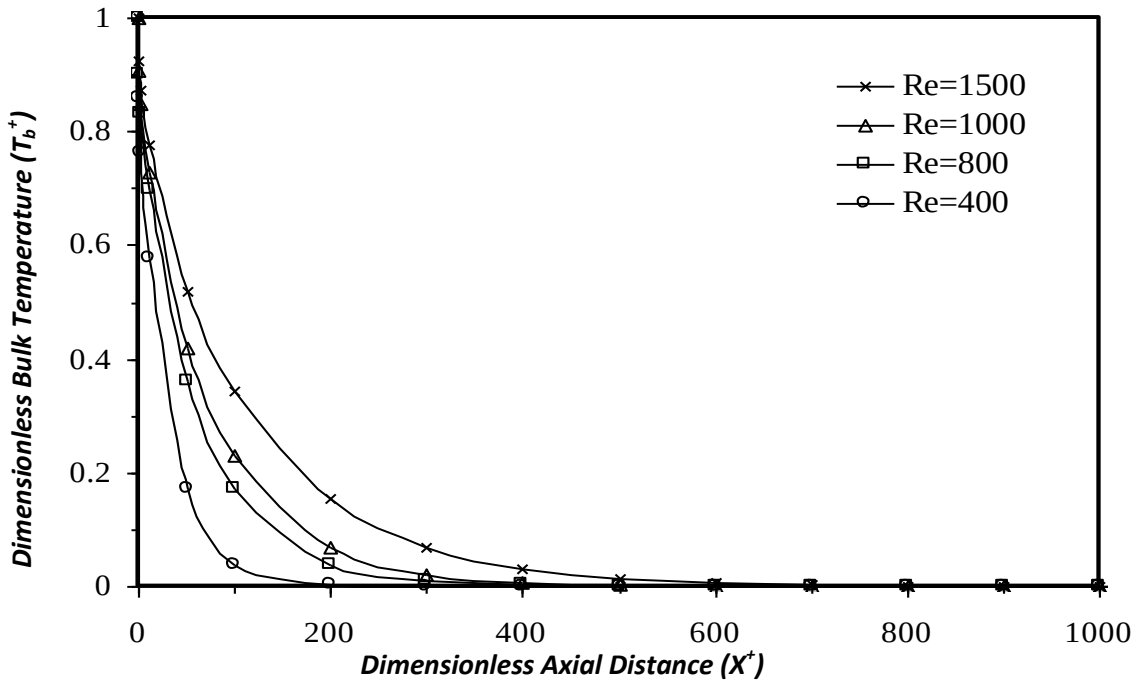

Fig. 4.23 Effect of Reynold Number on the Local Dimensionless Bulk Liquid Temperature (semi-parabolic velocity profile) Pr=1. S=0.1 .

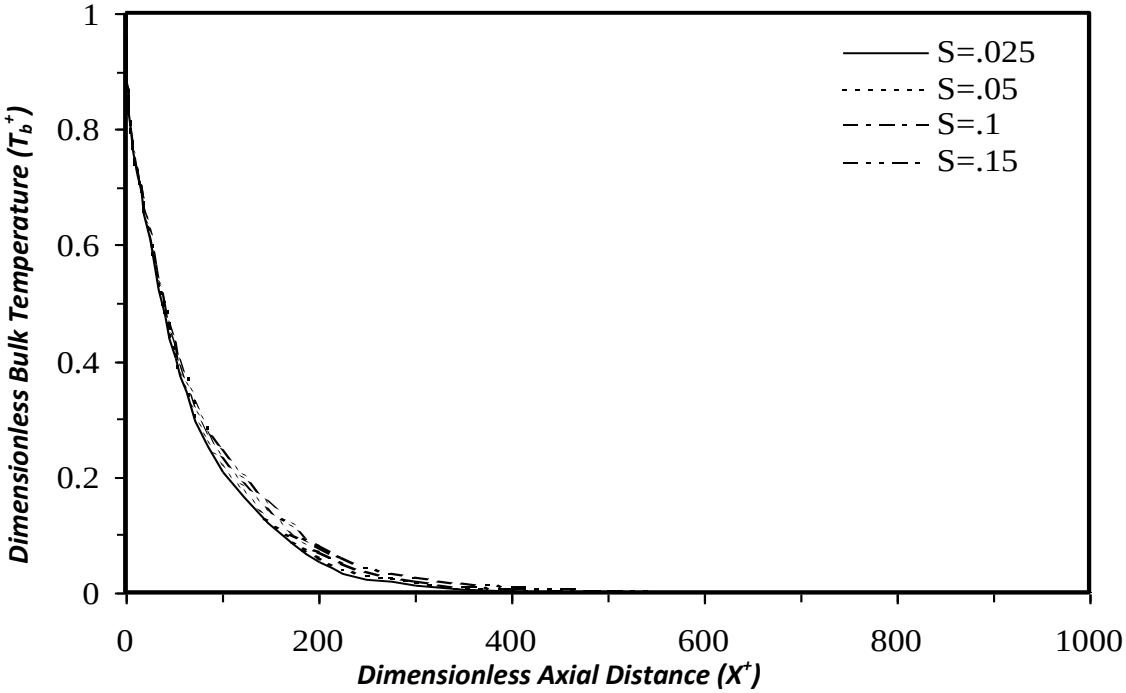

Fig. 4.24 Effect of Subcooling Number on the Local Dimensionless Bulk Liquid Temperature (semi-parabolic velocity profile) Re=1000 Pr=1.0 .

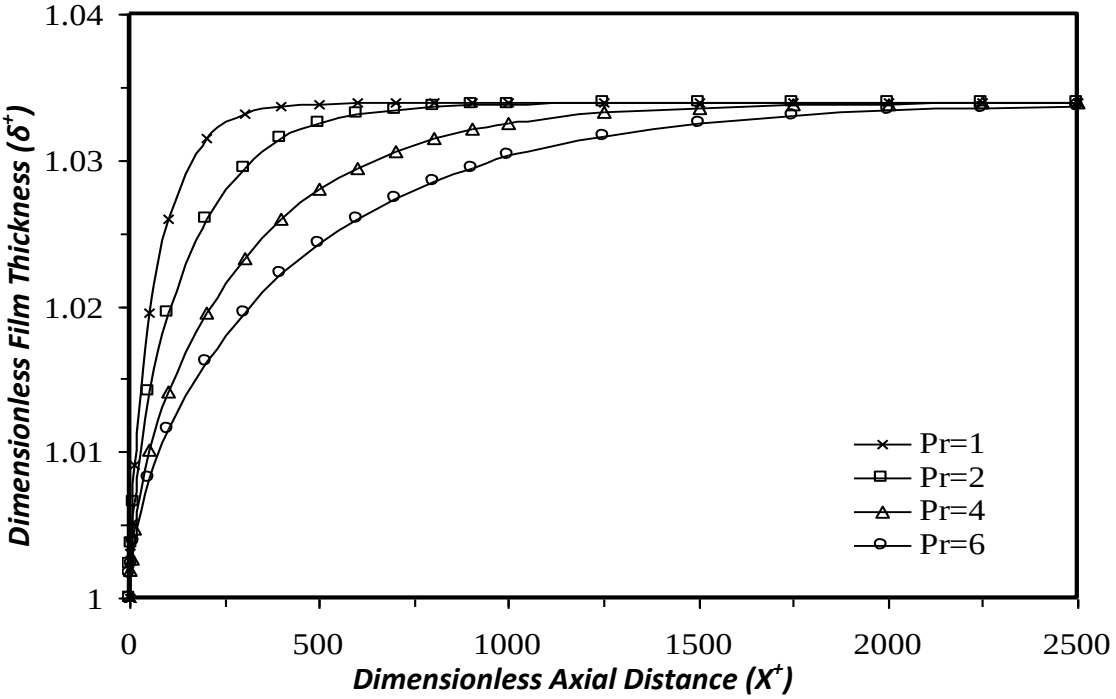

Fig. 4.25 Effect of Prandtl Number on the Local Dimensionless Film Thickness (semi-parabolic velocity profile) Re=1000. S=0.1 .

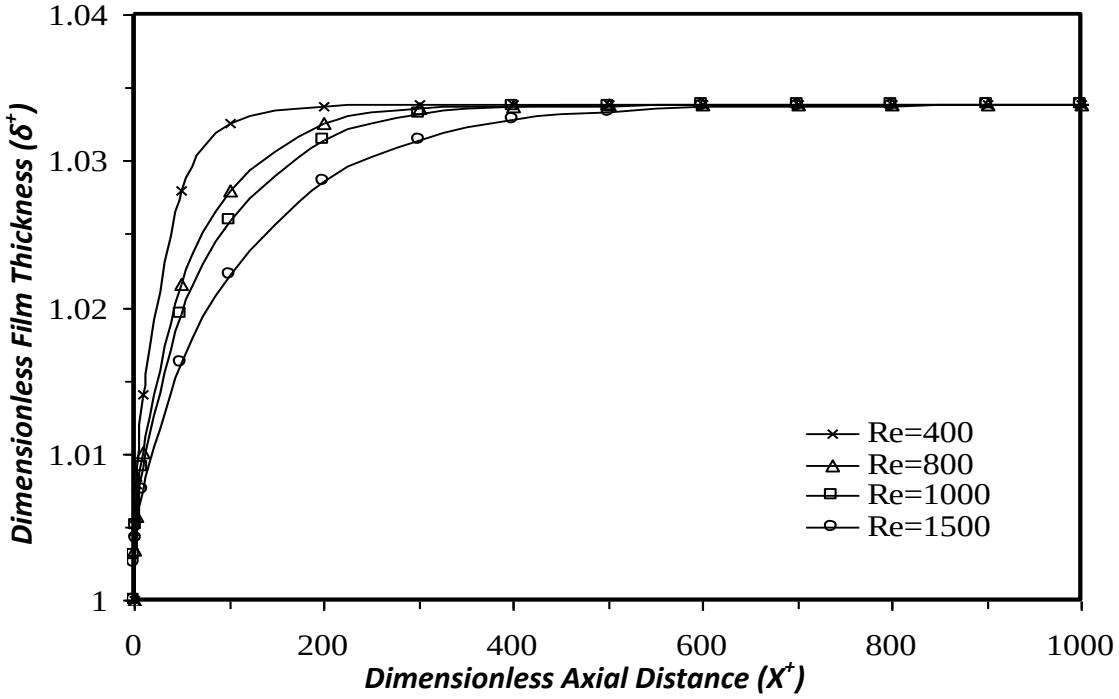

Fig. 4.26 Effect of Reynold Number on the Local Dimensionless Film Thickness (semi-parabolic velocity profile) Pr=1. S=0.1 .

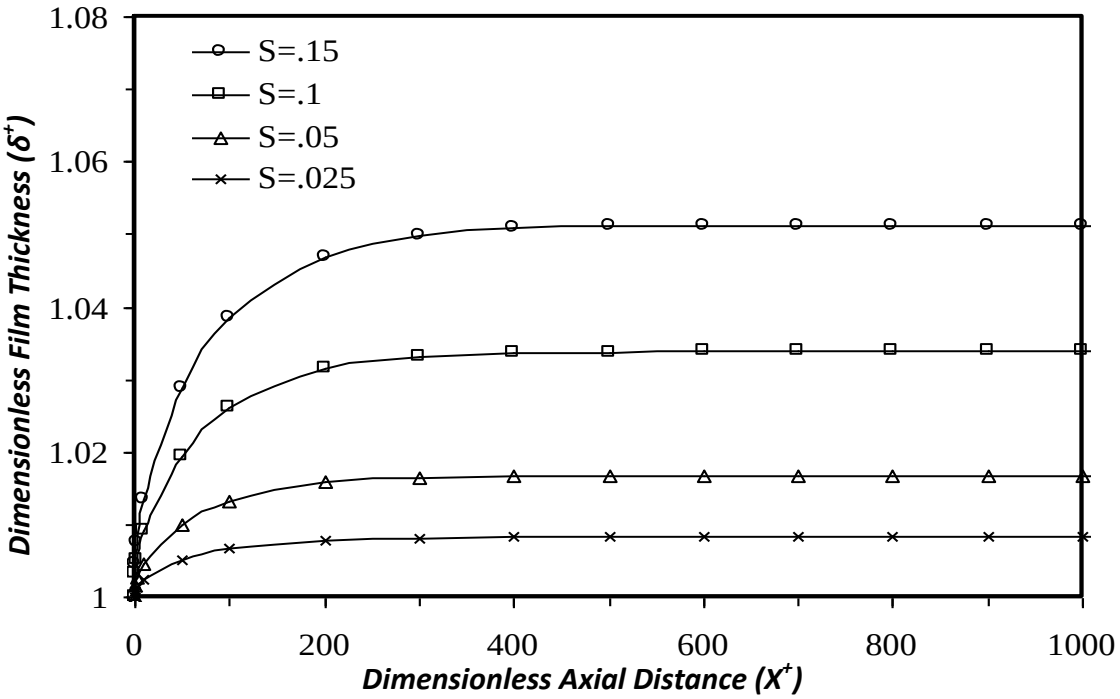

Fig. 4.27 Effect of Subcooling Number on the Local Dimensionless Film Thickness (semi-parabolic velocity profile) Re=1000. Pr=0.1 .

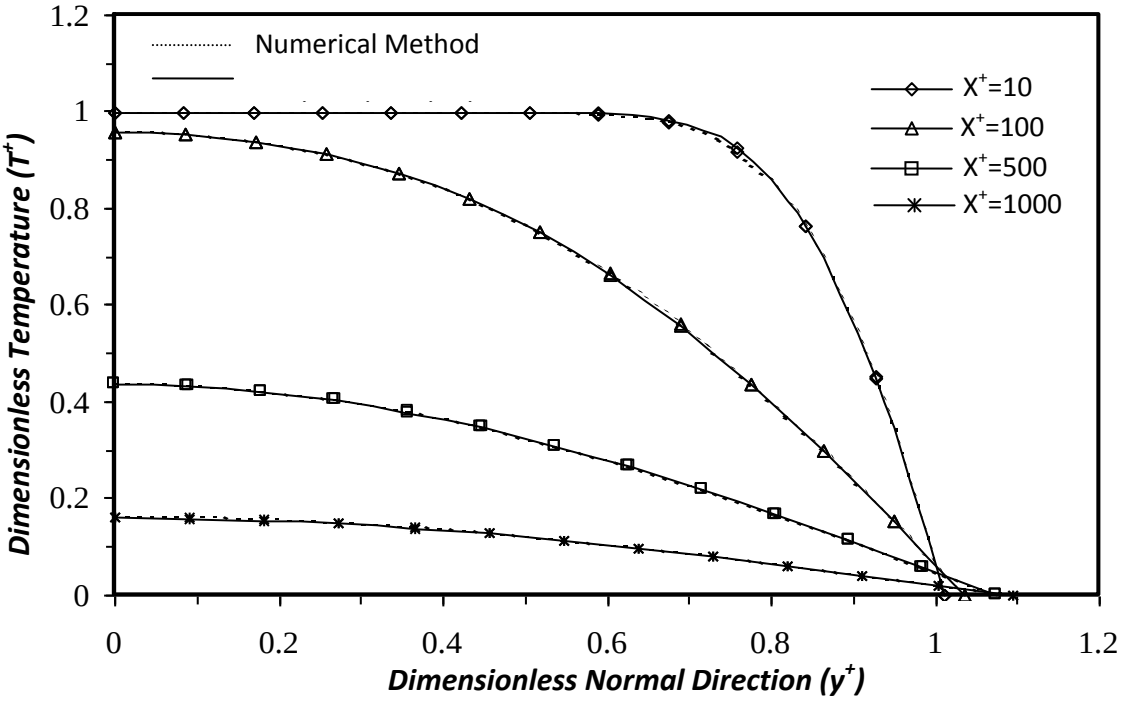

Fig. 4.28 Comparison Between the Dimensionless Liquid Temperature Distribution Obtained by Numerical and Analytical Methodes (uniform velocity profile)

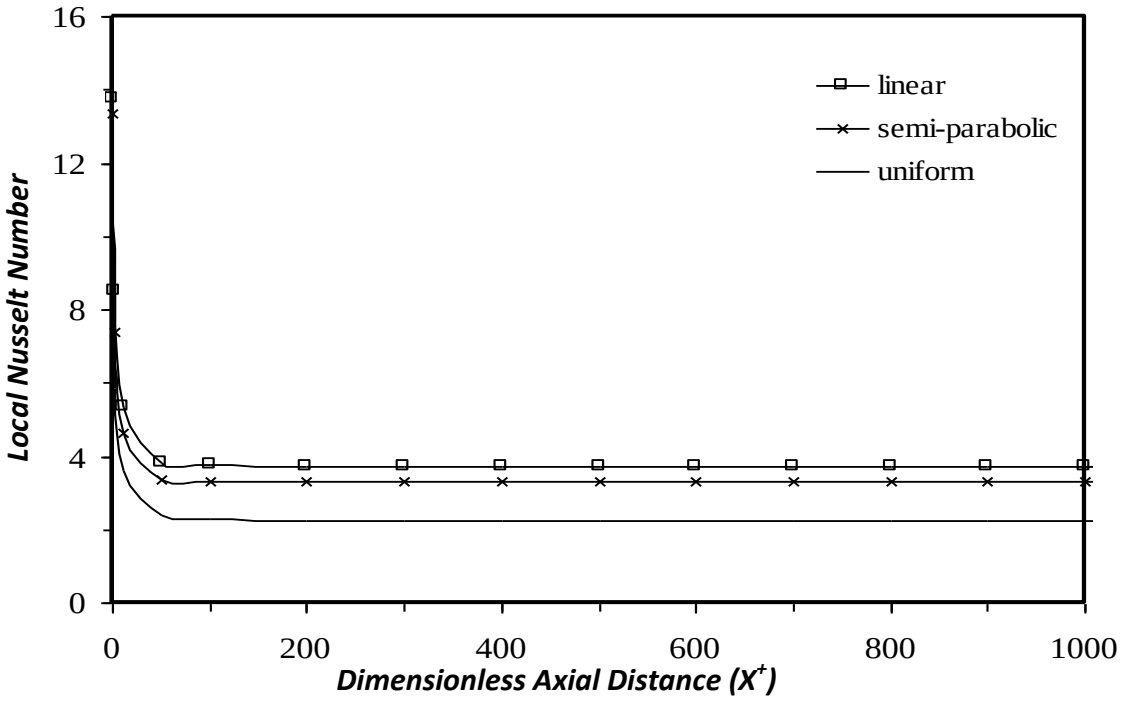

Fig. 4.29 Effect of Velocity Profile on the Local Nusselt Number Re=1000. Pr=1. S=0.1 .

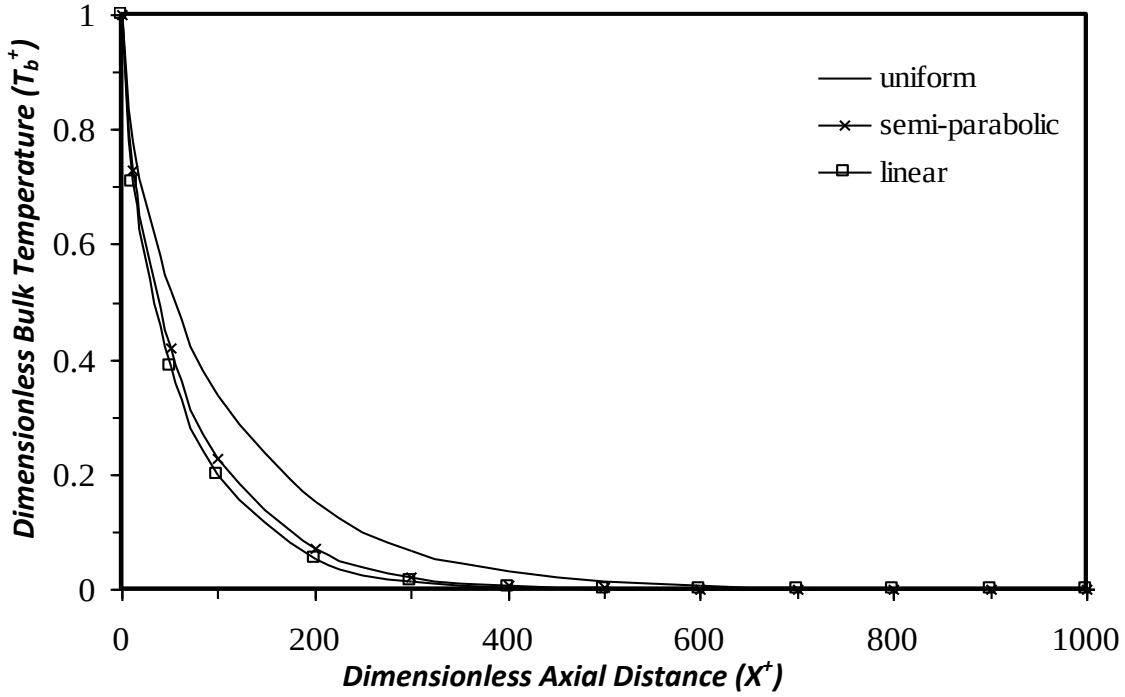

Fig. 4.30 Effect of Velocity Profile on the Local Dimensionless Bulk Liquid Temperature Re=1000. Pr=1. S=0.1 .

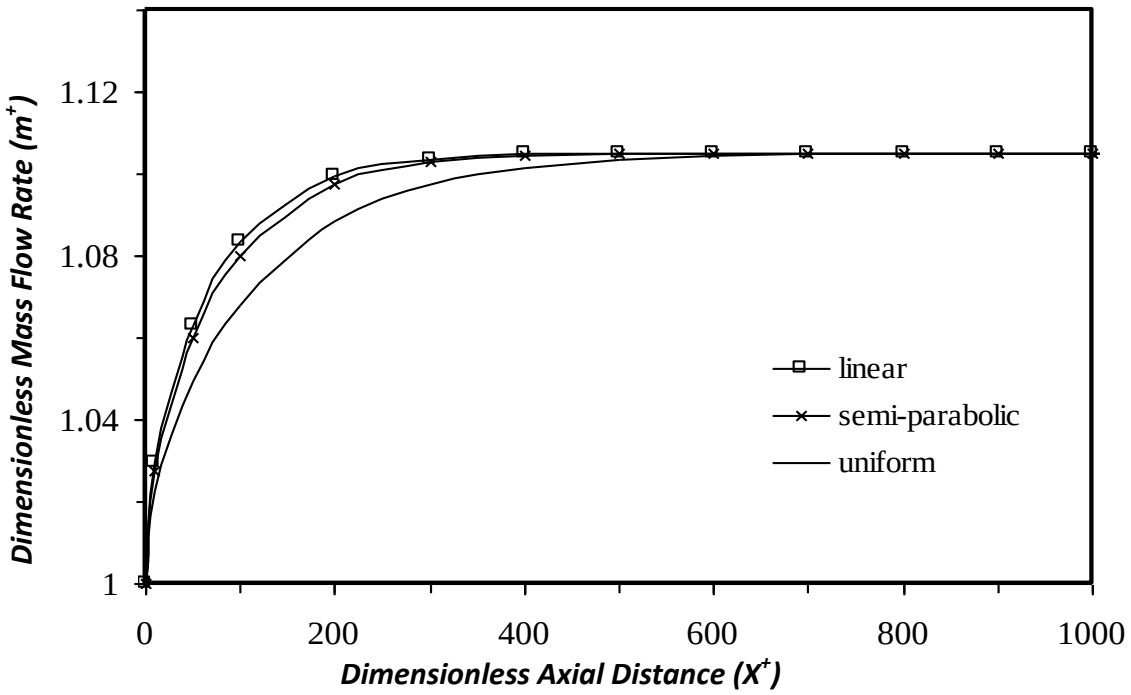

Fig. 4.31 Effect of Velocity Profile on the Local Dimensionless Mass Flow Rate Pr=1. Re=1000. S=0.1 .

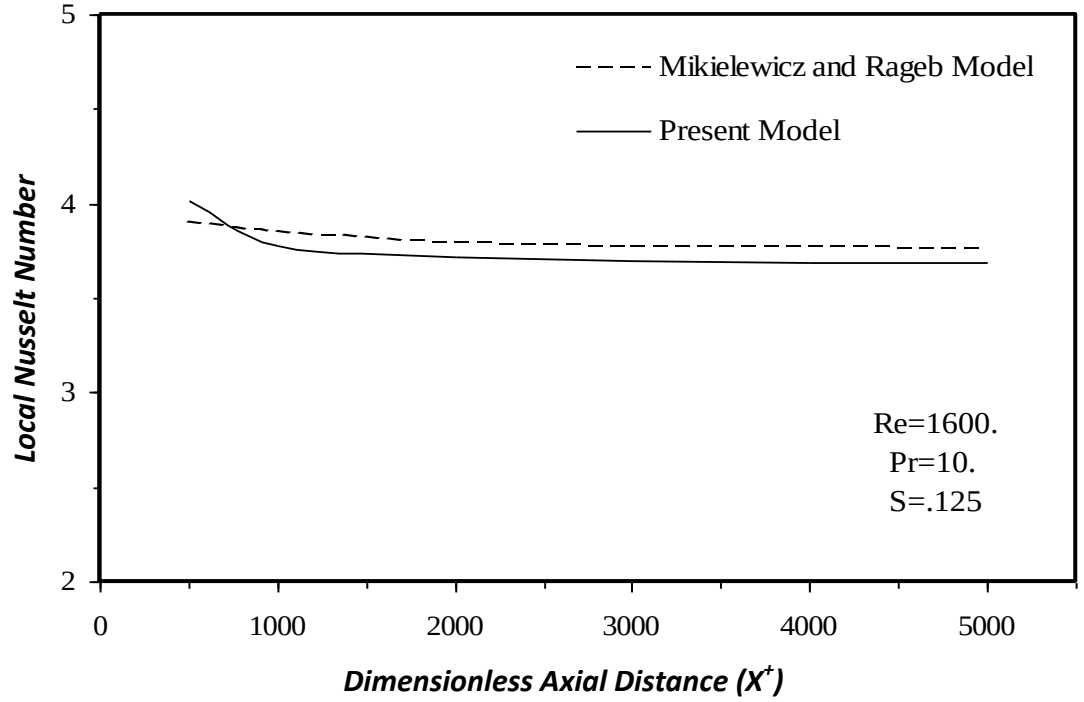

Fig. 4.32 Comparison Between Theoretical Local Nusselt Number from Mikielewicz and Rageb*[7]* and Local Nusselt Number from the Present Model(linear velocity profile).

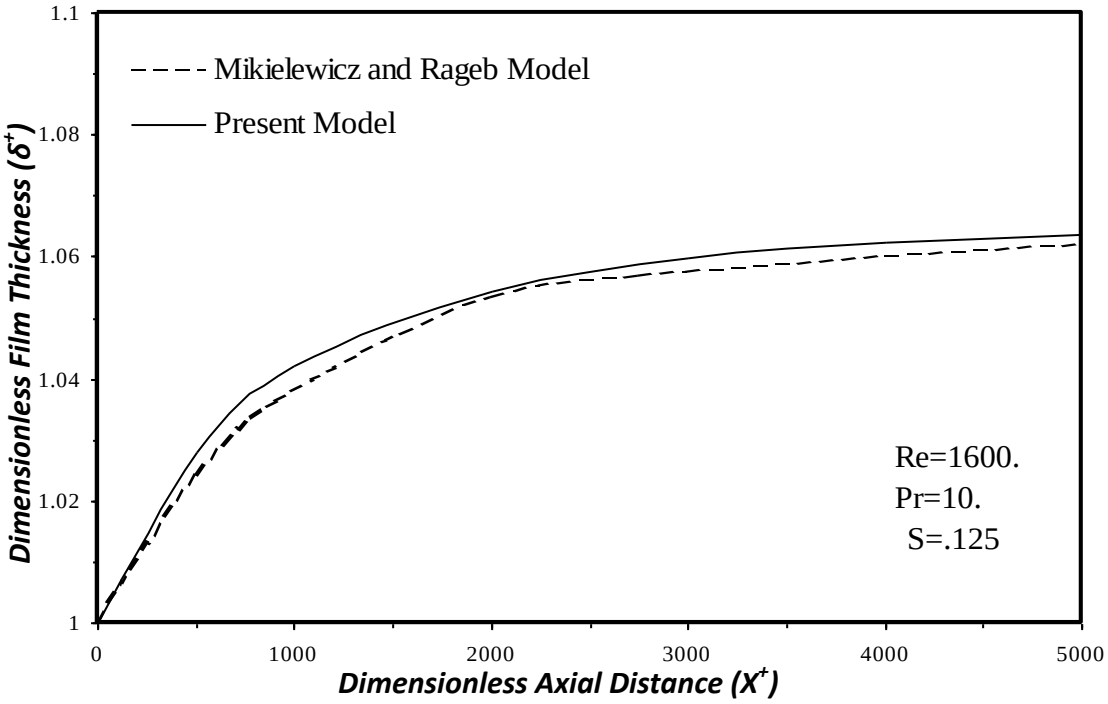

Fig. 4.33 Comparison Between Theoretical Local Film Thickness from Mikielewicz and Rageb*[7]* and Local Film Thickness from the Present Model(linear velocity profile).

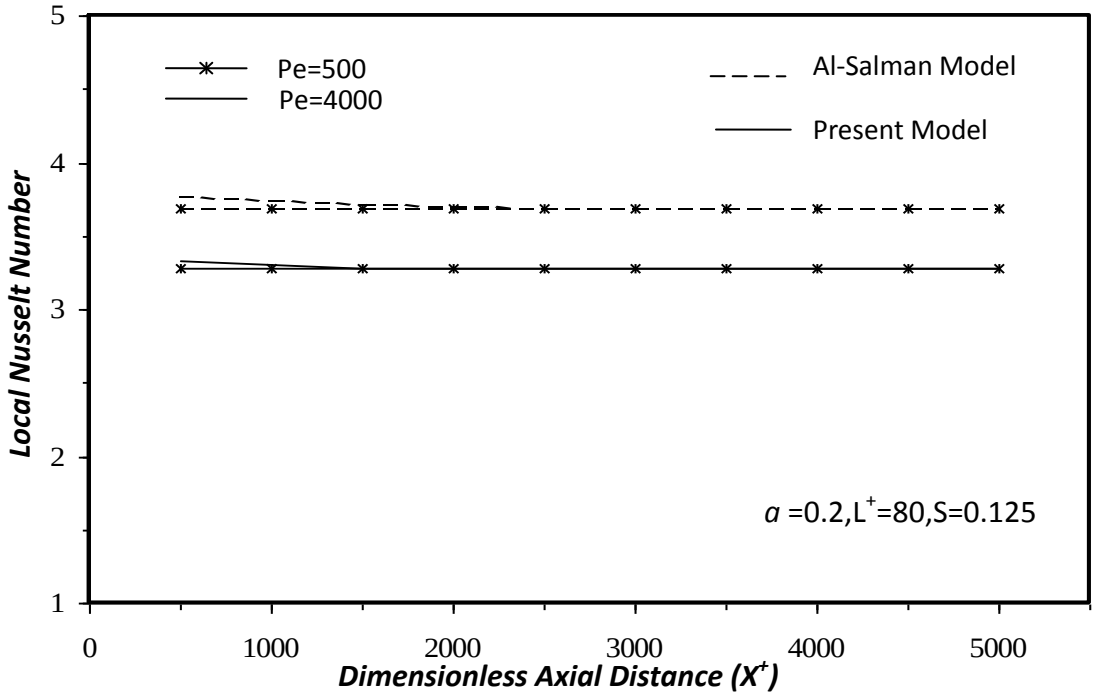

Fig. 4.34 Comparison Between Theoretical Local Nusselt Number from Al-Salman*[9]* and Local Nusselt Number from the Present Model(semi-parabolic velocity profile).

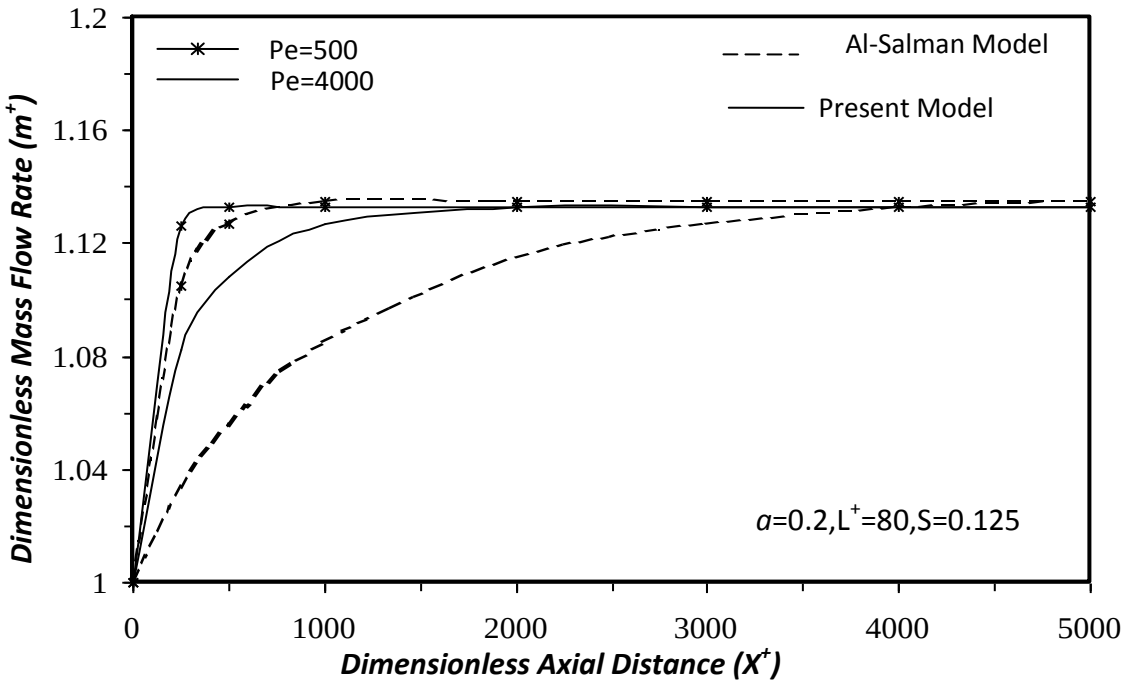

Fig. 4.35 Comparison Between Theoretical Local Mass Flow Rates from Al-Salman*[9]* and Local Mass Flow Rate from the Present Model

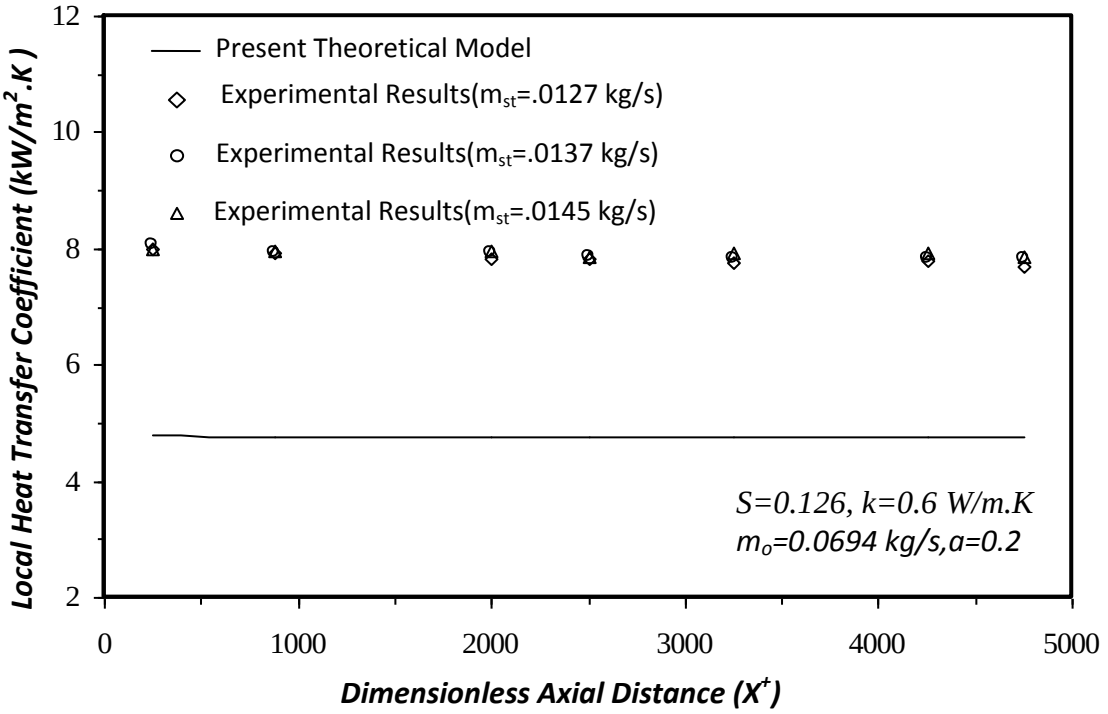

Fig. 4.36 Comparison Between the Present Theory and Experimental Data of Al-Salman*[9]*(semi-parabolic velocity profile).

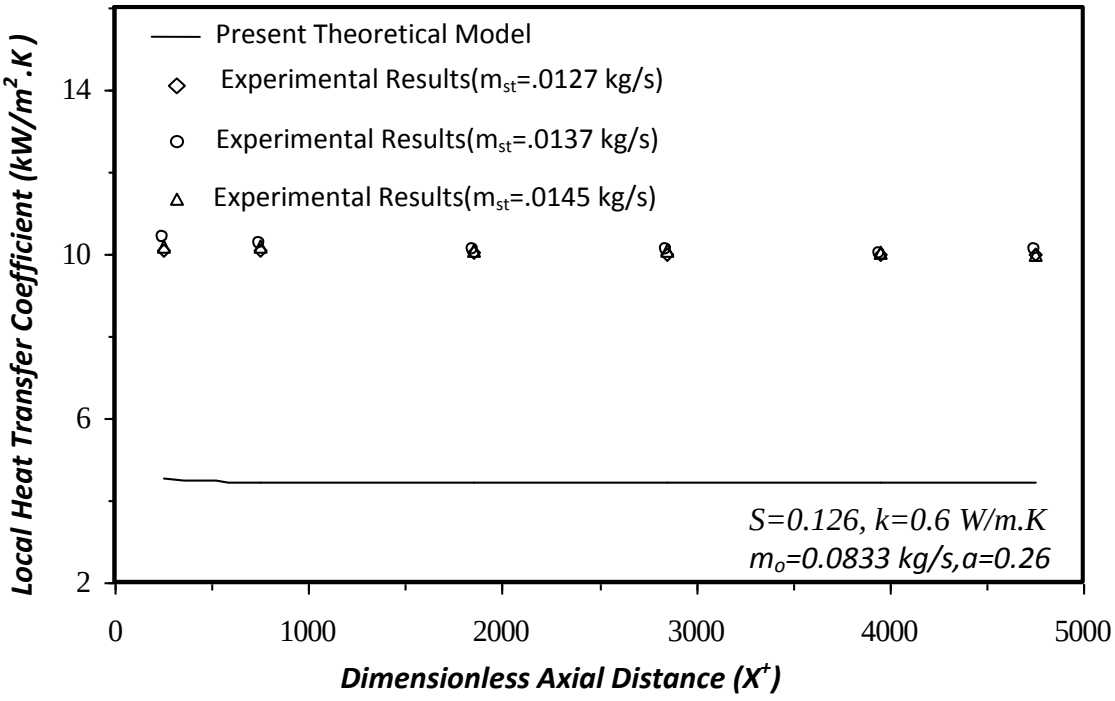

Fig. 4.37 Comparison Between the Present Theory and Experimental Data of Al-Salman*[9]*(semi-parabolic velocity profile).

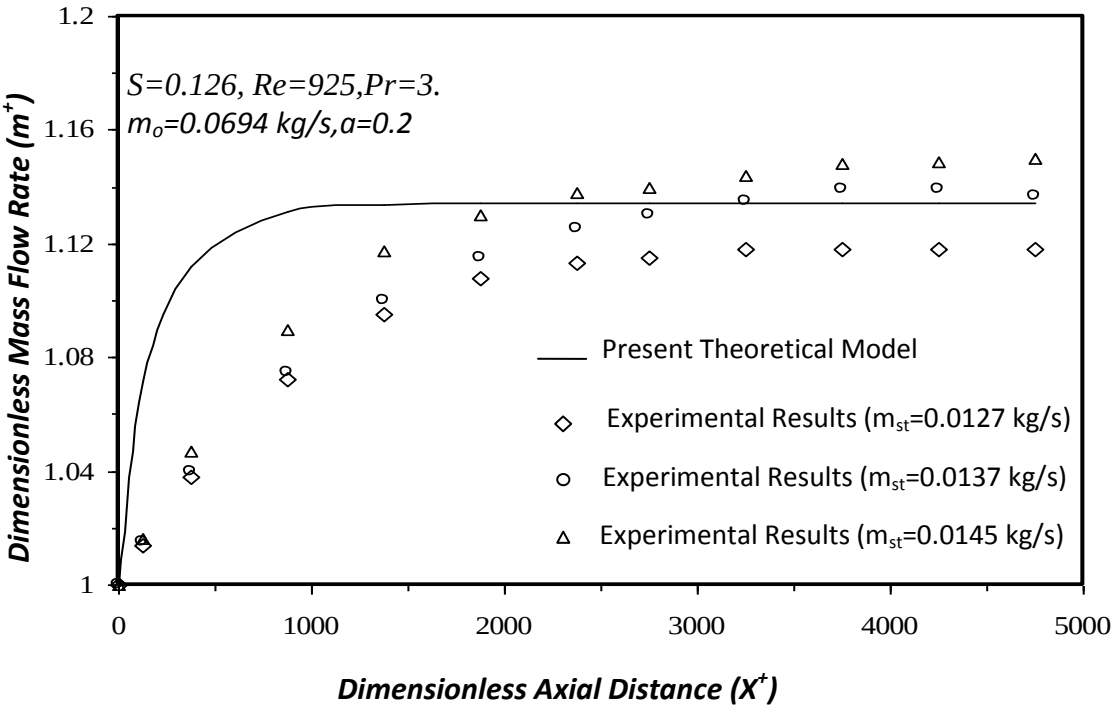

Fig. 4.38 Comparison Between the Present Theory and Experimental Data of Al-Salman*[9]*(semi-parabolic velocity profile).

Chapter five

CONCLUSIONS AND RECOMMENDATIONS

Chapter Five

CONCLUSIONS AND RECOMMENDATION

5.1 Conclusions

A theoretical model for direct contact condensation of saturated vapor on fully developed subcooled liquid film has been developed for three type of velocity profiles (uniform, linear and semi-parabolic). The characteristics of direct contact condensation process, such as local Nusselt number, local bulk temperature and local film thickness were evaluated a long the axial distance for each velocity profile. The present analysis implies that the condensation process is controlled by certain condensation parameters, these are Prandtl number, Reynolds number and subcooling number. The local Nusselt number and local bulk temperature are found to be increases with increasing Prandtl number or Reynolds number, while the film thickness is reduced. Nearly negligible effect of subcooling number on the local Nusselt number and local bulk temperatue is noted, while the film thickness increases with increasing subcooled number. The main conclusions concern the effect of variation of velocity profiles and the new methods of solution followed in this work are the following:

1. The developed theoretical methods based on the actual velocity profile and temperature gradient showed different results than that obtains using the models based on average values of both velocity and temperature gradient.
2. The results demonstrated that the linear velocity profile gives best performance of condensation than other type of velocity profile.

3. A numerical procedure is developed for semi-parabolic velocity profile, can be used to solve other problems which are more complicated using other velocity profile.
4. The comparison of theoretical result of the local Nusselt numbers with the available theoretical result gives satisfactory agreement. Also, the comparison of the local heat transfer coefficients with the published experimental data gives accepted results.

5.2 Recommendations

The present work could be extended to include the following topics:

1. Extension the model parameters to case of non-adiabatic surface with or without super heated the vapor.
2. This study may also be extended to taking into a count the effect of noncondensable gas which lead to increase the resistance of heat transfer.
3. The direct contact condensation process can be studied for the case of curvature solid surface.
4. The present analysis can be extended to include another type of velocity profile.

REFERENCES

References

[1] Bell, K. J. and Mueller, A. C., "Wolverine Engineering Data Book II", Wolverine Tube Inc., 2001 .

[2] Herman Merte, JR., "Condensation Heat Transfer," Advances in Heat Transfer, Vol.9, pp.181-268, 1973.

[3] Kim, H. J., Lee, S. C. and Bankoff, S. G.," Heat Transfer and Interfacial Drag in Countercurrent Steam-Water Stratified Flow", Int. J. Multiphase Flow, Vol.11, No.5, pp.593-606, 1985.

[4] Celata, G. P., Cumo, M. D., Annibale, Farello, G. E., and Facari, G., "A Theoretical and Experimental Study of Direct Contact Condensation on Water Turbulent Flow", Exp. Heat Transfer, Vol. 2, pp. 129-148, 1989.

[5] Karapanatsios T. D., Kostoglou, M., and Krabelas, A. J., " Local Condensation Rates of Steam-Air Mixtures in Direct Contact With a Falling Liquid Film", Int. J. Heat and Mass Transfer, Vol. 38, No. 5, pp.779-794, 1995.

[6] Al -Jabery, H. M., "Direct Contact Condensation on Laminar Sub-Cooled Wavy Liquid Film", M.Sc. Thesis, University of Basrah, College of Eng., 2001.

[7] Mikielewicz, J. and Rageb, A.M. A.," Simple Theoretical Approach to Direct-Contact Condensation on Subcooled Liquid Film", Int. J. Heat Mass Transfer, vol.38, No.3, pp. 557-562, 1995.

[8] Davis, J. and Yadigaroglu, G., "Direct Contact Condensation in Falkner- Skan Flows", ASME Int. Mech. Eng. Congress & Explosion Proceedings of IMECE' 02, New Orleans, Louisiana, USA, pp.1-10, Nov., 17-22, 2002.

[9] Al-Salman, K. Y. Y, "Analysis of Direct Contact Condensation on Subcooled Wavy Thin Falling Liquid Film", Ph.D. Thesis, University of Basrah, College of Eng.2002.

[10] Nusselt, W."Die Oberlachenck Condensation Des Wasserdampfes" Z.Vereines Deutscher Ingerieure, Vol. 60, pp. 541-546, 1916.

[11] Murty, N. S. and Sastri, V. M., "Condensation on A Falling Liquid Film", Fifth Int. Heat Transfer Conference, Tokyo, Vol. 3, pp.331-335, (1974.(

[12] Finkelstein, Y. and Tamir, A., "Interfacial Heat Transfer Coefficients of Various Vapors in Direct Contact Condensation," Chem. Eng. Journal, Vol.12, pp. 199-209,1976.

[13] Bankoff, S.G.," Some Condensation Studies Pertinent to LWR Safety", Int. J. Multiphase Flow, Vol.6, pp. 51-67, 1980.

[14] Segav, A. and Collier, R. P.," A Mechanistic Model for Counter Current Steam-Water Flow", Trans. of the ASME, Vol.102, pp.688-693, 1980.

[15] Kim, H. J. and Bankoff, S.G.," Local Heat Transfer Coefficients For Condensation in Stratified Countercurrent Steam-Water Flows", Trans. of the ASME, Vol.105, pp. 706-712, 1983.

[16] Bankoff, S. G. and Kim, H., J.," Local Condensation Rate in Nearly Horizontal Stratified Counter Current Flow of Steam and Cold Water", AICHE Symp. Ser.79, pp. 209-223, 1983.

[17] Lim, I. S., Tankin, R. S. and Yuen, M. C.," Condensation Measurement of Horizontal Co-current Steam Water flow", ASME. J. Heat Transfer, Vol. 106, pp. 425-432, 1984.

[18] Celata, G. P., Cumo, M., Farello, G. E. and Focardi, G.," Direct Contact Condensation of Steam on Slowly Moving Water" Nuclear Eng. and Design, Vol.96, pp.21-31, 1986.

[19] Celata, G. P., Cumo, M., Farello, G. E. and Focardi, G.," Direct Contact Condensation of Superheated Steam on Water", Int. J. Heat Mass Transfer, Vol. 30, No. 3,pp. 449-458, 1987.

[20] Rageb, A.M. A.," Theoretical Analysis of the Direct contact Condensation on the Heated Surface", Proc. Second Basrah Conference of Mech. Eng. Research, pp. 1-14, 1993.

[21] Karapantsios, T. D. and Karabelas, A. J.," Direct Contact Condensation in the Presence of Noncondensables over Free-Falling Films with Intermittent Liquid Feed", Int. J. Heat Mass Transfer, Vol. 38, No.5, pp. 795-805, 1995.

[22] Karapanatsios T. D., Kostoglou, M., and Krabelas, A. J., " Direct Contact Condensation of Dilute Steam/ Air Mixture on Wavy Falling Film", Chem. Eng. Comm., Vols. 141-142, pp. 261-285, 1996.

[23] Rageb, A. M. A., "Condensation on A Falling Laminar Liquid Film at the Entrance Length' Abhath Al-Yarmouk, Basic Sciences and Engineering, Vol. 8, No. 1, pp. 9-35, 1999.

[24] Benedek, S.," Heat Transfer at the Condensation of Steam on Turbulent Water Jet", Int. J. Heat Mass Transfer, Vol.19, pp. 448-450, 1976.

[25] Kim, S. and Mills, A. F.," Condensation on Coherent Turbulent Liquid Jets: Part I-Experimental Study", Trans. of the ASME, Vol.111, pp.1068-1074, 1989.

[26] Kim, S. and Mills, A. F.," Condensation on Coherent Turbulent Jets: Part II- a Theoretical Study", Trans. of the ASME, Vol.111, pp.1075-1082, 1989.

[27] Lui, T. L., Jacobs, H. R. and Chen, K.," An Experimental Study of Direct Condensation on a Fragmenting Circular Jet", Trans. of the ASME, Vol.111, pp. 585-588, 1989.

[28] Celata, G. P., Cumo, M. D., Farello, G. E., and Facari, G., "A Comprehensive Analysis of Direct Contact Condensation of Saturated Steam on Subcooled Liquid Jets", Int. J. Heat and Mass Transfer, Vol. 32, No. 4, pp.639-654, 1989.

[29] Ford, J. D., and Lekic, A.," Rate of Growth of Drops During Condensation", Int. J. Heat and Mass Transfer, Vol.16, pp.61-64, 1973.

[30] Lekic, A. and Ford, J. D.," Direct Contact Condensation of Vapor on A Spray of Subcooled Liquid Droplets", Int. J. Heat Mass Transfer, Vol.23, pp.1531-1537, 1980.

[31] Hijikata, K., Mori, Y. and Kawaguchi, S.," Direct Contact Condensation of Vapor to Falling Cooled Droplets, Int. J. Heat Mass Transfer, Vol.27, No.9, pp.1631-1640, 1984.

[32] Celata, G. P., Cumo, M., D'Annibale, F. and Farello, G. E.," Direct Contact Condensation of Steam on Droplets", Int. J. Multiphase Flow, Vol.17, No.2, pp.191-211, 1991.

[33] Özisk, "Heat Transfer Basic Approach", McGraw-Hill, N.Y., 1975.

[34] Benjamin, Gebhart, "Heat Conduction and Mass Diffusion", McGraw-Hill, N.Y, 1993.

[35] Hildeberand, F.B., Advanced Calculus for Application, 2nd edition, PRENTICE-HALL, Inc., N. J., 1976.

[36] El-Ariny, A. S, and Aziz, A., "A Numerical Solution of Entrance Region Heat Transfer in Plane Couette Flow", Trans. ASME, J. Heat Transfer, Vol. 98, No. 3, pp.427-431, 1976.

[37] Carnaham, B., Luther, H.A, and Wilkes, J. O., Applied Numerical Methods, Wiley, N, Y., 1969.

[38] Schlichting, H., "Boundary Layer Theory,"6th Edition, McGraw-Hill, N. Y., 1968.

APPENDICIES

Appendix A: Using the orthogonal Property to obtain the Multiplying factor.

$\phi_n(x)$ are said to be orthogonal on interval (a, b) if the integral of the product $\phi_m \phi_n$ over that interval vanishes[ ]:

$$\int_a^b \phi_m(x)\phi_n(x)dx = 0 \qquad m \neq n \tag{a.1}$$

More generally, the functions $\phi_m(x)$ and $\phi_n(x)$ are said to be orthogonal with respect to a weighting function *R(x),* on an interval (a,b) if

$$\int_a^b R(x)\phi_m(x)\phi_n(x)dx = 0 \qquad m \neq n \tag{a.2}$$

we have seen that the problem

$$\frac{d^2g}{dy^2} + \lambda^2 R(y)g = 0 \qquad g(0) = 1 \quad g(1) = 1 \tag{a.3}$$

where *R(y)* are any function with respect to y .

Suppose now that λ_m and λ_n are any two different characteristics values of the problem considered and that the corresponding characteristic function are g_m and g_n respectively. That follows

$$\left.\begin{aligned} \frac{d^2g_m}{dy^2} + \lambda_m^2 R(y)g_m = 0 \\ \frac{d^2g_n}{dy^2} + \lambda_n^2 r(y)g_n = 0 \end{aligned}\right\} \tag{a.4}$$

If the first of these equations is multiplied by g_n and the second by g_m, and the resultant equations are subtracted from each other, there follows

$$(g_n \frac{d^2 g_m}{dy^2} - g_m \frac{d^2 g_n}{dy^2}) + (\lambda_m^2 - \lambda_n^2) R(y) g_n g_m = 0 \qquad \text{(a.5)}$$

and hence

$$(\lambda_m^2 - \lambda_n^2) \int_0^1 R(y) g_n g_m dy = \int_0^1 \left[g_n \frac{d^2 g_m}{dy^2} - g_m \frac{d^2 g_n}{dy^2} \right] dy \qquad \text{(a.6)}$$

Integrating the right ember by parts, w obtain

$$(\lambda_m^2 - \lambda_n^2) \int_0^1 R(y) g_n g_m dy = \left[g_n \frac{dg_m}{dy} - g_m \frac{dg_n}{dy} \right]_0^1 - \int_0^1 \left[\frac{dg_n}{dy} (\frac{dg_m}{dy}) - \frac{dg_m}{dy} (\frac{dg_n}{dy}) \right] dy \qquad \text{(a.7)}$$

Since the last integrated vanishes identically, there follows finally

$$(\lambda_m^2 - \lambda_n^2) \int_0^1 R(y) g_n g_m dy = \left[g_n(y) \frac{dg_m(y)}{dy} - g_m(y) \frac{dg_n(y)}{dy} \right]_0^1 \qquad \text{(a.8)}$$

In view of the fact that both $\phi_m(y)$ and $\phi_n(y)$ satisfy the conditions prescribed in the connection with equation (a.3) at the point *y=0.0* and *y=1.0* the right-hand member of equation (a.8) clearly vanishes, there follows

$$\int_0^1 R(y) g_n(y) g_m(y) dy = 0 \quad if \quad m \neq n \qquad \text{(a.9)}$$

That is, if the characteristics functions correspond to different characteristics number, then they are orthogonal with respect to the function R(y).Therefore, at the first case the multiplying factor becomes

$$R(y)g_m(y) = \cos(\lambda_n y) \qquad \text{(a.10)}$$

Since *R(y)*=1.

At the second case,

$$R(y)g_n(y) = y^{3/2} J_{-1/3}(\gamma_m y^{3/2}) \qquad \text{(a.11)}$$

Since *R(y)= y*

Appendix B: The Solution of Differential Equation Using Bessel functions.

The general Bessel equation can be written as [ ]

$$\frac{d^2R}{dy^2}+\left[\frac{1-2m}{y}-2\alpha\right]\frac{dR}{dy}+\left[p^2a^2y^{2p-2}+\alpha^2+\frac{\alpha(2m-1)}{y}+\frac{m^2-p^2\nu^2}{y^2}\right]R=0 \qquad \ldots(b.1)$$

and the corresponding solution of which is

$$R(y)=y^m e^{\alpha.y}\left\{AJ_\nu(ay^p)+BY_\nu(ay^p)\right\} \qquad \ldots(b.2)$$

where A and B are arbitrary constants which found from boundary conditions of problem.

When ν is not zero or not positive integer, the solution equation (b.2) can be taken in the form

$$R(y)=y^m.e^{\alpha y}.[AJ_\nu(ay^p)+BJ_{-\nu}(ay^p) \qquad \ldots(b.3)$$

where

$$J_\nu(y)=\sum_{k=0}^{\infty}\frac{(-1)^k(y/2)^{2k+\nu}}{k!\Gamma(\nu+k+1)}$$

and

$\Gamma(x)$ is the gamma function.

By comparing the differential equation

$$\frac{d^2g}{dy^{+2}}+\frac{9}{4}\gamma^2y^+g=0 \qquad \ldots(b.4)$$

with the above generalized Bessel equation we find

$$m = \frac{1}{2}, \qquad \alpha = 0, \qquad a = \gamma, \qquad \nu = \frac{1}{3}$$

and the solution of equation (b.4) becomes

$$g(y^+) = \sqrt{y^+}\,[A_2 J_{1/3}(\gamma y^{+3/2}) + A_3 J_{-1/3}(\gamma y^{+3/2})] \qquad \ldots(b.5)$$

which involves Bessel functions.

where A_2, A_3 are arbitrary constants.

The sketch of Bessel function ($J_{-1/3}(\gamma\delta^{+3/2})$) are shown in the below figure.

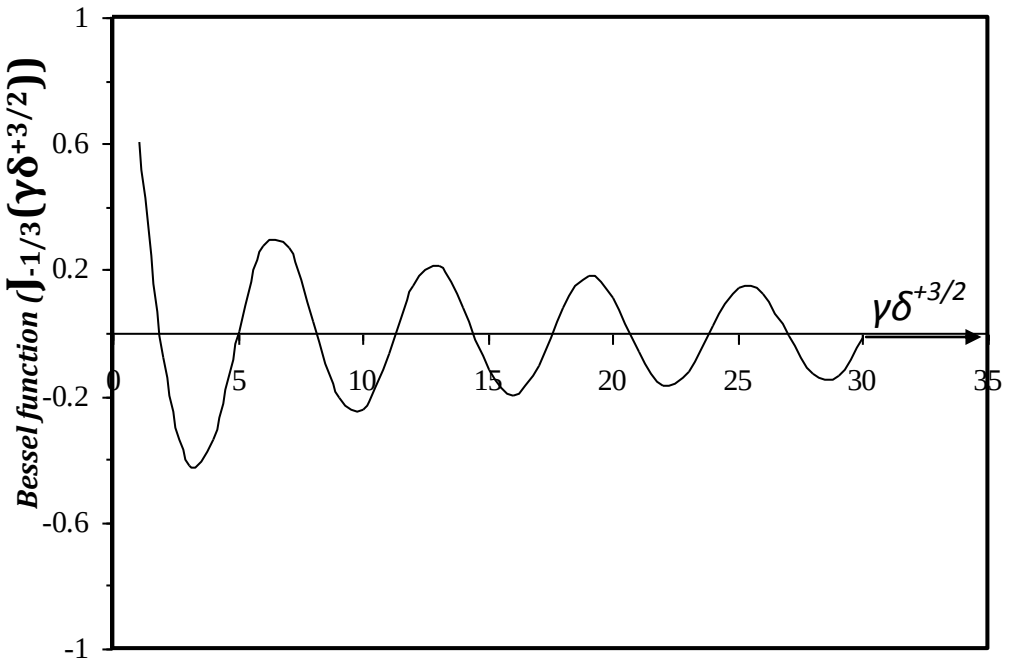

Figure B.1 Bessel function

Appendix C: Flow Chart for the Computer Program for the Uniform Velocity Profile case.

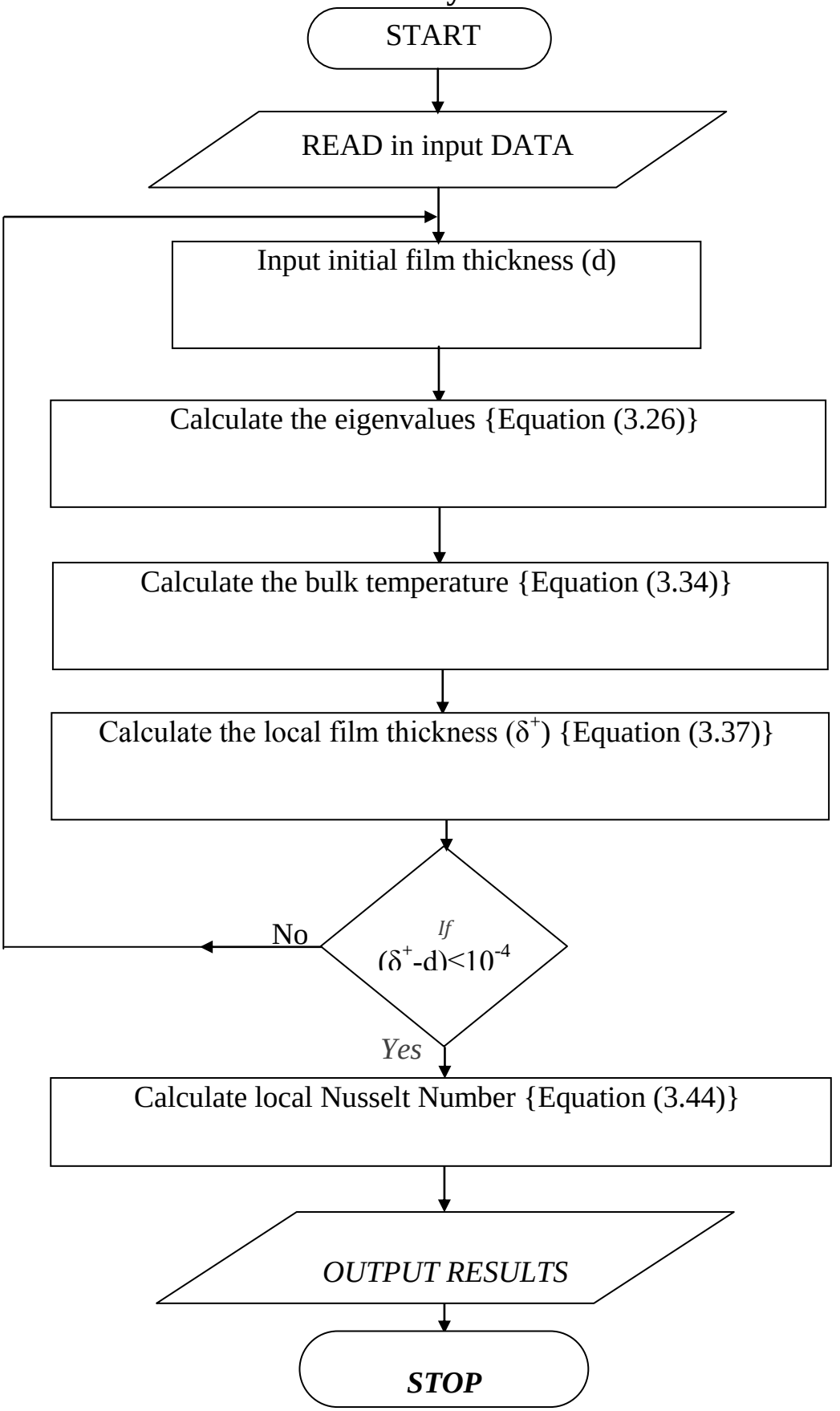

Appendix D: Flow Chart for the Computer Program for the Linear Velocity Profile case.

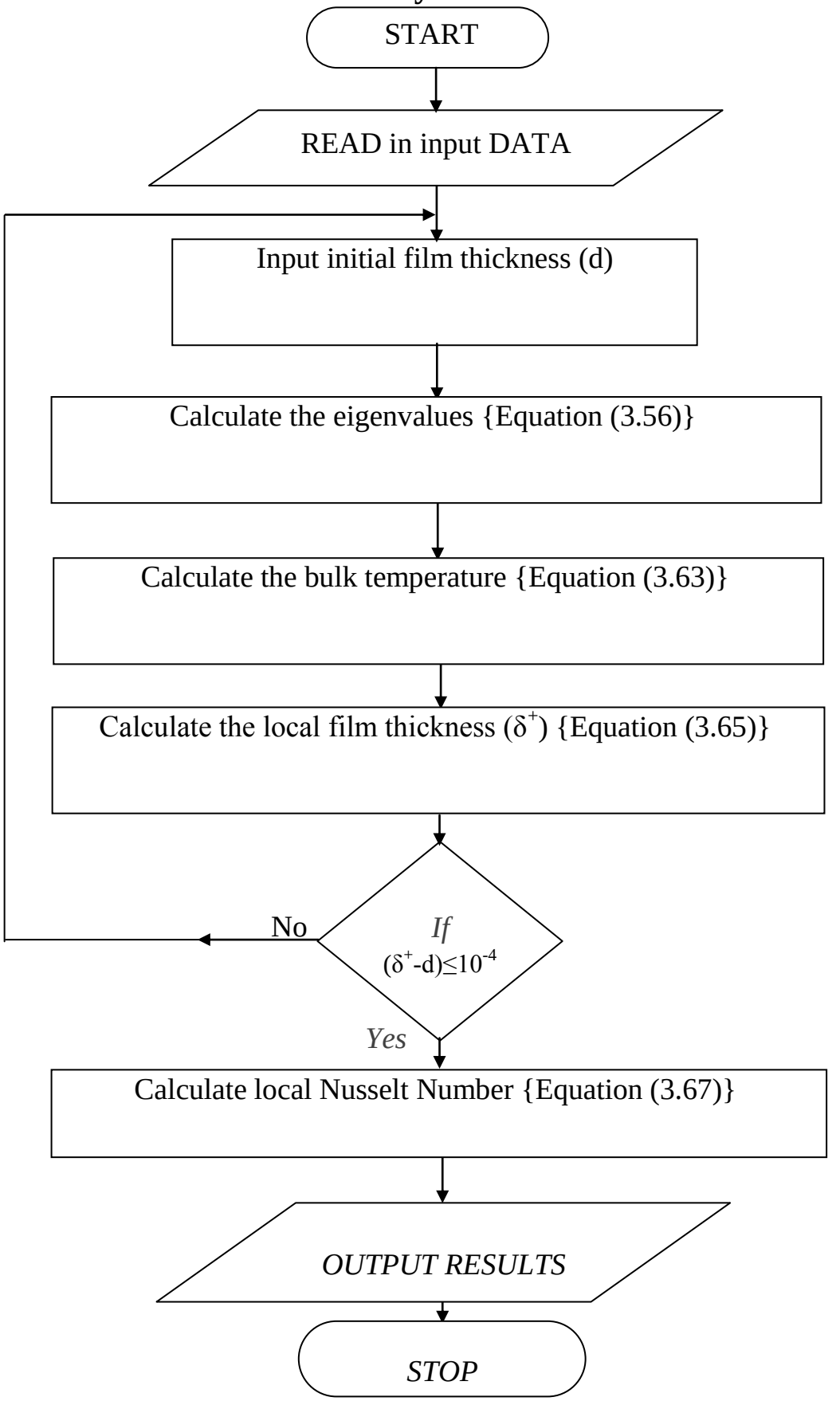

Appendix E: Flow Chart for the Computer Program for the Semi-parabolic Velocity Profile case.

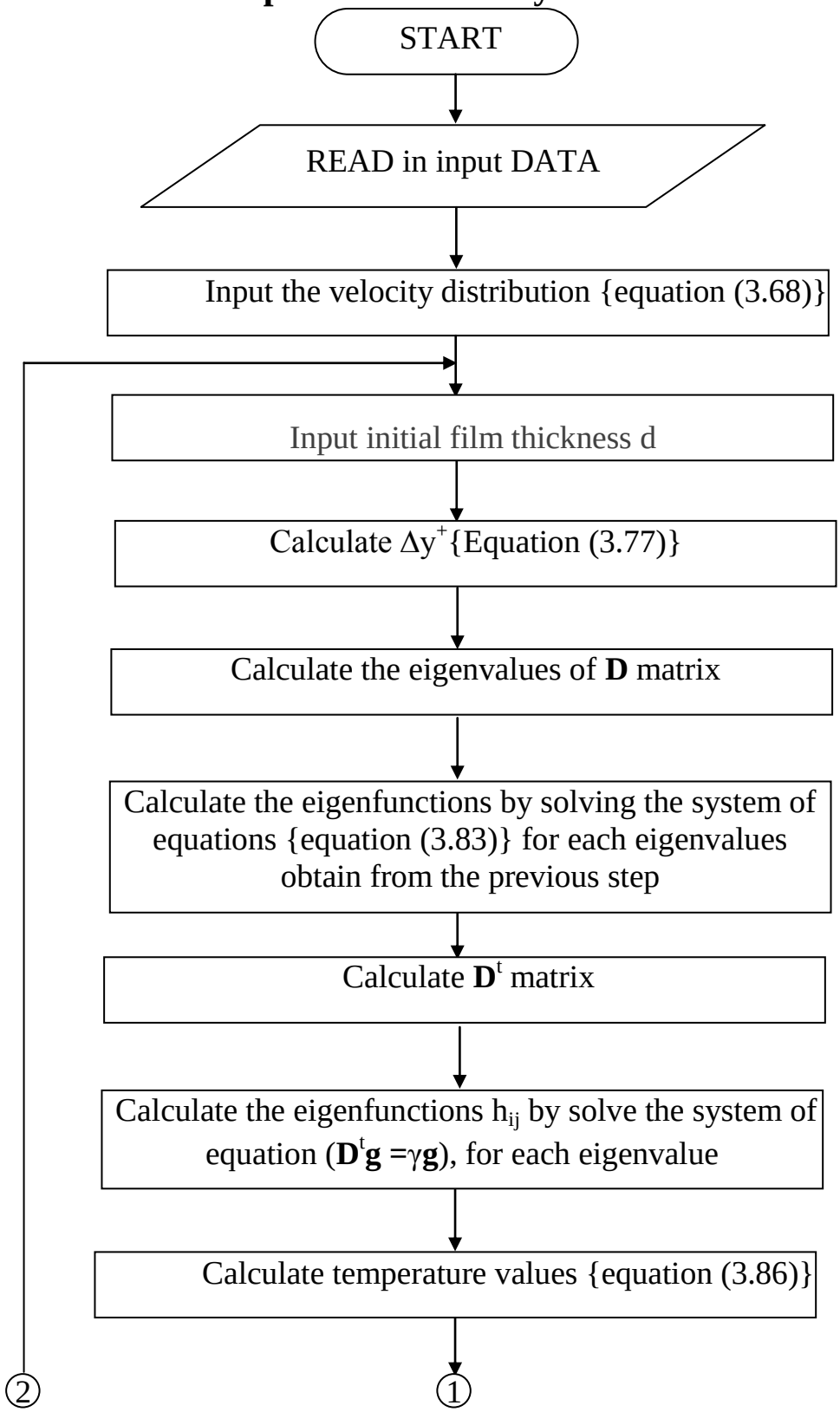

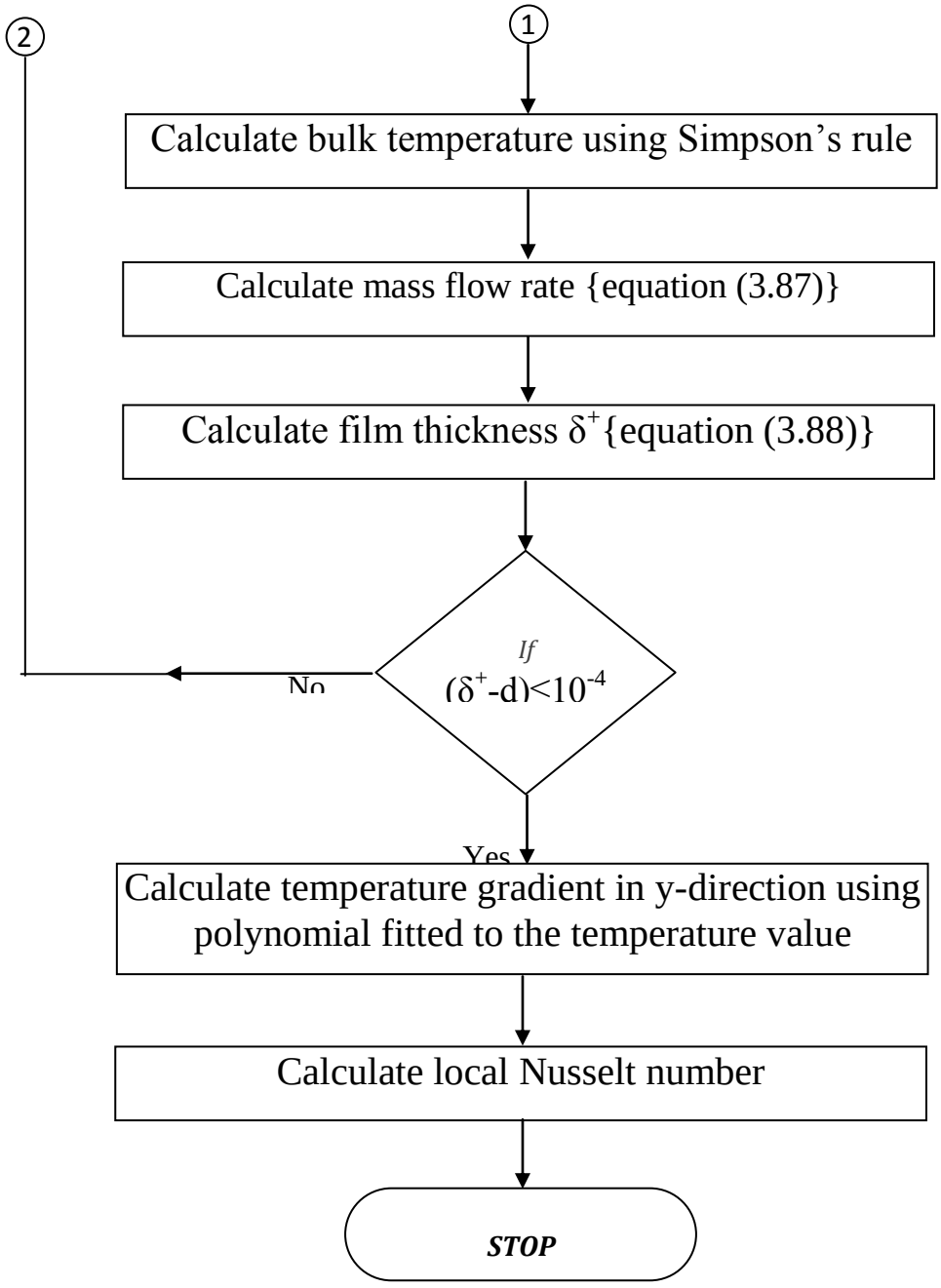
1
2
Calculate bulk temperature using Simpson's rule
Calculate mass flow rate {equation (3.87)}
Calculate film thickness δ^+ {equation (3.88)}
If
$(\delta^+ - d) < 10^{-4}$
No
Yes
Calculate temperature gradient in y-direction using polynomial fitted to the temperature value
Calculate local Nusselt number
STOP

الملخص

العمل الحالي عبارة عن بحث نظري لبيان تأثير السرع المختلفة على عملية التكثيف بالتماس المباشر لبخار مشبع على طبقة غشائية من السائل طباقية مبردة وتامة التشكيل تجري على سطح صلب معزول حرارياً. تم تطوير نموذج رياضي مستند على الموازنة الحرارية ومعادلة الطاقة الحرارية لوصف ادائية تكثيف البخار على طبقة رقيقة من السائل ولأنواع مختلفة من مقاطع السرع.النموذج الرياضي اخذ بنظر الاعتبار حالة كون السرعة وانحدار درجة الحرارة متغيرة على طول خط الجريان والذي يختلف عن اغلب النماذج حيث اعتبرت ثابتة. في هذه الدراسة انتخبت ثلاثة أنواع لتوزيع السرعة خلال طبقة السائل هي :السرعة المنتظمة,السرعة الخطية وسرعة الشبة القطع المكافئ.

استخدمت طريقة تحليلية لنوعين من توزيع السرعة هما السرعة المنتظمة و السرعة الخطية.أيضا تضمنت الدراسة تطوير طريقة عددية للنوع الثالث من السرع المستخدمة وهو سرعة شبة القطع المكافئ.

النتائج المستحصلة وضحت أن عوامل رئيسية تسيطر على عملية التكثيف هي رقم برانتل(Pr)ورقم رينولدز(Re)ورقم درجة التبريد(S). النتائج أعطت تصور عن العملية بدلالة عدد نيسلت, درجة الحرارة ألا جمالية و معدل التكثيف.

قورنت نتائج النموذج مع بعض الاستنتاجات التحليلية الأخرى وكان التقارب بين النتائج مرضٍ. ايظاً قورنت النتائج مع النتائج العملية لباحث أخر وكان التوافق بين النتائج مقبول.

تأثير توزيع سرعة طبقة السائل على التكثيف بالتماس المباشر

رسالة مقدمة إلى
كلية الهندسة – جامعة البصرة
كجزء من متطلبات نيل درجة ماجستير علوم
في الهندسة الميكانيكية

من قبل
عمار علي عجيمي
(بكالوريوس هندسة ميكانيكية)

شباط 2003